AN *AB INITIO* FUZZY DYNAMICAL SYSTEM THEORY: CONTROLLABILITY AND OBSERVABILITY

A Thesis
Presented to
The Academic Faculty

by

Attapong Terdpravat

In Partial Fulfillment
of the Requirements for the Degree
Master of Science in Mechanical Engineering

Georgia Institute of Technology
November 2004

AN *AB INITIO* FUZZY DYNAMICAL SYSTEM THEORY: CONTROLLABILITY AND OBSERVABILITY

Approved by:

Dr. Ye-Hwa Chen, Advisor

Dr. Augustine Esogbue

Dr. Kok-Meng Lee

Date Approved: November 2004

ACKNOWLEDGEMENT

I would like to thank my advisor, Professor. Ye-Hwa Chen, for his guidance and directions on this research. His knowledge and experience were vital to this work. I would also like to thank my reading committee members, Professor Augustine Esogbue and Professor Kok-Meng Lee, who have freely given me their time and experience.

My time as a graduate student has been enriched by a circle of friends who provided support and insights. I am deeply grateful for my family who has always been supportive and understanding. Special thanks go to Chayanin Kerdpholngarm who has helped me when I most needed and to Martin Kurnadi for his assistance. To my other friends and faculties who have influenced my time at Georgia Tech, Thank you.

TABLE OF CONTENTS

LIST OF TABLES

Table

LIST OF FIGURES

Figure

SUMMARY

The current research proposes a new framework that concerns the evolution of membership functions. Membership functions characterize fuzzy sets by assigning membership values over the relevant range. This creates smooth transitions between fuzzy sets corresponding to the degree of fulfillment each intermediate element has according to the operating definition of the concept. Through this approach, uncertainty in dynamical systems can be captured through membership functions. As a system evolves through time, so does its associated uncertainty. We introduce the concept of membership functions propagation as a dynamic description of uncertainty. Given a dynamical system with a set of initial states membership functions, the membership function propagation describes how these membership functions evolve over time with respect to the system. The evolution produces a set of propagated membership functions that have different size and shape from their predecessors. They represent the uncertainty associated with the states of the system at a given time.

This new description also confers new definitions for two important concepts in control theory, namely controllability and observability. These two concepts are re-introduced in a fuzzy sense, based on the concept of membership function propagation. By assuming convexity of the fuzzy set, criterions for controllability and observability are established and tested. Both concepts, along with the membership functions

propagation process are illustrated by MATLAB and SIMULINK simulations of an inverted pendulum and a 2 degree of freedom mechanical manipulator.

CHAPTER 1

INTRODUCTION

1.1 **Motivation: Uncertainty.**

Uncertainty can be characterized as *vagueness*, *imprecision* and *randomness* [9]. *Vagueness* refers to the fact that concepts in natural languages do not have well-defined boundary and the meaning of a word depends on the context of which it is used. In our daily lives, we accept crude descriptions and forego exact details because they would make communication tedious. For example, to describe a moderate weather, we simply use the term 'warm'. We usually do not give the precise information that the current temperature is 75 degree Fahrenheit with a wind-chill factor of 60 degree Fahrenheit gusting from the northwest at the speed of 5 mph. Instead, a single adjective suffices for communicating the necessary information and the complete detail is subsidiary. However, the same concept describes a different range of values if it is applied to say, a human body temperature.

Clearly, similar usage applies to all modifiers. They abbreviate a collection of assorted information in which the listeners can make further inference and implication about its scope according to a given context. Referring to the example above, upon being informed that the current temperature is warm, the listener can determine from his location and the current season that the temperature is possibly within the 70-80 degree Fahrenheit range.

Imprecision is the condition in which the possibility of error exists due to an inability to obtain exact and complete knowledge. Unfortunately imprecision in

measurement is inherent and this implies that the exact and complete measurement knowledge can not be obtained. All types of measurement are taken with reference to a standard. These standards can be further divided into fractional parts. However, we often find that these subdivisions prove too coarse for our application and another measurement instrument or technique may be used. A typical kilogram scale with a resolution of a hundred gram is appropriate for human weight. But for an object microscopically small, a different weight measurement technique with a much smaller resolution than a typical scale might be used. Ultimately, measurement can not be performed to an arbitrary degree of accuracy because the resolutions of the measuring devices have certain practical limits. Thus, the quest for precision reaches its limit when measurement falls between the resolutions of the best instrument and technique available. The truth ensues that in practicality, only a finite subdivision of a measurement standard is possible and therefore even the most precise instrument can not deny uncertainty.

Not only is that uncertainty prevalent in our daily lives, but also in sciences. In science and engineering, complex physical systems are represented through mathematical models. Often times, the resulting mathematical models are too complex for practicality and simplifications are needed for them to become feasible. One way to reduce the complexity is to simplify the model by exploiting the tolerance for uncertainty which can often appear in the forms of vagueness and imprecision as described above. Theoretically, such simplifying assumptions are absent; however, as Kaoru Hirota [15] puts it "There is a fundamental difference between the theoretically possible and the practically feasible". Surely, the resulting models are not perfect, but they are

manageable, valid solutions to complex problems which could be unfeasible if precision is required.

In contrast with the previous two aspects of uncertainty, *randomness* is not concerned with definitions, accuracy, or any other aspect of a particular concept. Instead, *randomness* describes the occurrence characteristic of an event. Another difference is that randomness, as treated in the probability theory, had received a long history of investigation ever since human began an ever-lasting infatuation with gambling. The introduction of statistical side of the probability theory dated back to the 1600's when Girolamo Cardano's book on gambling, *Liber de Ludo Alae* was published in 1663. Cardano was the first man to define the conventional format for expressing probability as a fraction [3].

Thus, for a long time, there remained a need for effective means to describe and quantify information in terms of its associated vagueness and imprecision. This need had been answered by the emergence of fuzzy theory in 1965.

1.2 **Developments of fuzzy theory.**

The publication of Professor Lofti A. Zadeh's seminal paper "Fuzzy Sets" in 1965 is generally accepted as the birth of fuzzy theory [16]. Professor Zadeh's interest was in using state variable approach in solving simultaneous differential equations. However, during the early 1960s he felt that the traditional framework were too precise and did not reflect many complex real-world problems [15]. For example, he noted that in many practical cases, the a priori data is far from being precise or do not have known probability distributions. Thus, in his seminal paper he proposed a different kind of

mathematics which deals with aspects of uncertainty distinct from probability theory. This new concept of uncertainty became fuzzy theory.

Initially, fuzzy theory encountered sharp criticism [8]. The main objections centered on the theory's core foundation of fuzzy sets. Fuzzy set accepts imprecision and therefore it was conceived as deviating from the traditional scientific focus on precision. Despite strong resistance, Zadeh continued to develop on the foundations of the fuzzy theory and slowly, the number of fuzzy followers grew.

By the 1970s, contributions to the foundations of fuzzy theory increased dramatically. Numerous publications followed the *fuzzification* trend. This process involves a generalization of the key mathematical sets from classical sets to fuzzy sets. Examples of such fuzzification include M.Mizumoto and K.Tanaka work on fuzzy automata and fuzzy grammars [12], Bezdek's work on fuzzy clustering [4] and H.J. Zimmermann's work on optimization [17]. Among these, notable contributions were made by E. Mamdani in the United Kingdom in 1974. In "Application of fuzzy algorithms for control of simple dynamic plant", fuzzy theory was applied to a steam generator controller and hence, the first fuzzy logic controller was developed [12]. Immediately after Mamdani showed that automatic learning and tuning of fuzzy controllers were possible, the first industrial application of the fuzzy theory emerged in 1976. It was a cement kiln controller that incorporates the experience of human operators developed by Blue Circle Cement and SIRA in Denmark. The kiln controller improved efficiency through smoother grinding and went into operation shortly after [15].

Hence forth, the fuzzy logic controller gained tremendous popularity which lead to the usual misunderstanding that fuzzy logic control is synonymous with fuzzy theory.

In fact, fuzzy control is a branch in the broad applications of fuzzy theory which includes examples cited above as well as fuzzy pattern recognition, fuzzy decision making, fuzzy arithmetic, etc.

The present time had seen many applications of fuzzy technologies, especially in Japan. The Japanese government endorsed collaboration between industries and universities by setting up a large scale research project, consortium and budgeted funding which facilitate knowledge transfers between the two communities. The result was a "fuzzy boom" in Japan, in which large companies deployed fuzzy technologies in all aspects, from consumer products such as vacuum cleaner, washing machines and rice cookers to public infrastructure such as subway and water treatment system. Today, a foreign word pronounced "fuzzy" means intelligence in Japanese [15].

1.3 Fuzzy sets.

Fuzzy set is a generalization of the classical set. A classical set is distinguished from another by a sharp boundary at some threshold value and therefore, they are also known as crisp set. In fuzzy theory, sharp boundary and crisp set are replaced by partial truth and fuzzy sets. The idea of partial truth facilitates information description especially those communicated through natural language. Natural language is prevalently vague. Particularly, the transition between descriptive terms such as hot and warm are not abrupt discontinuities. Instead, the transition is a smooth change over a range corresponding to the degree of fulfillment each temperature measure have according to the context of 'hot', 'warm', or 'cold'.

Smooth changes are better characterized by the idea of *partial membership* rather than the crisp, binary characterization of either 'hot' or 'warm' as employed by the

classical sets. For example, return the context of warm weather, depending on location and season, most people would agree that 70-75 degree Fahrenheit is warm. What about 77 degree Fahrenheit? Or even 80 degree Fahrenheit? Surely, not everybody think that 77 or 80 degree Fahrenheit is warm and some may declare that it is hot. As temperature gradually increases further, more people suggest hot weather rather than warm. When the transition between hot and warm weather occurs, the intermediate temperature readings, say 76, is not absolutely hot or absolutely warm. Such readings fell in between the two concepts, with some degree of relevance in both

Having a temperature reading fallen in between two concepts is an example of partial membership. An element can belong to two or more sets at the same time, and the degree at which it belongs to a particular set is reflected in its *membership grade* which is a value in the closed interval from 0 (not relevant) to 1 (fully relevant). This also means an element of a set can be part of its opposite: that is A can equal not-A. Partial membership is an expansion from classical set theory which allows only two possibilities for the relationship between an element and a set: Either an element 'a' belongs to a set 'A' or it is not. The expansion implies that certain logical relations are different when applied to fuzzy sets.

One way to define a crisp set is through using a characteristic function. A set K is defined by its characteristic function χ_K that declares which elements of the universal set, X belong to K as follows

$$\chi_K(x) = \begin{cases} 1 \text{ for } x \in K \\ 0 \text{ for } x \notin K \end{cases} \tag{I.3.1}$$

That is, the mapping of X to $\{0,1\}$ is binary; it is 1 when x is a member or 0 when x is not. This is formally expressed by

$$\chi_K : X \to \{0,1\} \tag{I.3.2}$$

In fuzzy theory, this process is generalized to the distribution of membership grades, which is performed by a *membership function*. A membership function is analogous to the characteristic function in the classical set theory in that it also maps an element of the universal set X to a set [0 , 1]. The major difference now becomes that the assigned number in the closed [0 , 1] has a quantitative meaning. The assigned value is the membership grade which correlates to the degree of compatibility of each element to the operating definition of that set.

Definition 1.1: Given a relevant universal set X, a membership function μ_A uniquely defines a fuzzy set A.

$$\mu_A : X \to [0,1] \tag{I.3.3}$$

For each $x \in X$, the membership function maps element of X to elements of the closed set [0,1].

In this manner, a classical set can be viewed as a special case of fuzzy sets whose membership function becomes a characteristic function

To see how one forms a fuzzy set, ten participants may be asked if any of the several temperature readings such as 60, 70, 80, and 90 degree Fahrenheit conform to the concept 'warm weather'. The concept 'warm weather', hence forth A, is a subset of the relevant universal set X, which includes all weather temperature e.g. cold, warm, chilly, hot, etc. The membership grade for each reading is derived from expert opinion, in this case, the participant's votes. Suppose none of the participants vote that 60 degree Fahrenheit is warm then the temperature reading of 60 receives a membership grade of 0. If two participants vote 64 degree as warm, then the membership grade for 64 degree

Fahrenheit is 2 divides by the total number of votes 10, or 0.2. Similarly, the voting process continues to give a membership grade from the [0,1] interval to each temperature reading *x* from *X*. The temperature reading with their associated grades can be as follows

Table 1.1: Temperature readings and the their membership grades for 'warm weather'

Temperature readings (deg. Fahrenheit)	Number of Votes	Membership Grades
60	0	0
62	1	0.1
64	2	0.2
66	3	0.3
68	4	0.4
70	7	0.7
72	10	1
74	10	1
76	10	1
78	8	0.8
80	6	0.6
82	4	0.4
84	3	0.3
86	2	0.2
88	1	0.1
90	0	0

Equivalently, a graphical representation of the above is as follows:

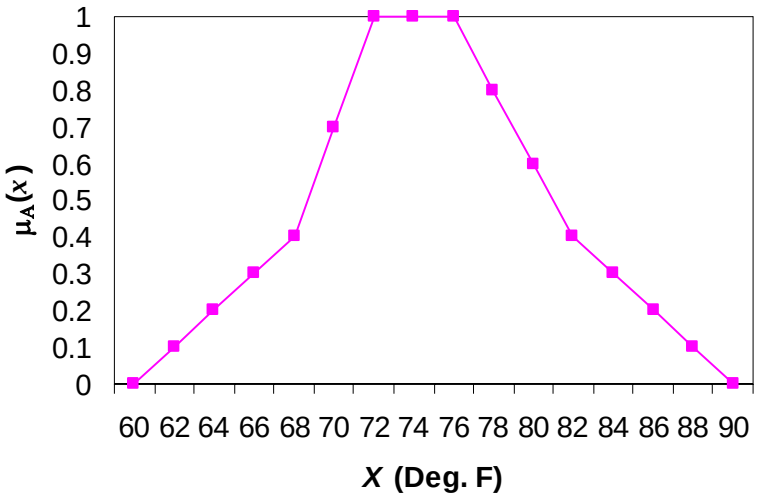

Figure 1.1: Membership function for warm weather.

Another way of representing a fuzzy set is through its list representation. The above fuzzy set can be represented by a list as

$$A = 0/60+0.1/62+0.264\ldots\ldots\ldots+0.3/84+0.2/86+0.1/88+0/90 \qquad \text{(I.3.4)}$$

The number that precedes the symbol / is a membership grade associated with a reading after it. Here, the symbol / stands for the correspondence between each temperature readings and its membership grade instead of division.

The voting process described above is one way in which a fuzzy set can be formed. It can be repeated for other concepts such as cold and hot with a possible result shown below.

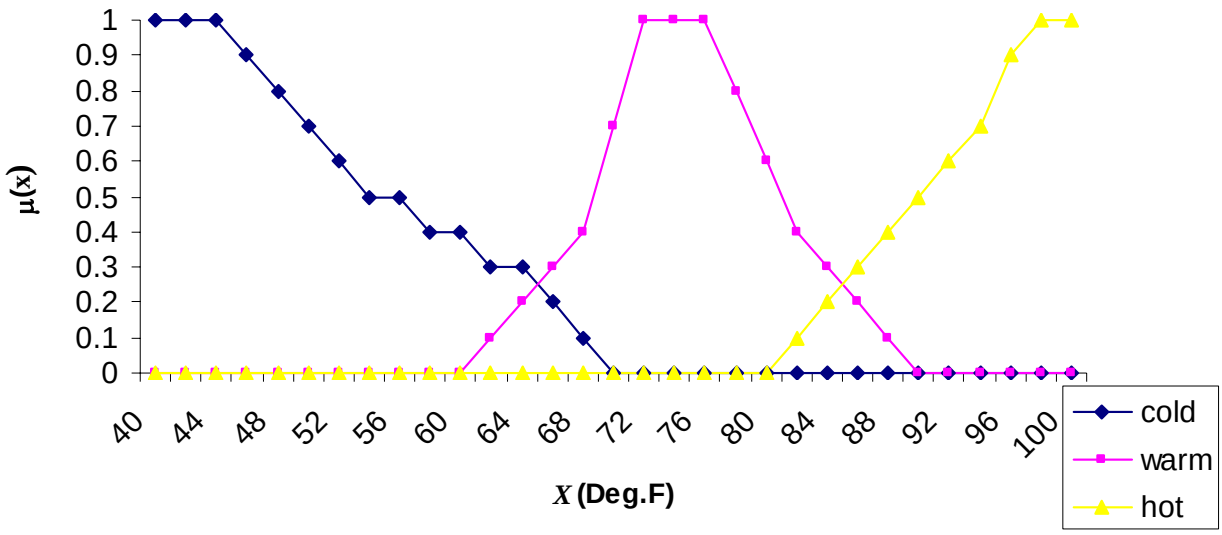

Figure 1.2: Membership functions for cold, warm and hot weather.

The overlapping sets are good demonstration for the idea of partial membership. As shown, by the temperature ranges from 60-76 and 80-92 degree Fahrenheit. The first temperature interval is a transition from cold to warm weather while the second interval is a transition from warm to hot. One reading may have different membership grades for each set. Consider the reading 62, its cold and warm membership value are 0.6 and 0.1 respectively. This illustrates that we consider 62 degree Fahrenheit to fit the concept of cold weather rather well while the reading is less appropriate for warm weather. Note that the membership grades are not required to add up to 1 for each temperature reading.

Typically, the shapes of fuzzy sets are drawn from expert opinion, tuning, empirical evidence etc. Consequentially, the exact transition from no membership to full membership can be hard to realize. However, most applications of fuzzy set theory are not sensitive to the actual shapes of the membership functions. Therefore simple shapes suffice and they are usually preferred as a result [9].

1.4 Alpha cuts and other fundamental properties of fuzzy sets.

1.4.1 Alpha cuts.

With a well-defined membership function, a fuzzy set can have another useful representation called α-cuts. The α-cuts provide an easy way to connect fuzzy sets to classical sets by generating crisp subsets of A denoted as A^{α}. A^{α} impose a restriction that its member must includes any x whose degree of membership is greater than or equal to a selected value $\alpha \in [0, 1]$.

Definition 1.2: Given a fuzzy set A defined on a relevant universal set X, the α-cuts are defined as

$$A^{\alpha} = \{x \mid A(x) \geq \alpha\} \tag{I.4.1}$$

A variant of the α-cuts is the strong α-cuts, denoted $A^{\alpha+}$ and defined as

$$A^{\alpha+} = \{x \mid A(x) > \alpha\} \tag{I.4.2}$$

For example, the α-cuts of 0.6 for the warm weather set defined above, $A^{0.6}$ includes all temperature from 70 to 80 degree Farenheit.

$$A^{0.6}=\{70,72,74,76,78,80\} \tag{I.4.3}$$

with the strong α−cut

$$A^{0.6+}=\{70,72,74,76,78\} \tag{I.4.4}$$

As seen from (I.4.3) and (I.4.4), the α−cut or the strong α−cut of a fuzzy set is a crisp sets.

1.4.2 Convexity of fuzzy sets.

An important and frequently applied property of a fuzzy set is their convexity. In the classical set theory, a set S is convex if and only if, for every pair of points in S, say

'*u*' and '*v*' and every real number 'λ' in the closed interval [0,1], the point '*g*' that is a linear combination of *u* and *v* also lies in *S*.

Formally, the above definition of convexity is as follows

$$g = \lambda u + (1-\lambda)v \in S \tag{I.4.5}$$

In other words, *S* is convex if and only if the line segment joining *u* and *v* is completely contained in *S*.

Convexity in fuzzy set theory expands on its classical counterpart. It requires that all α-cuts of a convex fuzzy set be convex. That is, let *u*, *v*, *g* and λ retain their former definitions when applied to A^{α},

$$g = \lambda u + (1-\lambda)v \in A^{\alpha} \tag{I.4.6}$$

and (I.4.6) is true for all $\alpha \in (0, 1]$. The exception of the 0-cut makes senses since it includes $\pm \infty$.

Figure 1.3 illustrates convex and non-convex membership functions. Hereafter, all membership function mentioned in this work are assumed to be convex.

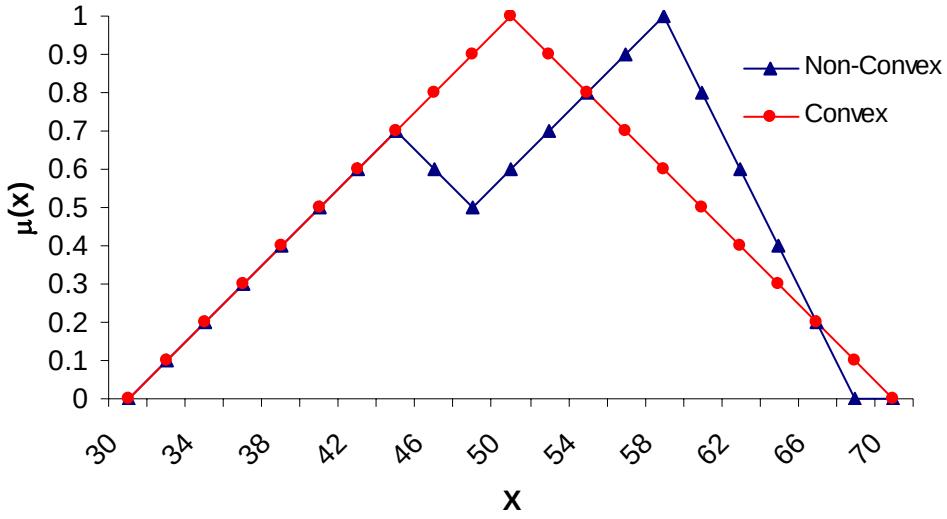

Figure 1.3 Non-convex and convex membership functions.

1.4.3 Standard fuzzy set operations

There are three basic set operations that can be readily generalized to fuzzy sets. These are called the standard fuzzy set operations, which are the standard fuzzy complement, the standard fuzzy intersection and the standard fuzzy union.

Given two fuzzy sets A, B, and the universal set X, the standard fuzzy union between A and B is denoted as A Y B. The operation is defined for all $x \in X$ by the following equation

$$(\text{A Y B})(x)=max[A(x),\text{B}(x)] \tag{I.4.7}$$

where *max* denotes the maximum operator, which is associative and therefore (I.4.7) can be extended to any finite number of fuzzy sets.

Similarly, the standard fuzzy intersection denoted as A I B is defined by the following equation

$$(\text{A I B})(x)=min[A(x),\text{B}(x)] \tag{I.4.8}$$

where *min* denotes the minimum operator, which can also be extended to any finite number of fuzzy sets because of its associative property.

Finally, the standard complement $\overline{A}$ of fuzzy set A is defined by the equation

$$\overline{A}(x) = 1 - A(x) \tag{I.4.9}$$

1.4.4 The decomposition theorem.

As seen, a fuzzy set can be decomposed into multiple crisp sets by specifying a series of α values so that each α–cut creates a slice of the membership function. Conversely, it is easy to see that the original membership function can be reconstructed by superimposing these slices in order.

In fact, this is the case: an important property of the α-cuts is that it can be used to regenerate the membership function. As a general property, the sizes of the α-cuts either remain the same or decrease as α value increases. This statement is intuitive since a higher α value charges a higher degree of compatibility and therefore less and less elements comply. According to Figure 1.1:

$$A^{0.6}=\{70,72,74,76,78,80\} \tag{I.4.10}$$

$$A^{0.8}=\{72,74,76,78,80\} \tag{I.4.11}$$

It can be shown that for any $\alpha_i > \alpha_j$

$$A^{\alpha i} \subseteq A^{\alpha j} \tag{I.4.12}$$

which implies $A^{\alpha i} \cup A^{\alpha j} = A^{\alpha j}$ and $A^{\alpha i} \cap A^{\alpha j} = A^{\alpha i}$. Consequently, reconstruction of the original fuzzy set A can be achieved by simply taking the standard fuzzy union over all the α–cuts of A. However, before this task could initiate, a special fuzzy sets ${}_{\alpha}A$ needs to be defined as being the product between the α and their associated α–cuts set as follows

$${}_{\alpha}A = \alpha \cdot A^{\alpha} \tag{I.4.13}$$

The collection of these special fuzzy sets ${}_{\alpha}A$ for all α $\alpha \in [0,1]$ can represent the original fuzzy set A.

Theorem 1.1: For every fuzzy set A defined within a universal set X

$$A = \bigcup_{\alpha \in [0,1]} {}_{\alpha}A \tag{I.4.14}$$

where ${}_{\alpha}A$ is defined by (I.4.13) and $\cup$ denotes the standard fuzzy union.

Theorem 1.1 is referred to as the **first decomposition theorem** of fuzzy sets, which is a useful method of representing fuzzy sets by their α–cuts. Similar development leads to the second decomposition theorem that utilizes the strong α–cuts of instead of the α–cuts. However, it is omitted because the first decomposition theorem alone is sufficient for later development.

As seen, the α–cuts representation is useful not only because it bridges fuzzy and crisp sets but also it provides a mean of which we can transform, manipulate and apply standard computations to fuzzy sets as will be shown in the following chapter.

1.4.5 Fuzzy subsethood.

From the classical set theory, set *F* is a subset of *G* if and only if every member of *F* is a member of *G*. This is written as

$$F \subseteq G \tag{I.4.15}$$

Similarly, the idea of fuzzy subset is defined as follows. Given two fuzzy sets *A* and *B* defined in the universal set *X*, *B* is a subset of *A* if for every element *x* in *X*, its membership grade in *B* is less than or equal to its membership grade in *A*.. This can be written as

$$B \subseteq A \Leftrightarrow \mu_B(x) \le \mu_A(x) \qquad \forall x \in X \tag{I.4.16}$$

Like other properties of fuzzy sets, subsethood can be extended to degree of subsethood. However, to facillitate its explanation, we must first define a quantity of fuzzy sets called scalar cardinality. For a fuzzy set *B,* its scalar cardinality |*B*| is defined by the formula

$$| B | = \sum_{x \in X} \mu_B(x) \tag{I.4.17}$$

$|B|$ may be thought of as the total number of elements in the set B. However, since each element can have partial membership in B, the summing process must reflect this fact by weighting each element with the corresponding membership grade that results in (I.4.17).

Now, the degree pf subsethood, say between set B and set A, should reflects how much of B belongs to A. This is accomplished by the formula

$$S(B, A) = \frac{1}{|B|}\left(|B| - \sum_{x \in X} \max[0, \mu_B(x) - \mu_A(x)] \right) \quad \text{(I.4.18)}$$

Since B and A are related by (I.4.16), the summation of (I.4.18) counts how many times (I.4.16) is violated. The scalar cardinality of B in the denominator is merely a normalizing factor that keeps the degree of subsethood between 0 (B is not a subset of A) and 1(B is a subset of A). (I.4.18) can be experssed more conveniently as follows

$$S(B, A) = \frac{|B \cap A|}{|B|} \quad \text{(I.4.19)}$$

1.5 Fuzzy theory vs. probability theory.

This section aims to clarify the general confusion between the roles of fuzzy and probability theory. Fuzzy theory is an alternative model for describing information. It benefits from the unique capability to describe aspects of uncertainty that probability theory is thought to be insufficient for. The differences between these two concepts can be viewed as the difference between *possibility* and *probability*. While probability theory focuses on the aspect of whether a random event does or does not occur and if so, what is its expectation, fuzzy theory focuses on the uncertainty in the concept itself due to imprecision in empirical observation or vagueness in natural language. As such, the two

theories are simply different tools for different problems and thus, they are not two competing methods as widely misunderstood.

To a great extent, the world is a matter of degree. Science reviewed that matter changes smoothly and continuously in the sense that a sweeping statement like "the sky is blue" can only be true in part. This is because an observation would show that the horizon is a gradual transition from white to blue and from blue to white to different shades of yellow near the shinning sun. Thus, an accurate description of the world would have to reflect this continuum of changes. However, there are certain circumstances that these degrees of changes simply degenerate to two truth values of true or false. For example, an individual belongs to two sexes: male or female, regardless of genders. Unfortunately, it has been a combination of convenience, habit and inheritance to project this binary world view to everything else, thus creating what Kosko called " the mismatch problem'[10]. That is, the world is gray but science and logic portray it as black-white.

Probability theory has proven powerful in a vast array of applications ranging from weather forecasting to stock portfolio holding. Nonetheless, it does little to alter or even challenge the black-white picture of the world [10]. Instead, it affirms this view and in essence, compounds to the mismatch problem by allowing practicioners to write off the shades of gray as black or white, before attaching the probability. This is made obvious by observing the requirement that an event either happen or not is fundamental to probability theory. To calculate a probability, we first need to consider all possible outcome, or the sample space. An event, which is a subset of that sample space, is

required to either occur (success) or not (failure). The probability is then calculated as a proportion of success and failure.

Consider a raffle with ten raffle number, 1,2,…,10, the sample space can be represented as S={1,2,3,…,10}. Suppose the winning condition is for a person to draw an even number, then the event would be E={2,4,6,8,10}. As such, the probability of winning this raffle can be calculated as the number of elements in the event set over the number of elements in the whole sample space, which is 0.5. The probability theory is useful in this class of problem where an outcome can be readily classified as either belonging to a set A or not-A. Thus, the accuracy of a probabilistic solution is reduced when this immediate classification is not possible. The probability theory cannot tolerate the notion that part of an event can be 'A' and 'not-A' at the same time because such event would simply be a misfit and a contradiction. It must be classified into either one of the two binary choices.

On the other hand, such contradiction is embraced by fuzzy theory and it is implemented by the membership grade of a fuzzy set. The same number has a different meaning when it is a membership grade than when it is a probability, consider the following example [11]. A prisoner must choose from two containers labeled 'D' and 'E'. Let P ={all deadly poison}, d={liquid in 'D' container}, and e={liquid in 'E' container} and $\mu_P(d) = 0.1 = \Pr(e \in P)$ as in the figure below

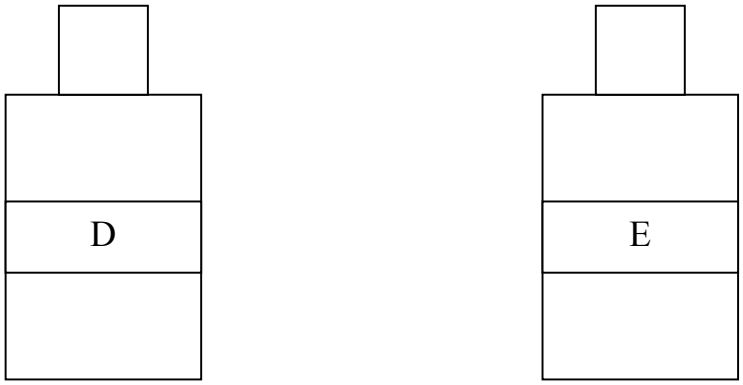

$\mu_P(d) = 0.1$ $\Pr(e \in P) = 0.1$

Figure 1.4: Two containers ‘D’ and ‘E’

Confronted with this pair of containers, the prisoner can immediately see that the container ‘D’ might contain liquid that is as dangerous as say, spoiled milk. It would not contain deadly liquids such as cyanide. That is, membership of 0.1 means that the contents of D are far from fatal. On the other hand, the probability that E is deadly “equals 0.1” means that over a long run of experiments, the contents of E are expected to be safe in about 90% of the trials. In the other 10% the contents will be fatal - 1 chance in 10. Thus, a logical choice is to opt for the spoiled milk.

Furthermore, suppose the prisoner has chosen ‘E’ and he survives, the probability $\Pr(e \in P)$ drops from 0.1 to 0, since the liquid in ‘E’ is not deadly. However, if he dies, then the probability $\Pr(e \in P)$ jumps to 1, since the liquid in ‘E’ is, in fact, deadly. This presents an interesting observation: as more information becomes available, the associated probability adjusts to reflect these changes. As in both cases, the probability $\Pr(e \in P)$ simply converges to 1 or 0. There is no more randomness. On the other

hand, the membership grade remains unchanged at $\mu_P(d) = 0.1$. As such, when more information can terminate randomness, fuzziness promises to stay as a prominent part of the future.

1.6 Research goal

The shape of a fuzzy set, as describe by the membership function, defines the transition of the degree of relevance of the intermediate elements from no membership to full membership. This, by far, has been the common extent of concern regarding the membership function. Different applications may use the membership function to describe different variables such as speed, position, temperature, dirtiness, traffic conditions etc. But the underlying application of fuzzy sets remains the same: to describe information whose membership function, created in an initial setting, preserve the same size and shape throughout its entire application. In other word, fuzzy sets are utilized as if they are static entities. Nothing has been said about how an initially defined membership function can develop over time with respect to a system.

The current research proposes a new framework that concerns the evolution of membership functions. We introduce the concept of membership function propagation as a dynamic description of uncertainty. This new description also confers new definitions for some control concepts, namely controllability and observability. These two concepts are re-introduced in a fuzzy sense, based on the concept of membership function propagation. A criterion for controllability and observability is stated, discussed and demonstrated by examples of selected physical systems.

1.7 Organization

The remaining chapters introduce the concept of membership function propagations and its applications to control theory. Chapter 2 presents an overview of the solution to the state equation and its extension to the membership function. A MATLAB simulation of an inverted pendulum is used as a sample dynamical system to illustrate the concept. Membership function propagation can be extended towards other applications of control theory. Chapter 3 discusses controllability and observability based on this extension. Contexts and conditions of which these properties hold are proposed. The inverted pendulum is revisited and simulation results are shown to ensure the validity of these contexts and conditions. Chapter 4 extends these concepts and characteristics to a 2-DOF mechanical manipulator. Modeling, linearization methods and simulations of the mechanical manipulator are presented and the same analysis done for the inverted pendulum is revisited under various conditions. Finally, the contributions of this work are highlighted and recommendations of future works are discussed in Chapter 5.

CHAPTER 2

MEMBERSHIP FUNCTION PROPAGATION

This chapter is divided into two main parts. The first part, from section 2.1-2.4, reviews the state equations of a linear time invariant system and their solutions. The second introduces the concept of membership function propagation as an application of fuzzy set theory on the solutions to state equations. An inverted pendulum is chosen as an example physical system to demonstrate the introduced concepts through MATLAB simulations.

2.1 State equations and linear time-invariant (LTI) systems

The first step toward understanding a physical system, regardless of whether it is chemical, electrical or mechanical, is to formulate a mathematical model of a relationship between its input (externally supplied quantities) and the dependent quantities that result from the effect of those input. The modeling process starts with identifying the physical variables of interest, such as velocity, positions, voltage, and current. The physical variables are then described by physical laws and constitutive relationships so that the behavior of the system in question can be predicted at any given time.

Naturally, the governing equations resulting from describing the system through physical laws produces n^{th} order differential equations. These n^{th} order differential equations can be difficult to solve in a sense that sometimes, they are also coupled and must be solved simultaneously. An efficient way to reduce this complexity is to rewrite n^{th} order equations by a collection of n first-order differential equations, which are known as the *state equations*. The state equations collectively represent the same information as

the original n^{th} order differential equations but they are all first-order equations that are easier to solve.

The transformation from the original n^{th} order differential equations to the state equations sometimes entails creating new variables. These new variables are not unique and maybe chosen to facilitate formulation of state equations. These variables are called *state variables*. Strictly, the collection of state variables is known as the state of the system. The state equation and the knowledge of the states of the system at a given time together give complete description of the system and allow for prediction of future states.

Linear Time Invariant systems, as the name implies, have two characteristics that makes it the simplest type of systems to analyze: linearity and time invariance. Linearity consists of homogeneity and additivity. A homogeneous system is one for which any scalar multiple of the input yields a proportional output. An additive system is one for which output of the sum is the sum of each output. To formally define linearity, we let a be a constant, u_1 and u_2 be the inputs to the system. Consider the action of the system to be represented by the symbol R, the output of the system is represented by $R(\cdot)$. Homogeneity and additivity amounts to satisfying the following two equations respectively

$$R(au_1)=aR(u_1) \tag{II.1.1}$$

$$R(u_1+u_2)=R(u_1)+R(u_2) \tag{II.1.2}$$

Time invariance refers to the fact that the system's output only depends on the difference between the current and initial time. That is, the actual time value is irrelevant as long as the difference between current and initial time are the same then the output of the system always remain the same.

The linear n^{th} order differential equations can be written in the matrix form as

$$\dot{X}(t) = AX(t) + Bu(t) \qquad \text{(II. 1.3)}$$

where $X \in \Re^n$, A $\in \Re^{nxn}$ is the state matrix, B $\in \Re^{nxm}$ is the input matrix, and $u \in \Re^m$ is the control signal. Similarly, the output of the system, which is a selection of the combination of the states and input, can be written as

$$Y(t) = CX(t) + Du(t) \qquad \text{(II.1.4)}$$

where $Y \in \Re^p$ is the output vector, C $\in \Re^{pxn}$ output matrix and D $\in \Re^{pxm}$ is the feedthrough matrix.

Together, (II.1.3) and (II.1.4) is the state equations of a linear time-invariant system. If the governing equations are time variant, the matrices in the state equations are simply written as a function of time i.e. *A(t),B(t),C(t),* and *D(t)*.

2.2 Equation of motion for the inverted pendulum

Consider an inverted pendulum shown in figure 2.1; the governing equations may be derived using the Lagrangian mechanic.

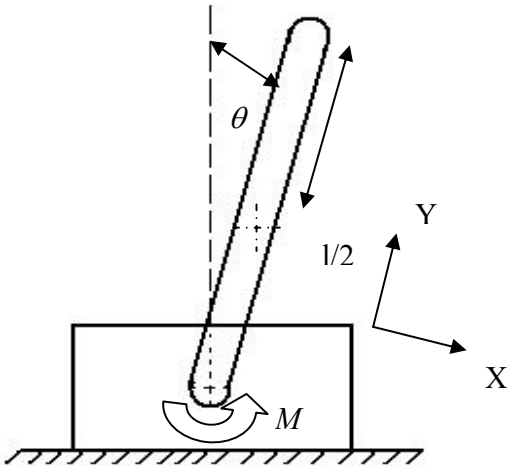

Figure 2.1: An inverted pendulum.

The Lagrangian mechanic is an alternative way of writing the equation of motions. In contrast to the Newtonian mechanic which uses Newton's second laws to derive the equation of motion, the Lagrangian mechanic based its principle on the system's mechanical energy (kinetic and potential). Therefore, it is convenient to define the Lagrangian function to be the difference between the system's kinetic energy (T) and the potential energy (V).

$$L = T - V \tag{II.2.1}$$

For each generalized coordinate, j, the Lagrangian equations which are differential equations of the following form can be written:

$$\frac{d}{dt}\left(\frac{\partial L}{\partial \dot{q}_j}\right) - \frac{\partial L}{\partial q_j} = Q_j \tag{II.2.2a}$$

by substituting (II.2.1)

$$\frac{d}{dt}\left(\frac{\partial T}{\partial \dot{q}_j}\right) - \frac{\partial T}{\partial q_j} + \frac{\partial V}{\partial q_j} = Q_j \qquad \text{j} = 1,2,3,..., \text{m} \tag{II.2.2b}$$

where q_j is generalized coordinate, $\dot{q}_j$ is the generalized velocity and Q_j is the generalized force. Notice that the potential energy is independent of the generalized velocity and therefore it is dropped out of the first term (II.2.2b).

Since we are concerned about the position of the pendulum, the obvious choice for the generalized coordinate is the only angle, hence $q=\theta$. However, the process is not as simple when it comes to determining the generalized force. To maintain the same level of explanation consistency, we return to the basic definition of generalized force.

Generalized force is derived from the concept of virtual work. The virtual work of a system is the amount of work done if a particle in the system is given a virtual (infinitesimal) displacement δr. The virtual work may be evaluated by taking the dot product between the virtual displacement δr and each individual force $\sum_i F$ in the system. For the system of *m* generalized coordinate, it can be shown that the virtual displacement is

$$\delta r = \sum_{j=1}^{m} \frac{\partial r}{\partial q_j} \delta q_j \tag{II.2.3}$$

The virtual work becomes

$$\delta W = \left(\sum_i F \right) \cdot \delta r = \sum_{j=1}^{m} \left(\sum_i F_i \cdot \frac{\partial r}{\partial q_j} \right) \delta q_j \tag{II.2.4}$$

First, we must note that friction at the pivot point is assumed negligible in this problem. A generalized force is defined as the coefficient of the corresponding increment δq_i in the expression for virtual work [5]. From (II.2.4) and the definition of generalized force Q_j, it can be shown that

$$\delta W = \sum_{j=1}^{m} Q_j \delta q_j \tag{II.2.5}$$

In other words, the generalized forces are the force components in the respective directions of the generalized coordinate. This means, when the generalized coordinate q_j is an angle of rotation, Q_j is the moment [5]. In our case, the control torque, *M* are being applied at the pivot, hence the virtual work of the system can be derived as the amount of work done if the angle θ is given a virtual displacement, $\delta\theta$ by the torque *M*.

$$\delta W = \sum_{j=1}^{m} Q_j \delta q_j$$
$$\delta W = M\delta\theta \qquad \text{(II.2.6)}$$
$$Q = M$$

Since this is pure rotation, the kinetic energy only contains the rotational energy term:

$$T = \frac{1}{2} I \dot{\theta}^2 \qquad \text{(II.2.7)}$$

where I is the pendulum's inertia with respect to the pivot. Refer to figure 2.1, since our chosen reference frame XYZ (with Z pointing out from the page) is the principle axes, which means that the coordinate axes form a plane of symmetry for the pendulum, the product of inertia I_{xy}, I_{yz} and I_{xz} are zero. In addition, since the only angle θ, rotates around the Z axes, the only relevant inertia term is I_{zz}. Since the pivot is not the center of mass, the inertia with respect to the pivot is derived from the parallel axis theorems, which states that

$$I'_{xx} = I_{xx} + m(Y^2{}_o + Z^2{}_o)$$
$$I'_{zz} = I_{zz} + m(X^2{}_o + Y^2{}_o) \qquad \text{(II.2.8)}$$
$$I'_{yy} = I_{yy} + m(X^2{}_o + Z^2{}_o)$$

where I'_{pp} is the new moment of inertia at pivot in the P axes, I_{pp} is the inertia in P axes at the center of mass, m is the mass, X_o, Y_o and Z_o are the translated distance in their respective directions. In this case, Y_o is the only shifted distance which is $\frac{l}{2}$.

$$I = I'_{zz} = \frac{1}{12} ml^2 + m(0^2 + \left(\frac{l}{2}\right)^2) = \frac{1}{3} ml^2 \qquad \text{(II.2.9)}$$

The next step is to calculate the potential energy. The center of gravity is placed at half length, therefore.

$$V = mg\frac{l}{2}\cos\theta \tag{II.2.10}$$

The partial derivatives are

$$\begin{aligned}
\frac{\partial T}{\partial \dot{\theta}} &= I\dot{\theta} \\
\frac{d}{dt}\left(\frac{\partial T}{\partial \dot{\theta}}\right) &= I\ddot{\theta} \\
\frac{\partial T}{\partial \theta} &= 0 \\
\frac{\partial V}{\partial \theta} &= -mg\ \frac{l}{2}\sin\ \theta
\end{aligned} \tag{II.2.11}$$

Lastly, the Lagrangian equations can be formed by substituting (II.2.7) to yield

$$I\ddot{\theta} - mg\frac{l}{2}\sin\theta = M \tag{II.2.12}$$

which can be simplified to give

$$\ddot{\theta} - 3g\frac{l}{2}\sin\theta = \frac{M}{I} \tag{II.2.13}$$

2.3 Linearization of the equation of motion

Note that although (II.2.13) is time invariant, it is not linear. The non-linear term, namely $3g\frac{l}{2}\sin\theta$, can be linearized by applying the Taylor series expansion for the general function *f(x)*.

$$f(x) \approx f(x_0) + \frac{\partial f(x)}{\partial x}|_{x_o}\left(x - x_0\right) \tag{II.3.1}$$

Next, the operating point x_0 is selected. One must be careful to choose x_0 such that $f(x_0)$ is zero, otherwise the condition for homogeneity and additivity may be violated. In this case, it is $x_0 = 0$ gives $3g\frac{l}{2}\sin(0) = 0$ and $3g\frac{l}{2}\sin\theta$ becomes

$$\begin{aligned} 3g\frac{l}{2}\sin\theta &\approx 3g\frac{l}{2}\sin(0) + 3g\frac{l}{2}\cos(0)(\theta - 0) \\ &= 3g\frac{l}{2}(\theta) \end{aligned} \tag{II.3.2}$$

Hence, the linearized equation of motion is

$$\ddot{\theta} - 3g\frac{l}{2}\theta = \frac{M}{I} \tag{II.3.3}$$

2.4 Solution to the state equations.

Recall the state equations (II.1.3) and (II.1.4). The effort in solving these equations mainly focuses on (II.1.3) since it is a system of differential equations. Once the solution $X(t)$ is obtained, it becomes a simple matter to determine $Y(t)$.

An integrating factor can be used to solve (II.1.3) as follows:

$$\begin{aligned} e^{-At}[\dot{X}(t) &= AX(t) + Bu(t)] \\ e^{-At}\dot{X}(t) - e^{-At}AX(t) &= e^{-At}Bu(t) \\ \frac{d}{dt}\left[e^{-At}X(t)\right] &= e^{-At}Bu(t) \end{aligned} \tag{II.4.1}$$

integrating both sides over a dummy variable τ from t_0 to t and rearrange to yield

$$\begin{aligned} e^{-At}X(t) - e^{-At_0}X(t_0) &= \int_{t0}^{t} e^{-A\tau}Bu(\tau)d\tau \\ X(t) &= e^{At}e^{-At_0}X(t_0) + \int_{t0}^{t} e^{At}e^{-A\tau}Bu(\tau)d\tau \end{aligned}$$

or

$$X(t) = e^{A(t-t_0)}X(t_0) + \int_{t0}^{t} e^{A(t-\tau)}Bu(\tau)d\tau \qquad \text{(II.4.2)}$$

The above expression gives a complete trajectory of the states *X(t)* given a known state and input matrix, A and B. The reciprocal of the integrating factor, namely, the matrix exponential e^{At} is also known as the state transition matrix.

In the case of the inverted pendulum, the state variables X_1 and X_2 are chosen to be the angle θ and the angular velocity $\dot{\theta}$ respectively. The linearized equation of motion can be written in the state space representation as follows

$$\begin{aligned} X_1 &= \theta \\ X_2 &= \dot{\theta} \\ \dot{X} &= \begin{bmatrix} 0 & 1 \\ -\frac{3g}{2l} & 0 \end{bmatrix} X + \begin{bmatrix} 0 \\ \frac{3}{ml^2} \end{bmatrix} M \\ Y &= \begin{bmatrix} 1 & 0 \end{bmatrix} X \end{aligned} \qquad \text{(II.4.3)}$$

with $A = \begin{bmatrix} 0 & 1 \\ -\frac{3g}{2l} & 0 \end{bmatrix}$, $B = \begin{bmatrix} 0 \\ \frac{3}{ml^2} \end{bmatrix}$, $C = \begin{bmatrix} 1 & 0 \end{bmatrix}$, and $D = 0$. Hence, equation (II.4.2) can be used to calculate the states and output at any time *t*, given a set of initial conditions.

2.5 Extension of the solution to the state equations to membership function.

The generalized solution presented in the last section has one intrinsic requirement: the precise and accurate knowledge of the input. This requirement is often impractical in the real world due to what L.A Zadeh refers to as *the principle of incompatibility* [15]. Basically, it states that high precision comes with high cost. To see how, consider a dart game: a trivial challenge would be to land two darts on the same segment of the board from a specified distance. Usually, this does not take very long for even an amateur player to accomplish. However, if a player was asked to land a second dart within 1 centimeter radius of the first, the player would go through many attempts.

In fact, most people would give up after a short while depending on each individual's determination. The point is that the cost (the time it takes to accomplish a task) increases as the demanded precision of that task increases.

This principle holds true for other systems besides a dart player. The complexity and cost for developing a precise system, say aligning a high-precision optical measurement device, increases in an exponential manner. On the other hand, the pay-off from that increased complexity saturates after a certain point. At that point, the small incremental pay-off becomes unworthy of the added effort and complexity. This is analogous to an economic principle of *diminishing returns* which states that there is a point beyond which the application of additional resources yields less than proportional increases in return.

For many dynamical systems, the precise knowledge of the input can be costly while the exact knowledge of the output may not be necessary. However, an input $X(t_0)$ must still be given to an algorithm to approximate the possible values of the final states and output, $X(t)$ and $Y(t)$. Clearly, a random guess producing a single value for an initial condition is unacceptable. Thus, this is where applications of fuzzy theory become greatly beneficial. Each possible value of the initial conditions along with its degree of possibility is represented by a set of membership functions. These membership functions, instead of a set of single values, are considered as input into the system. Consistently, the outputs of the system remain in the membership function form and they are produced by a process called *membership functions propagation*, which is an extension of the solution to the state equations to the membership functions.

Briefly, the membership functions propagation process decomposes the initial membership function into discrete intervals. For a linear system, equation (II.4.2) is applied to each interval to generate a snapshot of the membership functions at each instant. Thus, one can form a propagation history of the membership functions from compiling all the computed snapshots from initial to final time. The propagation history also reflects the nature of the system's uncertainty as the shape and size of each snapshot varies.

Perhaps the greatest benefit of the membership functions propagation process is presented on the flipped side. It provides a definite answer regarding what ranges of outputs are possible from a set of uncertain input. That is, for a given system, not just any amount of output deviation can be the result of the initial uncertainty. Instead, for a certain amount of initial uncertainty, there is a specified set of possible output values. This is useful in investigating such claims as "due to uncertainties in the input, the experimental result deviates by 3 radians". Of course, the ranges of possible outputs depend on the size of the initial membership function, the beginning uncertainties. Nevertheless, those values with zero final membership grade are impossible thereby, this resolve any doubt that the output might fall outside the specified range as a result of uncertainty in the input.

For an introductory purpose, consider the n^{th}-order linear state equation with no external input ($u(t)$=0).

$$\dot{X}(t) = A(t)X(t) \quad , \quad X(t_0) = X_0 \tag{II.5.1}$$

where $A(t)$ is a $n \times n$ real time-varying matrices. The solution to the above can be derived from equation (II.4.2) by truncating the input term, which reduces the solution to

$$X(t) = \phi(t, t_0) X_0 \qquad \text{(II.5.2)}$$

where the matrix exponential $e^{A(t-t0)}$ is denoted here as $\phi(t, t_0)$. Note that in the absence of input, the state transition matrix solely governs the motion of the state vector in the time interval (t_0, t).

Defining a_{ij} to be an element in the i^{th} row and j^{th} column of the state transition matrix,

$$\phi(t, t_0) = \begin{bmatrix} a_{11} & . & . & a_{1n} \\ . & . & . & . \\ . & . & . & . \\ a_{n1} & . & . & a_{nn} \end{bmatrix}$$

an equivalent representation of (II.5.2) is as follows

$$X(t) = \phi(t, t_0) X_0 = \begin{bmatrix} a_{11}X_1(0) + a_{12}X_2(0) + \ldots\ldots\ldots\ldots + a_{1n}X_n(0) \\ . \\ . \\ a_{n1}X_1(0) + a_{n2}X_2(0) + \ldots\ldots\ldots\ldots + a_{nn}X_n(0) \end{bmatrix}$$

or

$$X_i\ (t) = \sum_{j=1}^{n} a_{ij}(t) X_j\ (0) \quad \text{for } i = 1,..n \qquad \text{(II.5.3)}$$

In the other words, $X_i\ (t)$ is a weighted sum of all $X_j\ (0)$ having a_{ij} as their associated weight.

Definition 2.1 Consider a dynamical system described by (II.5.1), with known initial state information described by fuzzy sets $X(0)=[X_1(0),\ldots.,X_n(0)]^T$. Assuming convex fuzzy sets, for any $\alpha \in [0, 1]$ an α-cut representation of X_i can be expressed as

$$X_i^{\alpha} = [\underline{X}_i^{\alpha}, \overline{X}_i^{\alpha}] \quad \text{for all } i = 1,...n \tag{II.5.4}$$

where $\underline{X}_i^{\alpha}$ and $\overline{X}_i^{\alpha}$ are, respectively, the minimum (lower cut) and the maximum (upper cut) of all X that belongs to X^{α}.

The first step is to transform each membership functions into the α−cuts representation as shown above, having a lower and upper cut. Assuming that the state transition matrix $\phi(t, t_0)$ is well defined for the time interval [t_0, t], both the lower and upper cuts of X_i at time t can be computed by treating the original cuts ($X_1(0)^{\alpha}$)as crisp points and apply (II.5.3) directly. The computation is as follow

$$\underline{X}_1^{\alpha}(t) = a_{11}\underline{X}_1^{\alpha}(0) + a_{12}\underline{X}_2^{\alpha}(0) + ... + a_{1n}X_n^{\alpha}(0)$$

$$\overline{X}_1^{\alpha}(t) = a_{11}\overline{X}_1^{\alpha}(0) + a_{12}\overline{X}_2^{\alpha}(0) + ... + a_{1n}\overline{X}_n^{\alpha}(0)$$

and

$$\underline{X}_2^{\alpha}(t) = a_{21}\underline{X}_1^{\alpha}(0) + a_{22}\underline{X}_2^{\alpha}(0) + ... + a_{2n}\underline{X}_n^{\alpha}(0)$$

$$\overline{X}_2^{\alpha}(t) = a_{21}\overline{X}_1^{\alpha}(0) + a_{22}\overline{X}_2^{\alpha}(0) + ... + a_{2n}\overline{X}_n^{\alpha}(0)$$

or

$$\underline{X}_i^{\alpha}(t) = \sum_{j=1}^{n} a_{ij}(t)\underline{X}_j^{\alpha}(0) \quad \text{for } i = 1,..n$$

$$\overline{X}_i^{\alpha}(t) = \sum_{j=1}^{n} a_{ij}(t)\overline{X}_i^{\alpha}(0) \quad \text{for } i = 1,..n \tag{II.5.5.a}$$

In other words, each α-cut of X_i at time t is a linear combination of the α-cuts of X_i at time $t = t_0$ in the same manner as (II.5.3). For each cut, the linear combination is applied twice for both the upper cut and the lower cut. This allows us to obtain all

necessary information of the α-cuts of $X_i(t)$ from known initial membership function. All that is left at this point is to invoke the decomposition theorem, which allows the construction of the membership function at time *t* from the α-cuts.

The process just described is the *Membership Functions Propagation (MFP)*. Equation (II.5.5) allows the α-cuts to be computed when there is no input. When the input is not zero, one simply computes the integral term $\int_{t0}^{t} e^{A(t-\tau)} Bu(\tau) d\tau$ at the specified time as normal. The term is simply added on to each α-cut as it is a constant and therefore requires no set operation, as shown in (II.5.5.b).

$$\underline{X}_i^{\alpha}(t) = \sum_{j=1}^{n} a_{ij}(t)\underline{X}_j^{\alpha}(0) + \int_{t0}^{t} e^{A(t-\tau)} Bu(\tau) d\tau \quad \text{for } i = 1,..n$$

$$\overline{X}_i^{\alpha}(t) = \sum_{j=1}^{n} a_{ij}(t)\overline{X}_i^{\alpha}(0) + \int_{t0}^{t} e^{A(t-\tau)} Bu(\tau) d\tau \quad \text{for } i = 1,..n \quad \text{(II.5.5.b)}$$

2.6 Sample calculations.

An example calculation of the membership function propagation process is shown below. For the demonstrative purpose, simple triangular shape membership functions are selected for both X_1 and X_2 as shown in figure 2.2. The MATLAB program that is used to perform the computation can be founded in appendix A (NTEST12 and NT2).

The state transition matrix can be computed from the known *A* matrix (II.4.3) as

$$\phi(t, t_0) = \begin{bmatrix} \cosh(\omega \cdot t) & a \cdot \sinh(\omega \cdot t) \\ -b \cdot \sinh(\omega \cdot t) & \cosh(\omega \cdot t) \end{bmatrix} \qquad \text{(II.6.1)}$$

where the constant a is 0.82, b is 1.21 and with the angular frequency, ω of 1.21 radian per second.

Figure 2.2 below shows the initial membership functions for X_1 and X_2 both center at 3 radian and radian per second respectively.

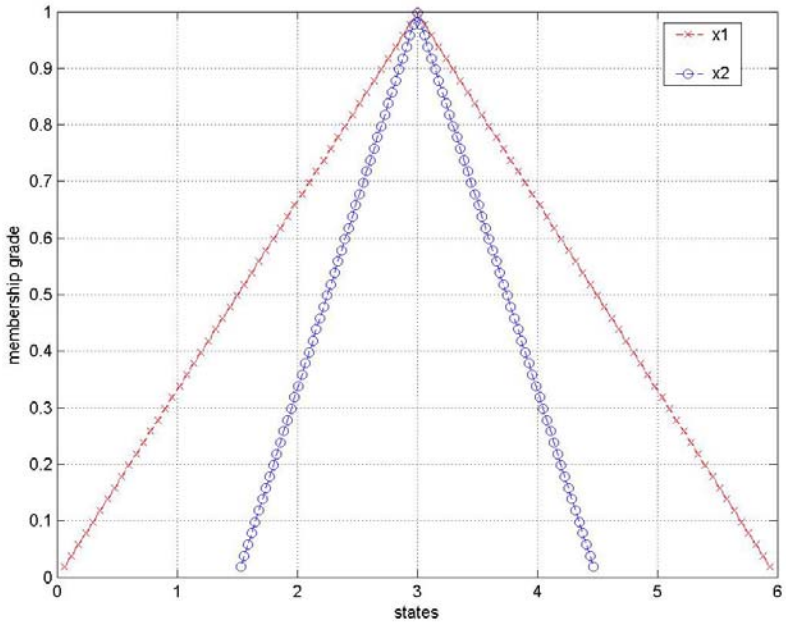

Figure 2.2: Initial membership functions.

From the figure above, the alpha cut of $X_1(0)$ can be easily obtained as shown below.

Table 2.1 α cut of $X_1(0)$

α cut X_{10}	$\underline{X}_1^{\alpha}(0)$	$\overline{X}_1^{\alpha}(0)$
0.2	0.66	5.34
0.4	1.26	4.74
0.6	1.86	4.14
0.8	2.46	3.54
1	3.00	3.00

Similarly, the alpha cut of $X_2(0)$ is

Table 2.2 α cut of $X_2(0)$

α cut X_{20}	$\underline{X}_2^{\alpha}(0)$	$\overline{X}_2^{\alpha}(0)$
0.2	1.83	4.17
0.4	2.13	3.87
0.6	2.43	3.57
0.8	2.73	3.27
1	3.00	3.00

Now, let $\underline{X}_i^{\alpha}(t)$ and $\overline{X}_i^{\alpha}(t)$ denotes the lower and upper limit of the propagated alpha cut, which can be calculated according to the equations (II.5.5).

Applying the equation:

$$\underline{X}_1^{0.2}(t) = \cosh(\omega \cdot \mathrm{t}) \cdot 0.66 + \mathrm{a} \cdot \sinh(\omega \cdot \mathrm{t}) \cdot 1.83$$

$$\overline{X}_1^{0.2}(t) = \cosh(\omega \cdot \mathrm{t}) \cdot 5.34 + \mathrm{a} \cdot \sinh(\omega \cdot \mathrm{t}) \cdot 4.17$$

And

$$\underline{X}_2^{0.2}(t) = \mathrm{b} \cdot \sinh(\omega \cdot \mathrm{t}) \cdot 0.66 + \cosh(\omega \cdot \mathrm{t}) \cdot 1.83$$

$$\overline{X}_2^{0.2}(t) = \mathrm{b} \cdot \sinh(\omega \cdot \mathrm{t}) \cdot 5.34 + \cosh(\omega \cdot \mathrm{t}) \cdot 4.17 \qquad \text{(II.6.2)}$$

The above process is repeated for all α-cuts. Choosing time to equal 1 second gives

Table II.3 Propagated cuts at 1 second.

α cut X_{10}	$\underline{X}_1^{\alpha}(t)$	$\overline{X}_1^{\alpha}(t)$
0.2	1.6	5.1
0.4	2.1	4.7
0.6	2.5	4.2
0.8	3.0	3.8
1	3.4	3.4

Now representing the membership function in as a list:

$$A^{\alpha} = 1/x_1 + 1/x_2 + 1/x_3 + 1/x_4 \ldots$$

As a reminder, the first number before the symbol "/" is a membership value. In this case it is either 1 or 0. 1 means that the element behind the dash symbol is included, belongs to the A^{α} subset with full membership. 0 means the opposite.

$$X_1^{0.2} = 1/1.6+1/2.1+1/2.5+1/3.0+1/3.4+1/3.8+1/4.2+1/4.7+1/5.1$$

$$X_1^{0.4} = 0/1.6+1/2.1+1/2.5+1/3.0+1/3.4+1/3.8+1/4.2+1/4.7+0/5.1$$

$$X_1^{0.6} = 0/1.6+0/2.1+1/2.5+1/3.0+1/3.4+1/3.8+1/4.2+0/4.7+0/5.1$$

$$X_1^{0.8}=0/1.6+0/2.1+0/2.5+1/3.0+1/3.4+1/3.8+0/4.2+0/4.7+0/5.1$$

$$X_1^{1}=0/1.6+0/2.1+0/2.5+0/3.0+1/3.4+0/3.8+0/4.2+0/4.7+0/5.1$$

Referring to Chapter 1, ${}_{\alpha}A(x)$ is a special set that can be formed by taking the multiplying the value of the alpha cut to the α-cuts subset. In terms of the representation above, the alpha value is multiplied to the number in front of the dash symbol only.

$${}_{\alpha}A(x)=\alpha\, A(x)^{\alpha}$$

$${}_{0.2}X_1=0.2/1.6+0.2/2.1+0.2/2.5+1/3.0+0.2/3.4+0.2/3.8+0.2/4.2+1/4.7+0.2/5.1$$

$${}_{0.4}X1=0.4/2.1+0.4/2.5+0.4/3.0+0.4/3.4+0.4/3.8+0.4/4.2+0.4/4.7$$

$${}_{0.6}X_1=0.6/2.5+0.6/3.0+0.6/3.4+0.6/3.8+0.6/4.2$$

$${}_{0.8}X1=0.8/3.0+0.8/3.4+0.8/3.8$$

$${}_{1}X_1=1/3.4$$

And finally, taking the standard fuzzy union completely constructs the fuzzy set according to the decomposition theorem. For the selected α-cuts:

$$\mathbf{A} = {}_{0.2}A \cup {}_{0.4}A \cup {}_{0.6}A \cup {}_{0.8}A \cup {}_{1}A$$

Hence,

$$X_1= 0.2/1.6+0.4/2.1+0.6/2.5+0.8/3.0+1/3.4+0.8/3.8+0.6/4.2+0.4/4.7+0.2/5.1$$

Finally, the figures below show the membership function propagation of X_1 and X_2.

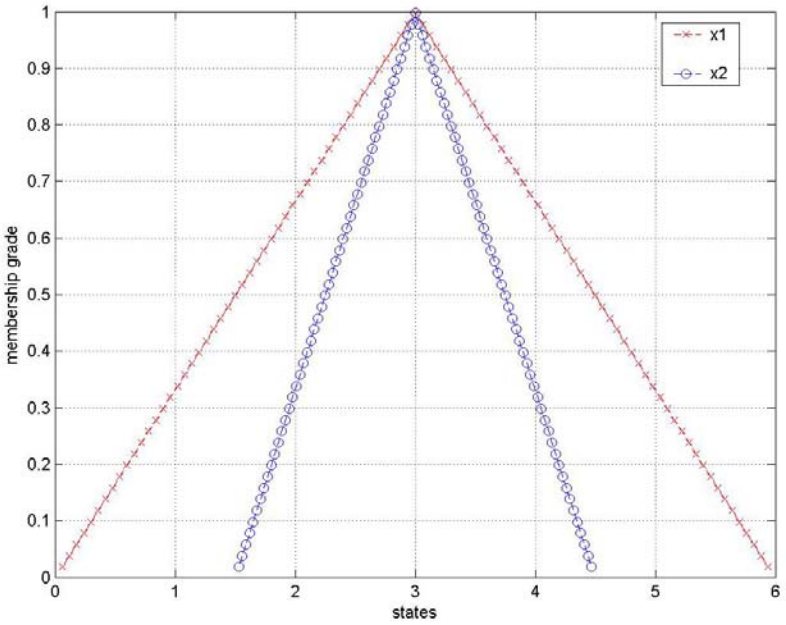

Figure 2.3(a) Membership functions at time t=0 second.

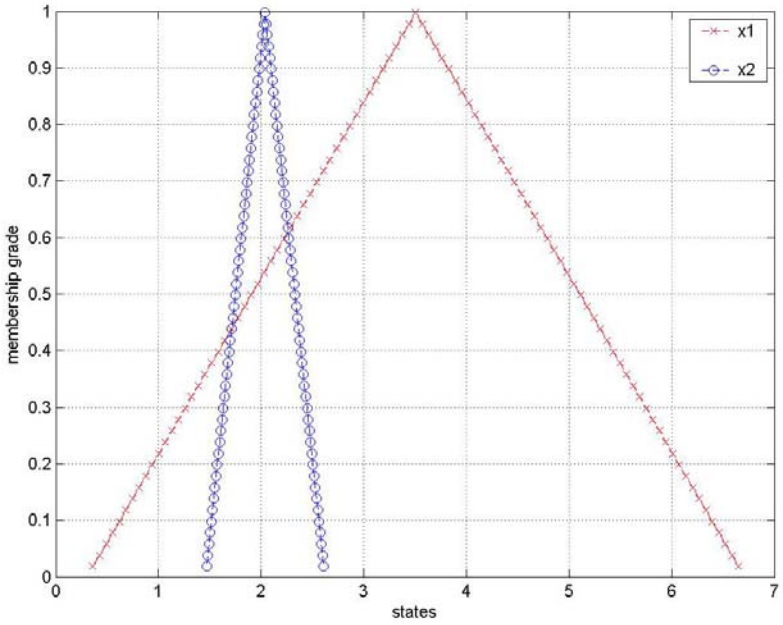

Figure 2.3(b) Membership function at time t=0.2 second

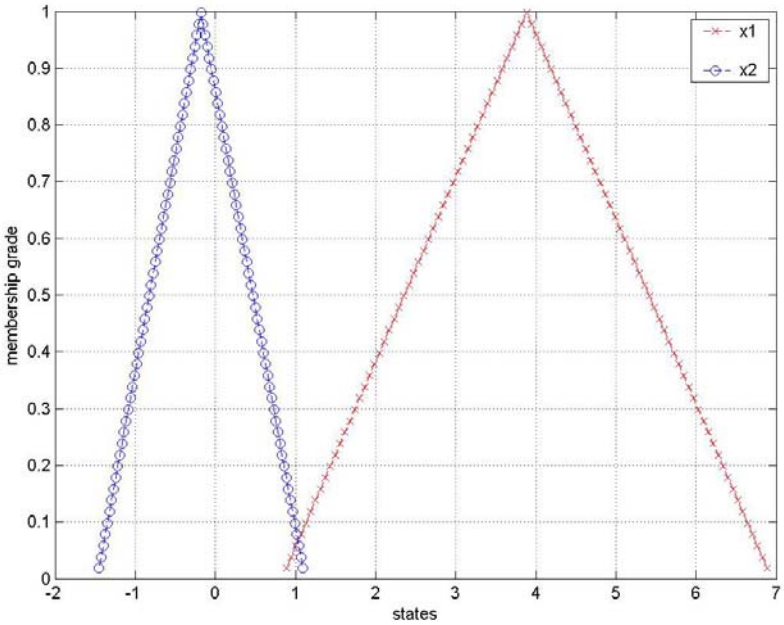

Figure 2.3(c) Membership function at time t=0.8 second

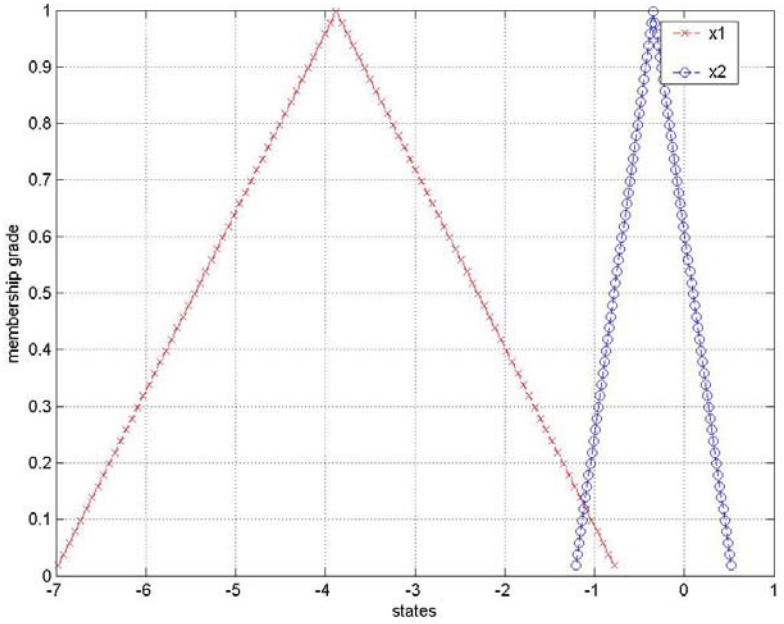

Figure 2.3(d) Membership function at time t=3 second

Notice that the shape of the membership functions emulates the behavior of the system. Especially, the width of the X_2 membership function reduces as the pendulum halt to change direction. The implication is: although the exact velocity of the pendulum is uncertain, it must be close to zero at this point in time. Hence the range of possible values also decreases to reflect this fact.

2.7 Pole placement by state feedback: A case study.

Pole placement problem arises as a test for the validity of the membership function propagation. For a controllable system, pole placement methods utilize a control law that stabilizes the system. The output can be driven to the origin from using a state feedback controller. The control law can be

$$u(t) = KX(t) + r \tag{II.7.1}$$

Substitution into the general state equations yield

$$\begin{aligned} \dot{X}(t) &= AX(t) + BKX(t) + Br \\ Y(t) &= CX(t) + DKX(t) + Dr \end{aligned} \tag{II.7.2}$$

or

$$\begin{aligned} \dot{X}(t) &= (A + BK)X(t) + Br = \bar{A}X(t) \\ Y(t) &= (C + DK)X(t) + Dr = \bar{C}X(t) \end{aligned} \tag{II.7.3}$$

where K a $1xn$ gain matrix, r is a reference input which is chosen to be zero in this case. For a linear time-invariant system, the stability only depends on the location of the eigenvalues (poles) of the system which is now determined by the new matrix $\bar{A}$. Since K can be freely chosen, its proper selection places the eigenvalues on the left-half plane. This ensures that the system output eventually stabilizes and approaches the origin.

Although the procedures for selecting a gain matrix are not in the scope of this work, MATLAB commands exist for such procedure. The MATLAB program that was used can be found in Appendix A (MPP and NT2).

Similar to the previous example of a freely rotated inverted pendulum, the shape of the membership function should reflect the behavior of the system. Intuitively, when all the states of the system are eventually forced to zero, there should be no uncertainty left. This implies that both membership functions must converge to a crisp point at the origin, independent of any factor.

The propagation history shown below attests to this fact. The inverted pendulum is simulated with the same control law mentioned above. The resulting gain matrix and system eigenvalues are shown below. Regardless of the shape of the initial membership function, both the triangular and trapezoidal membership functions converge to origin.

Table 2.4 Gain matrix and Eigenvalues.

Gain Matrix K	[1.00 83.33]
Eigenvalues	[-1 , -1.5]

The following figures show the propagation history of triangular membership functions for X_1 and X_2

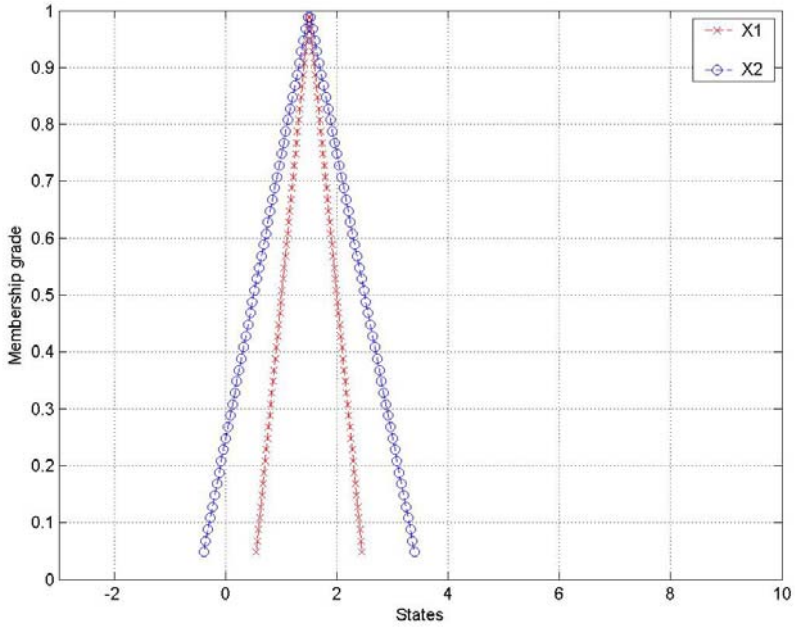

Figure 2.4(a) Membership functions at time t=0 second.

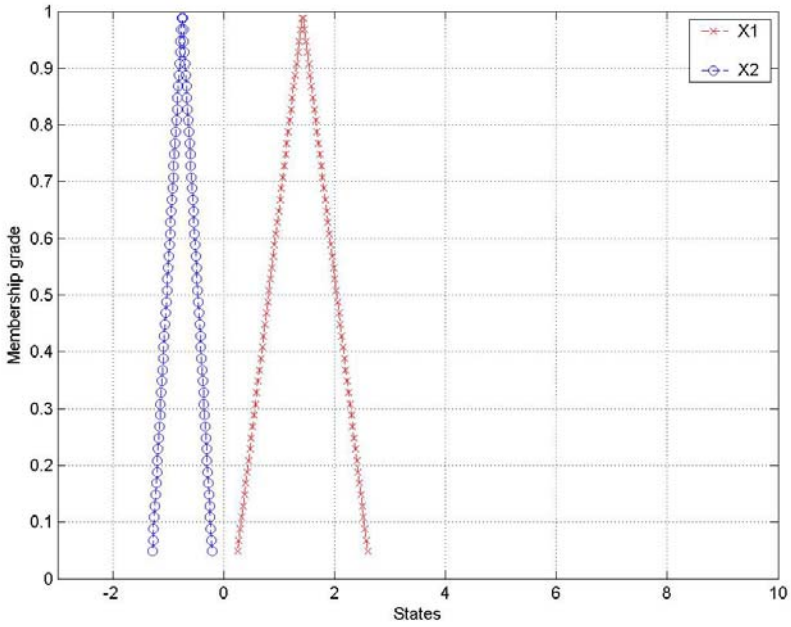

Figure 2.4(b) Membership functions at time t=1 second.

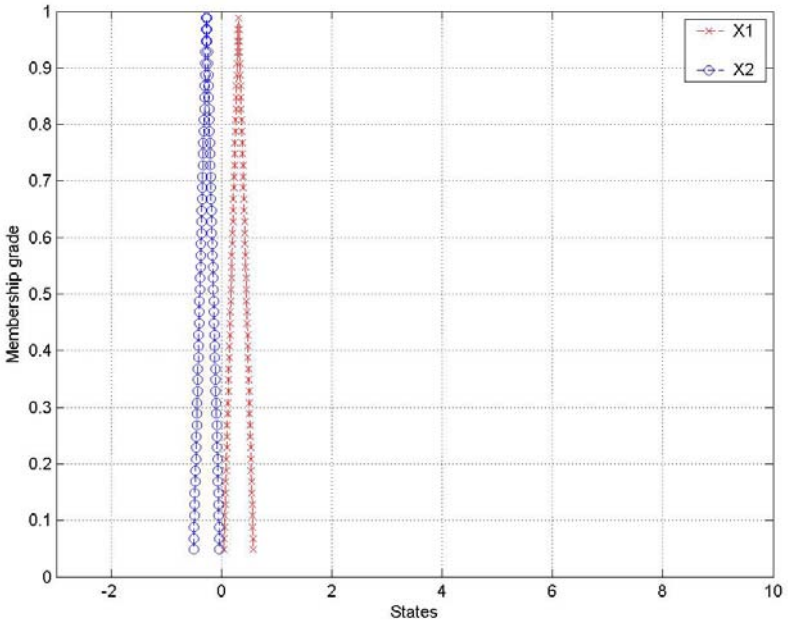

Figure 2.4(c) Membership functions at time t=3 second.

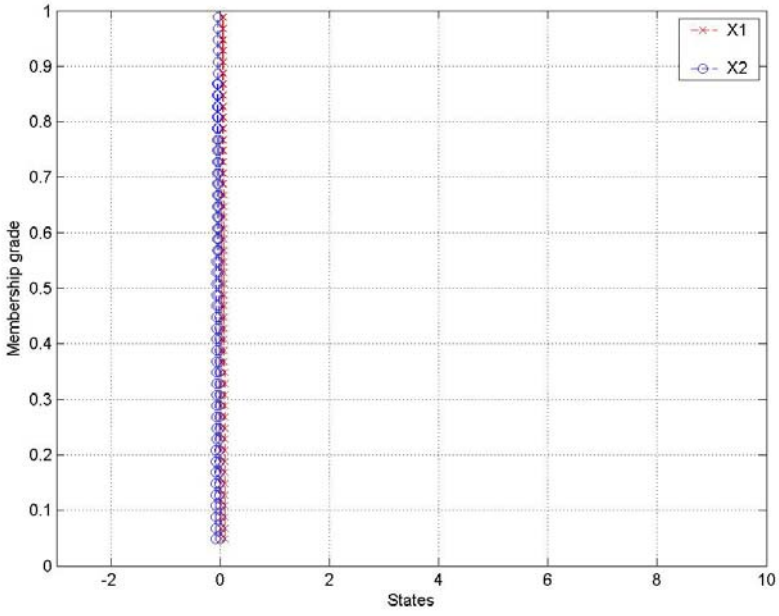

Figure 2.4(d) Membership functions at time t=5 second.

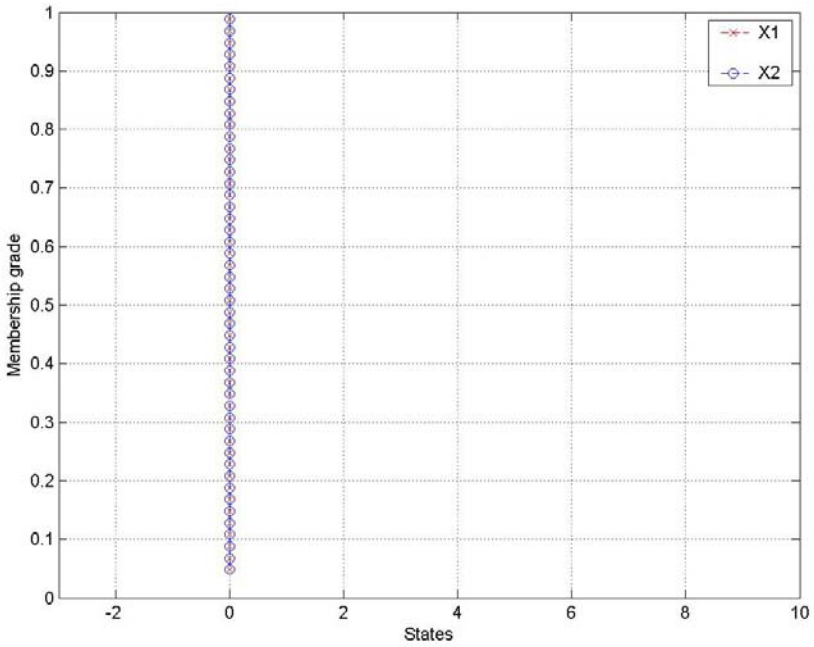

Figure 2.4(e) Membership functions at time t=10 second

The following figures show the propagation history of trapezoidal membership functions for X_1 and X_2

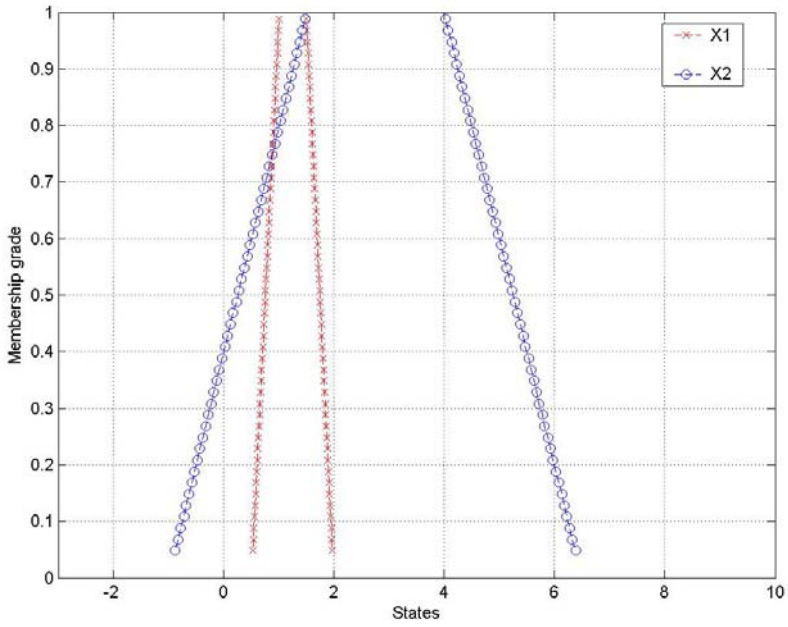

Figure 2.5(a) Membership functions at time t=0 second.

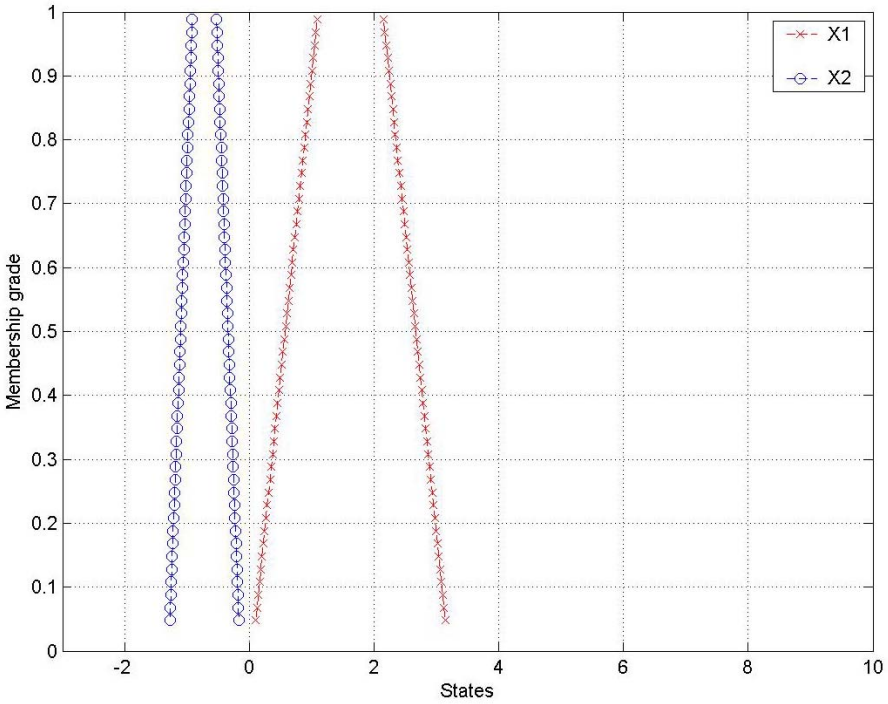

Figure 2.5(b) Membership functions at time t=1 second.

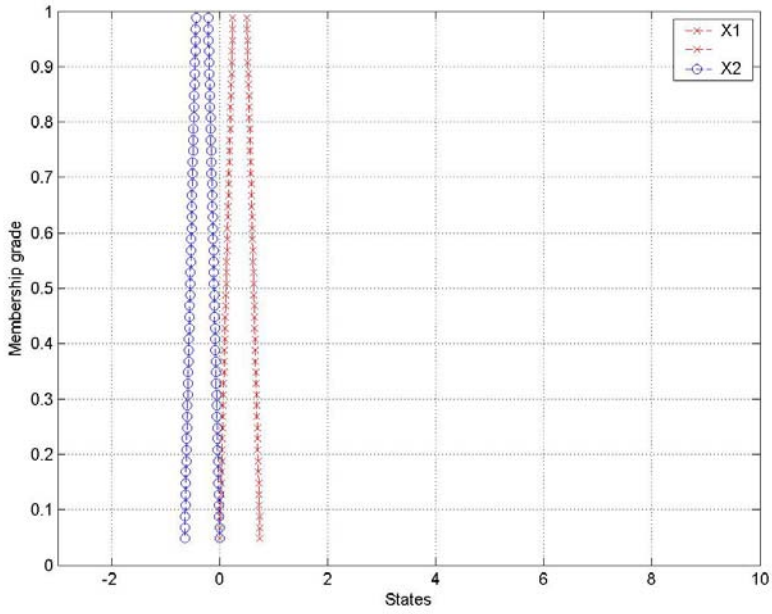

Figure 2.5(c) Membership functions at time t=3 second.

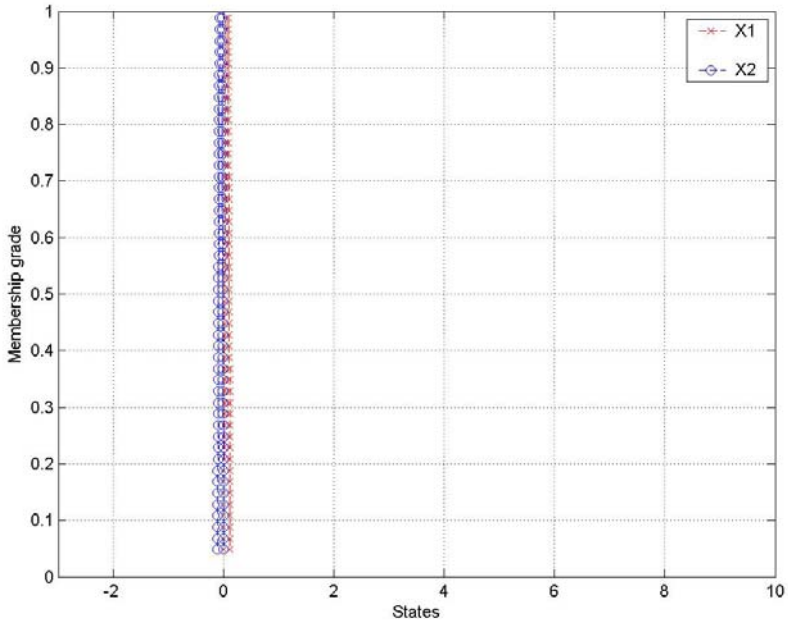

Figure 2.5(d) Membership functions at time t=5 second.

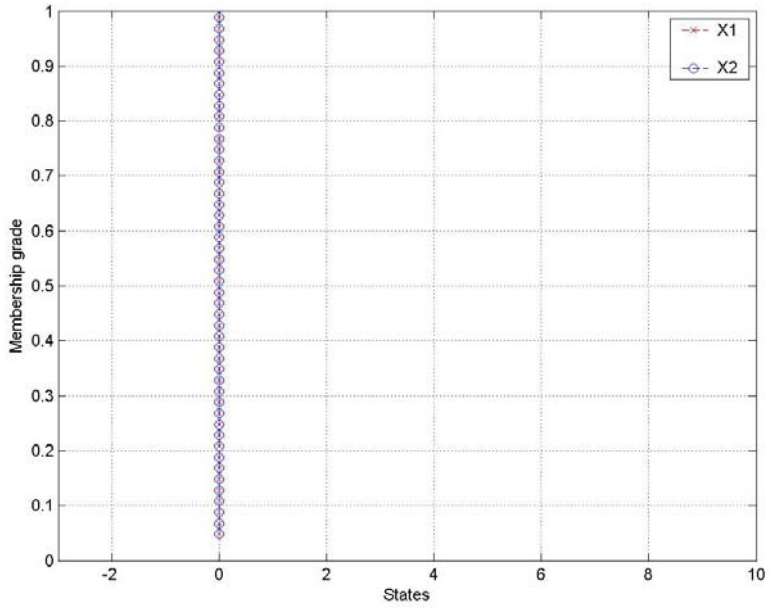

Figure 2.5(e) Membership functions at time t=10 second.

CHAPTER 3

CONTROLLABILITY AND OBSERVABILITY

Controllability and observability are the two basic concepts that arise in the control of dynamic systems. This chapter discusses the development of these two concepts in the fuzzy sense. Conditions under which these two concepts are valid under the new sense are proposed and as before, an inverted pendulum system is used as an example. Finally, various simulation results are presented as examples for both concepts and concerns regarding the completeness and validations of the proposed condition follow.

3.1 The general concept of controllability and observability.

Recall from Chapter 2 that the solution of the state equation (II. 1.3) is given by

$$X(t) = e^{A(t-t0)}X(t_0) + \int_{t_0}^{t} e^{A(t-\tau)}Bu(\tau)d\tau \qquad \text{(III.1.1)}$$

and the output is

$$Y(t) = C\left[e^{A(t-t0)}X(t_0) + \int_{t_0}^{t} e^{A(t-\tau)}Bu(\tau)d\tau\right] + Du(t) \qquad \text{(III.1.2)}$$

All these two equations provide is a computational formulation that gives the value of the states and the output at a specific time *t*. Hence, the only types of analysis that can be performed are specific inquiries about the state and output of the system which one must compute (III.1.1) and (III.1.2) to answer. As a result, no conclusion regarding the general property of the system can be made from these two equations alone.

Specifically, it is useful to answer the following two basic questions before any in depth analysis of the system can be performed.

(i) Is there a possible input signal that transfers the original states of the system to any desirable states in finite time?

(ii) Is it possible to determine the initial states from the output and input history over a finite time interval?

The answers to both questions are addressed by Kalman in the 1960's in what became known as the controllability and observability of the system respectively.

Controllability [1]: A dynamical system is controllable in an interval $[t_0, t_1]$ if there exists an input $u(t)$ that, when applied to the system from an initial state $X(t_0)$, transfers the system to the state $X(t_1)=0$. If this property holds regardless of the initial time t_0 or the initial state $X(t_0)$, the system is said to be completely controllable.

Basically, controllable systems are ones that can be manipulated as pleased. It implies that there is no inherent restriction in designing the control. On the other hand, uncontrollable system does not necessary mean that the system will never behave satisfactorily. The states can be divided into controllable and uncontrollable states, which mean that as long as the important variables are controllable, while the other uncontrollable states can be maintained within an acceptable region, the system is under control. Notice that controllability, as defined above, places no restrictions on what happen between time t_0 to t_1 or after t_1. That is, it does not require that the states stay at $X(t_{>}t_1)=0$.

Intuitively, since controllability is the coupling between the states and the input, one could guess whether a system is controllable or not by looking at the state equation

$$\dot{X}(t) = AX(t) + Bu(t) \qquad \text{(III.1.3)}$$

Frankly, if there is a link through which the input can affect the states, then the system is controllable. Otherwise, if the states behave independently of the input, then it can not be controlled. Therefore, the relationship between the states and the input is contained within the matrices pair A, which provides links between different states, and B, connects the states to the input.

Observability is the dual concept to controllability. From section 2.7, we see that to implement a control law such as

$$u(t) = KX(t) + r \tag{III.1.4}$$

the complete knowledge of the states *X(t)* is required. In practice, this may be too demanding as not all of the states are accessible to measurement. Therefore, an observer system must be built to calculate the inaccessible states from the output and input history, which are available.

The design of an observer system depends on the observability property of the original system. Observability is the coupling between the states and the output; hence the property is contained in the relationship between the matrices pair A and C.

Observability [1] : A dynamical system is observable in an interval $[t_0, t_1]$ if, for an initial state $X(t_0)$, knowing two functions *u(t)* and *Y(t)* over the same interval is sufficient information to uniquely solve for $X(t_0)$. If this property holds regardless of the initial time t_0 or the initial state $X(t_0)$, the system is said to be completely observable.

Note that the notion of observability depends solely on the capability to make measurement, i.e. an unobservable system may become observable if more information is available through improved measurements, etc. Hence, uncertainty plays a major role here which also links observability to the membership function propagation.

3.1.1 Tests and conditions for controllability and observability.

The most popular method to test for both properties of the system is through the fundamental tests for controllability and observability, which is as follows.

Fundamental test for controllability: A n-dimensional continuous-time LTI system is completely controllable if and only if the matrix

$$CO = \left[B \; AB \; \Lambda \; A^{n-1} B \right] \tag{III.1.5}$$

has rank n.

Fundamental test for observability: A n-dimensional continuous-time LTI system is completely observable if and only if the matrix

$$OB = \begin{bmatrix} C \\ CA \\ \mathrm{M} \\ CA^{n-1} \end{bmatrix} \tag{III.1.6}$$

has rank n.

From fairly lengthy proofs that are omitted from this work, both tests amount to the following conditions:

1. The rows of $e^{At}B$ are linearly independent for all t for complete controllability.

2. The controllability gramians, $W(t_0, t_1) = \int_{t0}^{t1} \phi(t_0, \tau) B(\tau) B^T(\tau) \phi^T(t_0, \tau) d\tau$ is invertible

for any t > 0.

3. The columns of Ce^{At} are linearly independent for all t for complete observability.

4. The observability gramians, $V(t_0, t_1) = \int_{t0}^{t1} \phi^T(t_0, \tau) C^T(\tau) C(\tau) \phi \; (t_0, \tau) d\tau$ is invertible

for any t > 0

3.2 Controllability in the fuzzy sense.

As seen from the last section, the essence of controllability is to transfer one set of initial states to another desired set. For a linear time invariant system, the sole requirement amounts to having linearly independent rows of the controllability matrix. This is no longer sufficient when regarding controllability in the fuzzy context, mainly because the crisp states are now replaced by membership functions. The effects are two folded. First, it no longer makes sense to talk about the desired sets as crisp states; they too, must be represented by membership functions. Such membership functions are termed *target membership functions* hereafter. Second, a new requirement for controllability must incorporate a relationship between the target and the original membership functions.

Perhaps the best way to arrive at the new requirement is through intuition. Consider an analogy of shooting a basketball; let the state variable be the distance of the ball from the basket. The initial state is the distance of the player making the shot, which can be described by a membership function "around the free throw line". From this uncertain information, it is not clear whether a random player could control his shot to land within a satisfactory region, which may be represented by a target membership functions "near the basket". It follows that if this particular player demonstrates consistent ability to land shots within this bound, then the membership function which represents the actual position of the shot landed is also contained within this bound. Hence, the player can reasonably claim that his shots can be controlled from "around the free throw line". On the other hand, if this is a novice player who seldom lands shots in the vicinity or if the acceptable region, the target membership function, is reduced to

"within a few inches around the basket", then the membership function representing the shots is not contained within the target membership function. The player can not make such claim in this case.

In the same manner, for all dynamical system, the shape and size of the membership function at time *t* reflects the bound of possible states. Surely, this is with respect to the behavior of that particular dynamical system: the inverted pendulum in section 2.6 swings indefinitely thus, the range of uncertainty changes corresponding to the shape of the membership functions. For the inverted pendulum with feedback system discussed in section 2.7, the states must converge to the origin after some time interval and the membership functions reflects this fact by their reduction to a crisp point.

With these facts in mind, it makes senses to say that if the membership function at time *t* can be contained within a prescribed target membership function, then the system is said to be controllable. Note that there is an additional freedom in this new definition for controllability: one could choose a prescribed target membership function to cover any range large or small. Thus, it is important to emphasize that this new definition of controllability always require an accompanying specific prescribed target membership function and the system is said to be controllable in the sense of that specific membership function only. There exists no such property as "generally controllable" for all prescribed membership functions.

To repeat, the basic requirement from the general concept of controllability applies here as well. The controls must be able to affect the different states independently as reflected in the ranks of the controllability matrix. The only difference is that the desired states now become the prescribed target membership function, which

must be large enough to sufficiently contain the membership functions of the states. Translate into formal language; the above idea is as follows.

Definition 3.1 Consider the following state equation

$$\dot{X} = f(X, u, t) \tag{III.2.1}$$

where X is the state, $u(t) \in \mathrm{R}^m$ is the control. Let $\mu_0(X_0 - \overline{X}_0)$ be a known membership function at time $t=t_0$ where $X_0, \overline{X}_0 \in \mathrm{R}^n$ are the states at t_0. Let $\mu^*_1(X(t_1) - \overline{X}_1)$ be the prescribed membership function where $\overline{X}_1$ to the set of states at time t_1, denoted X_1. For $X \in X_1$ The state equation (III.2.1) is said to be controllable in the context of $\mu^*_1(\cdot)$ if during the interval $[t_0, t_1]$ there exist an input $u[t_0, t_1]$ and a membership function $\hat{\mu}_1(\cdot)$ such that at time $t=t_1$ such that

$$\hat{\mu}_1(X - \overline{X}_1) \le \mu^*_1(X - \overline{X}_1) \tag{III.2.2}$$

The following figure demonstrates definition 3.1.

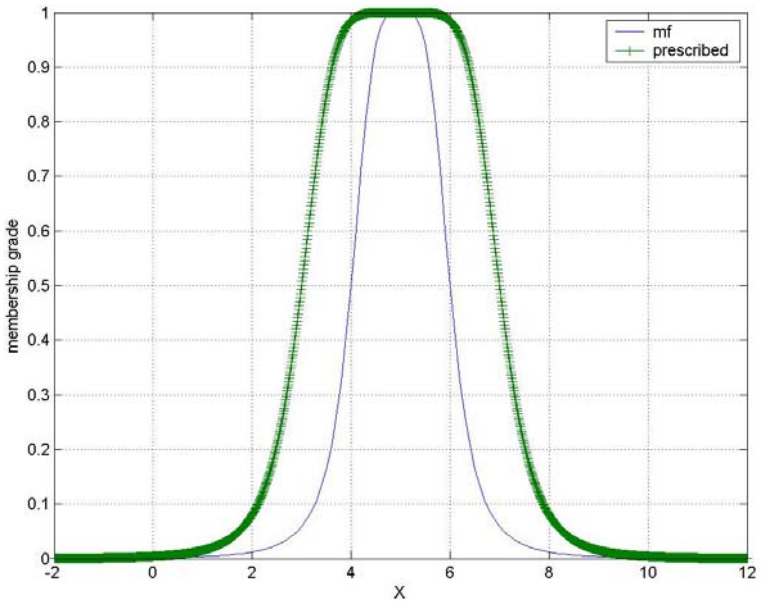

Figure 3.1 A prescribed target membership function that validates controllability.

For the linear system, existing control theory reduces definition 3.1 to the following.

Theorem 3.1 For a linear system, the state equation (III.2.1) can be expressed as

$$\dot{X}(t) = A(t)X(t) + B(t)u(t) \quad , \quad X(0) = X_0 \tag{III.2.3}$$

The state equation (III.2.3) is controllable in the sense of $\mu^*_1(\cdot)$ if and only if

(i) The rows of $\phi(t_0,\cdot)B(\cdot)$ are linearly independent on $[t_0,t_1]$.

(ii) $\exists \overline{X} \in X_1$ such that $\hat{\mu}_0(X - \overline{X}) \le \mu^*_1(X - \overline{X}_1)$, $\forall X, \overline{X}_1 \in X_1$.

The control can be

$$u(t) = -B^T(t)\phi^T(t_0,t)W^{-1}(t_0,t_1)[X_0 - \phi(t_0,t_1)\overline{X}_1] \tag{III.2.4}$$

where the controllability gramians remains unchanged, as it is independent of whether the states are represented by crisp points or membership functions.

$$W(t_0,t_1) = \int_{t0}^{t1} \phi^T(t_0,\tau)B(\tau)B^T(\tau)\phi^T(t_0,\tau)d\tau \tag{III.2.5}$$

The membership function at time *t* is calculated through the membership function propagation procedure discussed in the previous chapter. The forced response equation for each upper and lower cut is repeated here for convenience.

$$\overline{X}_i^{\alpha}(t) = \phi(t,0)\cdot\overline{X}_i^{\alpha}(0) + \int_0^t \phi(t,\tau)\cdot B\cdot u(\tau)d\tau$$

$$\underline{X}_i^{\alpha}(t) = \phi(t,0)\cdot\underline{X}_i^{\alpha}(0) + \int_0^t \phi(t,\tau)\cdot B\cdot u(\tau)d\tau \tag{III.2.6}$$

The proofs for theorem 3.1.(ii) starts by assuming convexity for both the prescribed target membership function $\mu^*_1(\cdot)$ and the propagated membership function $\hat{\mu}_0(\cdot)$.

Proof $\hat{\mu}_0(X-\overline{X}_1) \le \mu^*_1(X-\overline{X}_1)$ for $\forall X, \overline{X}_1 \in X_1$

Given $\exists \overline{X} \in X_1, \hat{\mu}_0(X-\overline{X}) \le \mu^*_1(X-\overline{X}_1)$

For convex fuzzy sets, it can be shown that [8]

$$\mu_1(\lambda X_a + (1-\lambda)X_b) \ge \min[\mu_1(X_a), \mu_1(X_b)] \qquad \text{(III.2.7)}$$

where $\lambda \in [0,1]$ and X_a and X_b are two points in the relevant universal set of which $\mu_1(\cdot)$ is defined. Apply (III.2.7) to $\hat{\mu}_0(\cdot)$ and consider $(X-\overline{X}_1)$ and $(X-\overline{X})$

$$\begin{aligned}
&\hat{\mu}_0(\lambda(X-\overline{X}_1)+(1-\lambda)(X-\overline{X})) \ge \min[\hat{\mu}_0(X-\overline{X}_1), \hat{\mu}_0(X-\overline{X})] \\
&\hat{\mu}_0(\lambda X-\lambda\overline{X}_1+X-\overline{X}-\lambda X+\lambda\overline{X}) \ge \min[\hat{\mu}_0(X-\overline{X}_1), \hat{\mu}_0(X-\overline{X})] \\
&\hat{\mu}_0(X-\overline{X}+\lambda(\overline{X}-\overline{X}_1)) \ge \min[\hat{\mu}_0(X-\overline{X}_1), \hat{\mu}_0(X-\overline{X})]
\end{aligned} \qquad \text{(III.2.8)}$$

pick λ=0

$$\hat{\mu}_0(X-\overline{X}) \ge \min[\hat{\mu}_0(X-\overline{X}_1), \hat{\mu}_0(X-\overline{X})] \qquad \text{(III.2.9)}$$

there are two cases:

A) when $\hat{\mu}_0(X-\overline{X}_1) > \hat{\mu}_0(X-\overline{X})$ then (III.2.9) becomes trivial

$$\hat{\mu}_0(X-\overline{X}) = \hat{\mu}_0(X-\overline{X}) \qquad \text{(III.2.10)}$$

B) when $\hat{\mu}_0(X-\overline{X}_1) \le \hat{\mu}_0(X-\overline{X})$ then (III.2.9) becomes

$$\hat{\mu}_0(X-\overline{X}) \ge \hat{\mu}_0(X-\overline{X}_1) \qquad \text{(III.2.11)}$$

From the given, we already have $\mu^*_1(X-\overline{X}_1) \ge \hat{\mu}_0(X-\overline{X})$. Therefore, from (III.2.11) it follows that $\mu^*_1(X-\overline{X}_1) \ge \hat{\mu}_0(X-\overline{X}) \ge \hat{\mu}_0(X-\overline{X}_1)$ and

$$\begin{aligned}
&\mu^*_1(X-\overline{X}_1) \ge \hat{\mu}_0(X-\overline{X}) \ge \hat{\mu}_0(X-\overline{X}_1) \\
&\mu^*_1(X-\overline{X}_1) \ge \hat{\mu}_0(X-\overline{X}_1)
\end{aligned} \qquad \text{(III.2.12)}$$

The definition of fuzzy subset is defined by the inequality given in (I.4.14), repeated here for convenience

$$B \subseteq A \Leftrightarrow \mu_B(x) \leq \mu_A(x) \qquad \forall x \in X \tag{I.4.14}$$

A comparison between (I.4.14) and theorem 3.1.(ii) reveals that the fuzzy sets A and *B* in (I.4.14) are analogous to the prescribed and propagated membership functions respectively. From (III.2.2) $\hat{\mu}_0(\cdot)$ becomes the propagated membership function at time $t=t_1$, or $\hat{\mu}_0(X-\overline{X})$. This membership function is simply required to be a subset of $\mu^*_1(X-\overline{X}_1)$ for the system to be controllable in the sense of $\mu^*_1(\cdot)$

In simple terms, the fuzzy subsethood requirement ensures that the uncertainty is bounded, and thus the behavior of the system can be controlled. This amounts to fitting one membership function inside another. The membership function propagation produces the membership function at time $t=t_1$. If this membership function is contained by some prescribed membership function that represents an acceptable region, then the system is said to be controllable in a sense of that prescribed target membership function.

3.2.1 Example of controllability.

The following subsection gives an example of controllable system in the new context. Recall the inverted pendulum from chapter 2, the linearized state equations are as follow

$$\begin{aligned} X_1 &= \theta \\ X_2 &= \dot{\theta} \\ \dot{X} &= \begin{bmatrix} 0 & 1 \\ -\frac{3g}{2l} & 0 \end{bmatrix} X + \begin{bmatrix} 0 \\ \frac{3}{ml^2} \end{bmatrix} M \end{aligned} \tag{III.2.13}$$

Suppose, the states are to be driven to the following desired location at $X_1 = 5$ radian and $X_2 = 10$ radian per second from a set of uncertain initial conditions represented by membership functions "near stationary". The task is completed at the final time 1 second.

From section 3.1.2, the first requirement of theorem 3.1 is equivalent to having n=2 linearly independent columns of the controllability matrix. The controllability matrix is computed as

$$\begin{aligned} CO &= \left[B \quad AB \quad \Lambda \quad A^{n-1}B \right] \\ AB &= \begin{bmatrix} \frac{3}{ml^2} \\ 0 \end{bmatrix} \\ CO &= \begin{bmatrix} 0 & \frac{3}{ml^2} \\ \frac{3}{ml^2} & 0 \end{bmatrix} \end{aligned} \qquad \text{(III.2.14)}$$

The rank of CO is 2 which equals n, the number of the state variables. Therefore, the inverted pendulum passes the fundamental controllability test.

Now, for the second condition from theorem 3.1, a membership function for each state at time t must be prescribed. For comparison, four different sets of membership functions are selected. The first set shows prescribed membership functions that have the same shape and size as the original initial membership functions, but displaced such that their core, those values with membership grade of 1, are centered at the desired states. The second set shows prescribed membership functions that have the same shape as the original membership function but have a much larger range. The third and fourth set show prescribed membership functions of different shapes and size.

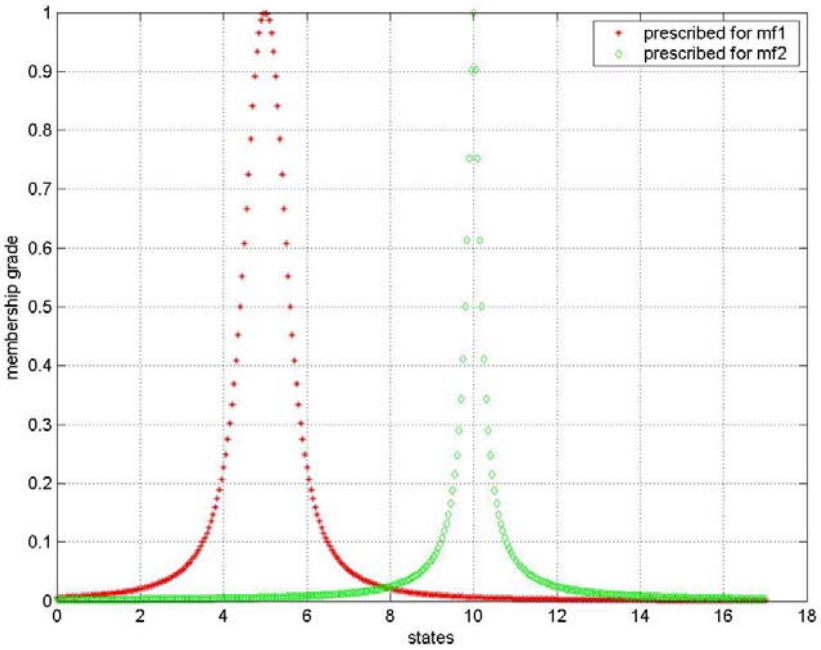

Figure 3.2 (a) Prescribed membership functions type 1.

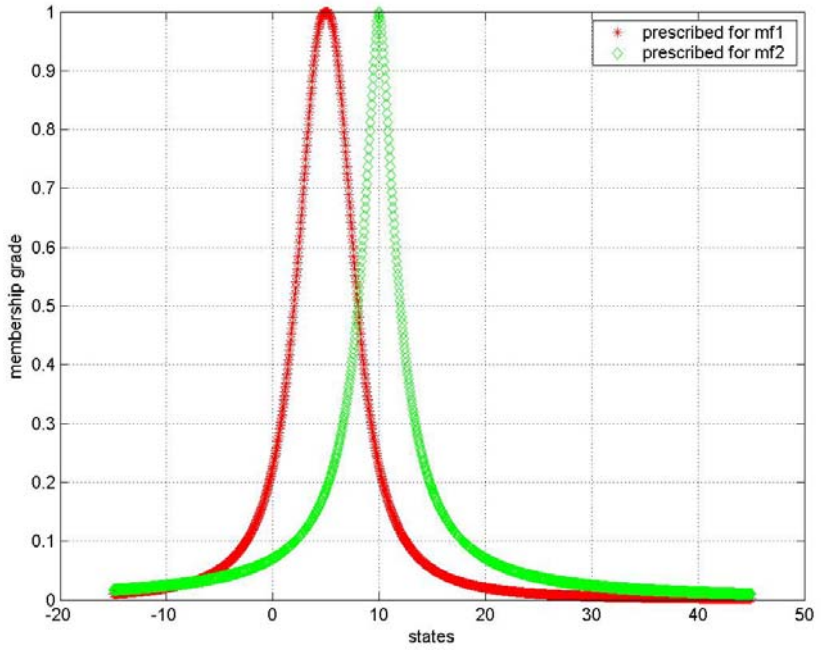

Figure 3.2 (b) Prescribed membership functions type 2.

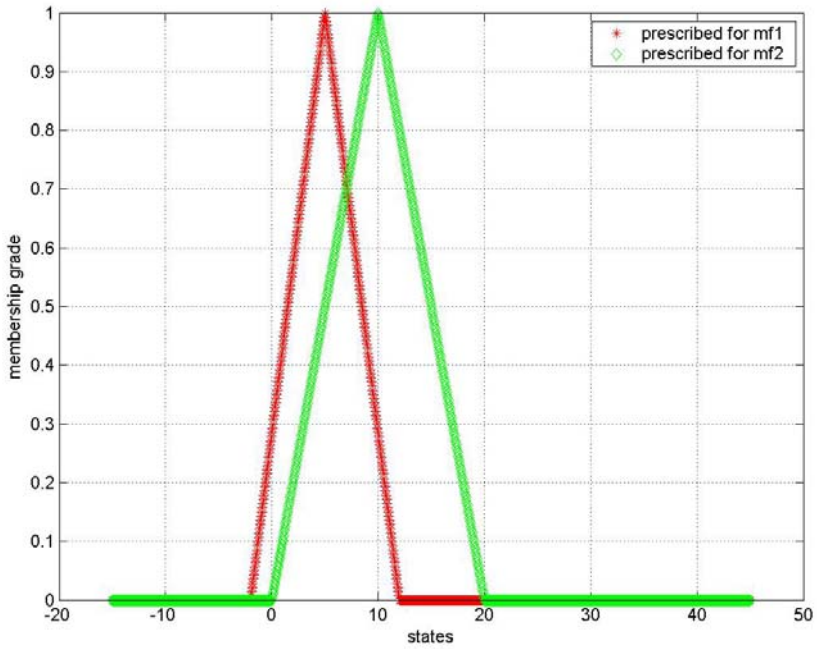

Figure 3.2 (c) Prescribed membership functions type 3.

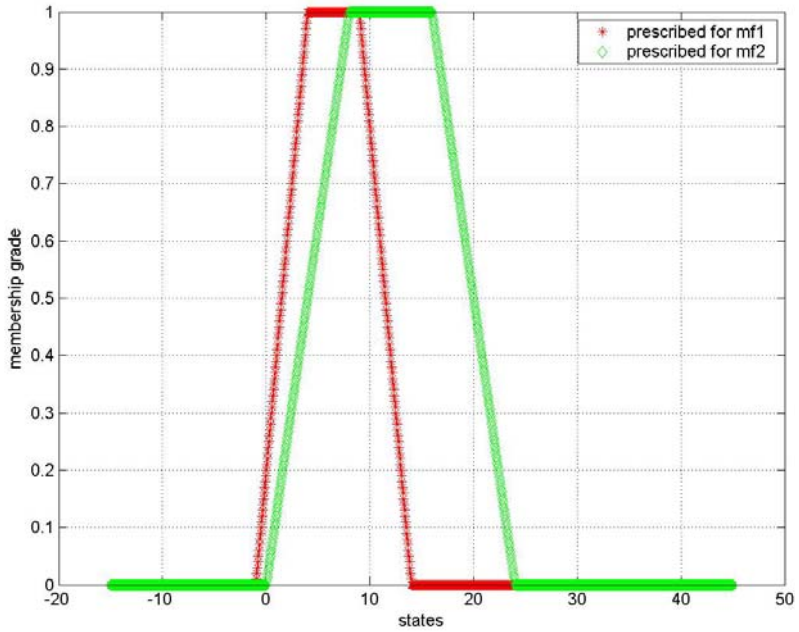

Figure 3.2 (d) Prescribed membership functions type 4.

For the time interval [0,1] the controllability gramians is invertible. The control *u(t)* can be calculated as in (III.2.4), applied to each alpha cuts as in (III.2.6) and the

membership function propagation procedure as described in section 2.6 yields the following propagation history. The MATLAB programs used is included in the appendix A (NTEST11S and NT2**)**

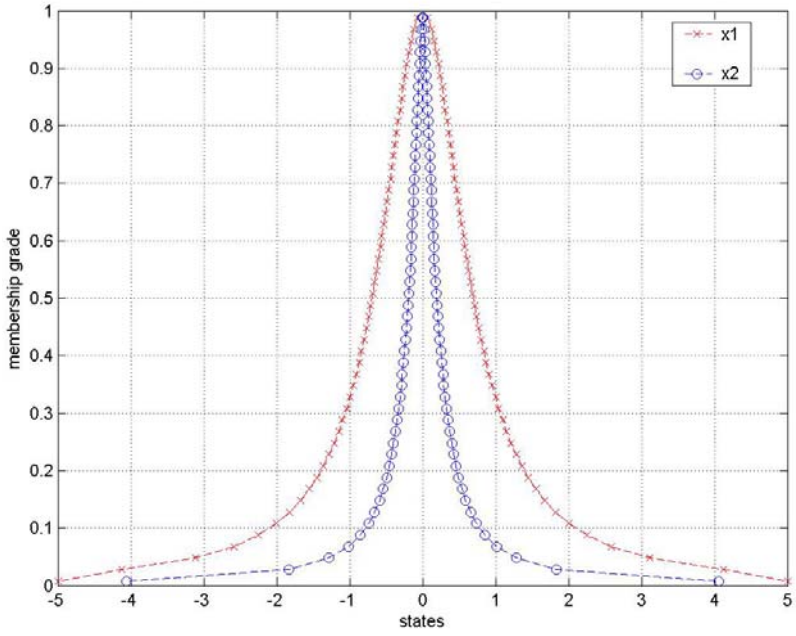

Figure 3.3 (a) Membership functions propagation at time t= 0 second.

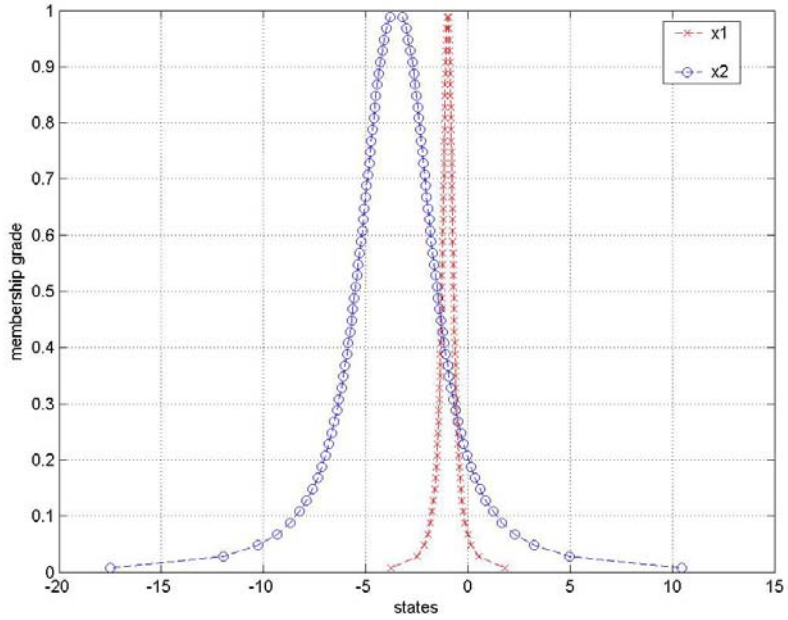

Figure 3.3 (b) Membership functions propagation at time t= 0.25 second.

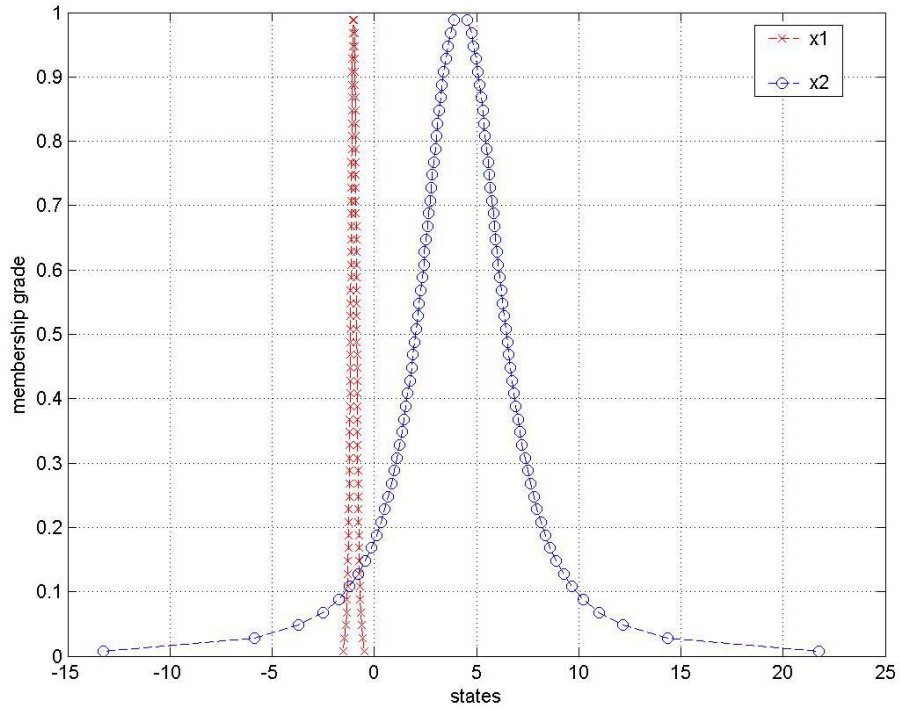

Figure 3.3 (c) Membership functions propagation at time t= 0.5 second.

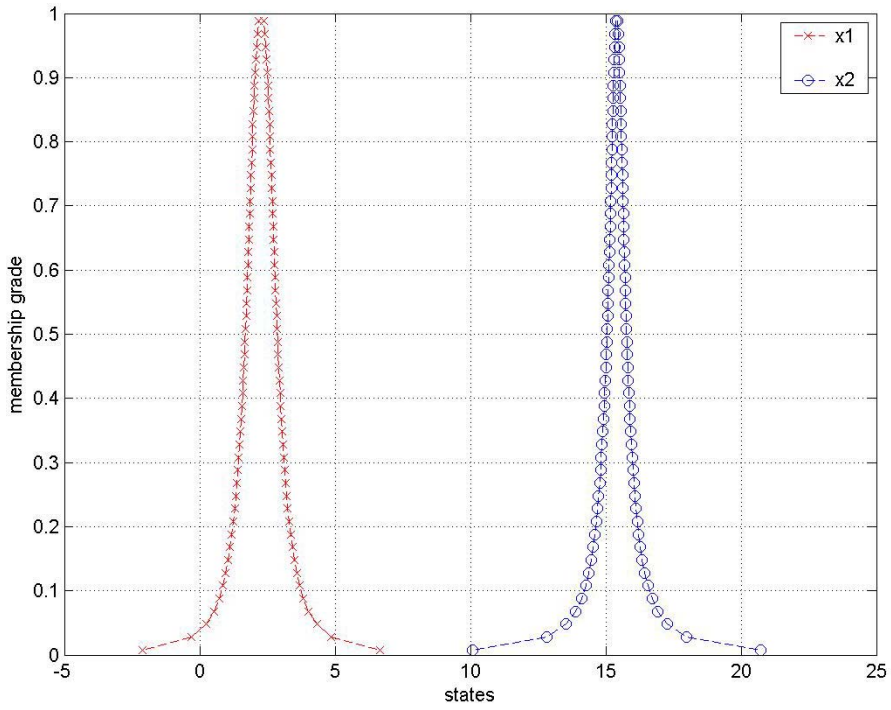

Figure 3.3 (d) Membership functions propagation at time t= 0.75 second

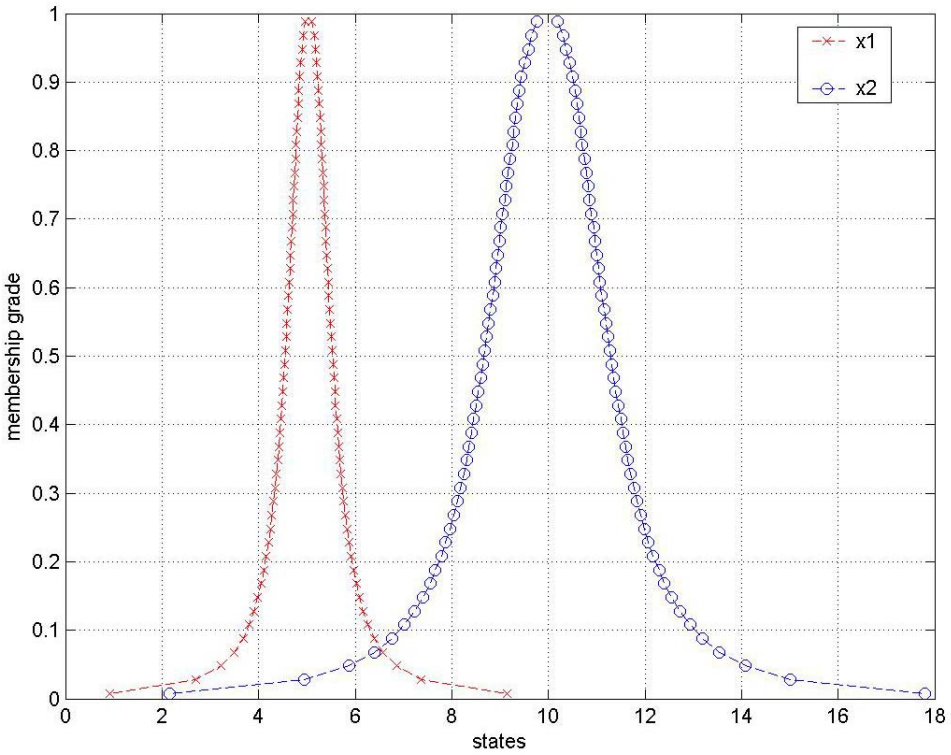

Figure 3.3 (e) Membership functions propagation at time t= 1 second

By superimposing the prescribed membership function to the final snapshot of the propagation history, the following figures show that the second and third case are controllable in the sense of their respective prescribed membership functions.

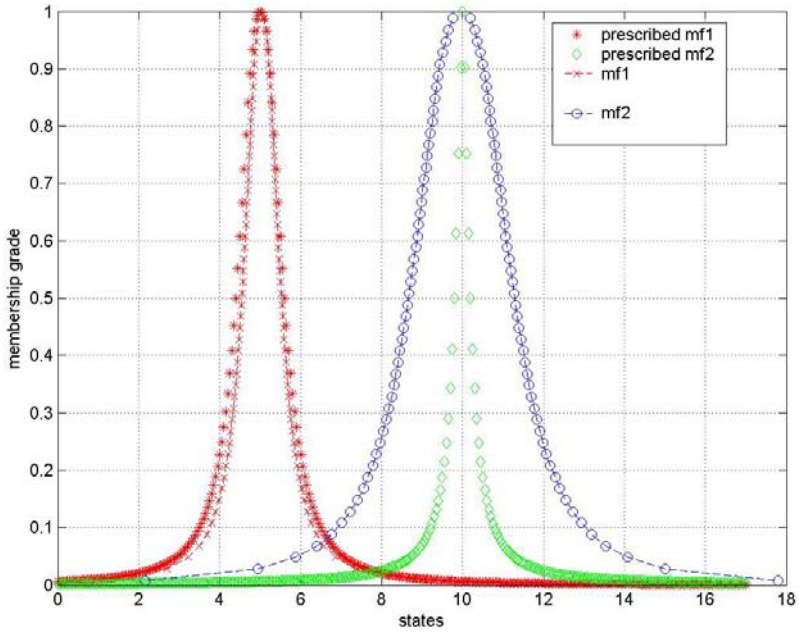

Figure 3.4 (a) Demonstrating controllability in the sense of prescribe membership functions type 1.

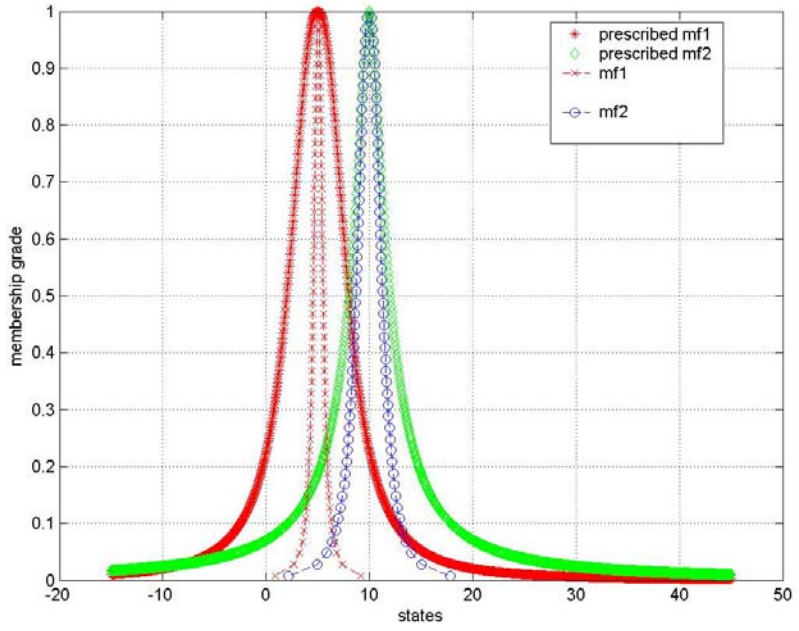

Figure 3.4 (b) Demonstrating controllability in the sense of prescribe membership functions type 2

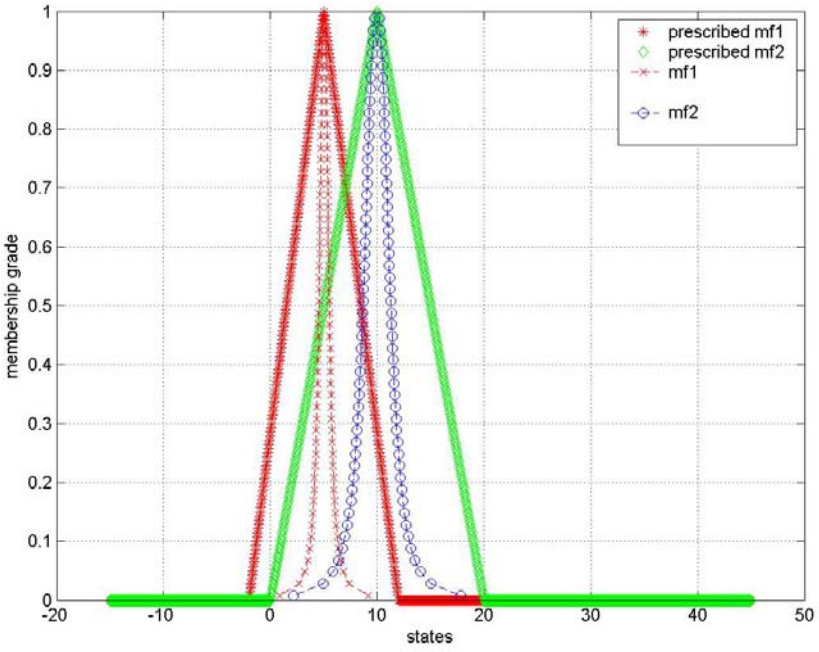

Figure 3.4 (c) Demonstrating controllability in the sense of prescribe membership functions type 3

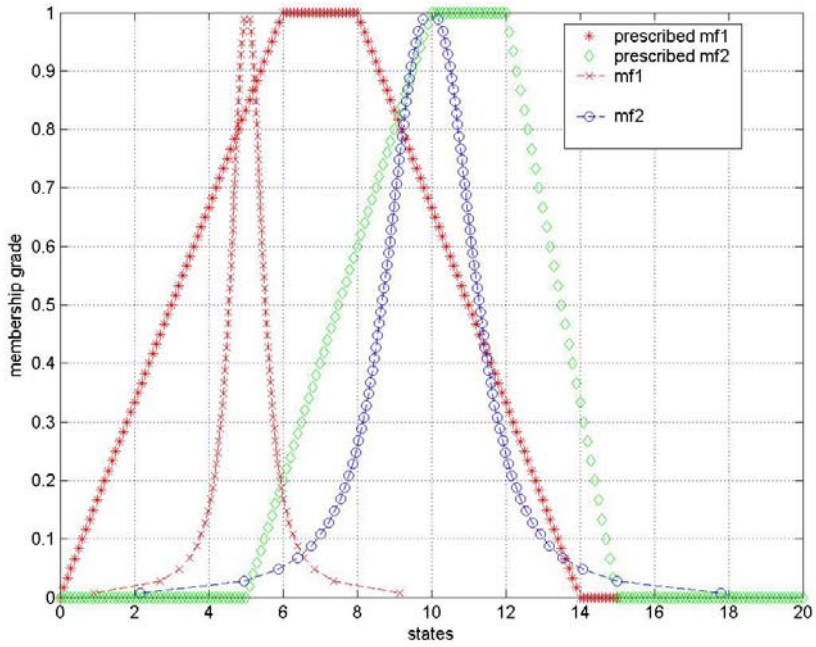

Figure 3.4 (d) Demonstrating controllability in the sense of prescribe membership functions type 4

The first and fourth cases violates 3.1.(ii) and the inverted pendulum is not controllable under the respective prescribed membership function. From figure 3.4(a), the prescribed membership function of X_2 can not contain the propagated X_2 membership function because the propagated membership functions at time t do not retain their original range. While the control term u(t)only translates the whole membership function through the state space, the state transition matrix stretches the range or the support (all states with non-zero membership grades). In the other words, the amount of uncertainty changes with respect to the behavior of the system: if the pendulum swings freely, it is difficult to guess where the pendulum might be after only a short instant. Therefore, there is more uncertainty and the range of the membership functions increase. Hence, the propagated membership functions can not be contained by the prescribed membership functions with the same shape and range as the original membership functions.

For the fourth case, although the range of the prescribed membership function is sufficient to cover the propagated membership function, the particular shape chosen for the prescribed membership function produces a contradiction to (III.2.2). This contradiction arises because some of the states from the propagated membership function have greater membership grades than the states from the prescribed membership function.

3.3 Observability in the fuzzy sense.

In parallel to controllability, membership functions also replace the crisp states for observability in the new context. Given known input and output membership functions history for the time interval $[t_1\ t_0]$, the observation task is to calculate the initial membership functions at time t_0 based on said knowledge.

Expectedly, the basic required conditions from the general observability concept hold. A relationship between the input, the output and the states must exists otherwise it is impossible to link these quantities. As before, the introduction of membership functions requires an additional condition that must be concerned with whether the uncertainty resulting from prediction of the initial membership function could be bounded.

Assuming that the basic requirement for general observability holds, the additional condition amounts to testing whether the predicted membership function is contained within another prescribed membership function. If the containment is successful, then the system is said to be observable in the sense of that prescribed membership function. Otherwise, a larger prescribed membership function can be selected to satisfy this requirement and the system is said to be observable in the sense of the new, larger membership function.

However, this implies that as long as the basic condition for general observablility is satisfied, one could always find a prescribed membership function that is sufficiently large for the additional condition. It becomes a question of usefulness at this point. Consider the analogy of identifying an archeological artifact. Suppose some dating technique is available for identifying the artifact as belonging to different eras with some uncertainty. As a result, only approximate statements like "this pottery piece belongs to an era that existed around 5,000 years ago" are possible. In addition, a membership function of this prediction could be formed. Then, it would be very useful if there is an era that spans the period of 10,000 years ago because we can firmly conclude that the artifact belongs to that era. On the other hand, if there are five distinct eras, each span on

average, 2,000 years each, then, hardly any conclusion is valid. In our context, we can say that the age of the artifacts is observable through the dating technique in a sense of the era that spans 10,000 years and not in the sense of any of the 2,000 years eras. This is because despite the fact that there is associated uncertainty regarding the dated artifacts, the uncertainty, as represented by the membership function is contained within a prescribed bound.

Observability is given the following definition:

Definition 3.2 Consider an output equation to the state equation (III.2.1)

$$y = g(x,u,t) \tag{III.3.1}$$

Let X and $\overline{X}_0$ belongs to the set of states at time t_0, denoted X_0. The output equation (3.4) is said to be observable in the sense of $\mu^*_1(\cdot)$ if the knowledge of $y[t_0,t_1]$ and the input $u[t_{0,}t_1]$ allow for the estimation of $\hat{\mu}_0(\cdot)$ such that

$$\hat{\mu}_0(X-\overline{X}_0) \le \mu^*_1(X-\overline{X}_0) \tag{III.3.2}$$

For the linear system, definition 3.2 reduces to the following.

Theorem 3.2 For a linear system, the output equation (III.2.1) becomes

$$Y(t) = C(t)X(t) + D(t)u(t) \tag{III.3.3}$$

The state equation (III.2.3) and (III.3.3) is observable in the sense of $\mu^*_1(\cdot)$ if and only if

(i) The columns of $C(\cdot)\phi(t_0,\cdot)$ are linearly independent on $[t_0,t_1]$.

(ii) $\exists\overline{X} \in X_0$ such that $\hat{\mu}_0(X-\overline{X}) \le \mu^*_1(X-\overline{X}_0)$, $\forall X \in X_0$.

The estimated membership function $\hat{\mu}_0(X-\overline{X})$, can be obtained by applying the following formula to each α-cuts as discussed in chapter 2.

$$\overline{X^{\alpha}}(0) = V^{-1}(t_0, t_1)\int_{t0}^{t1} \phi^T(t, t_0) C^T(t) \overline{\hat{Y}^{\alpha}}(t) dt$$

$$\underline{X_{\alpha}}(0) = V^{-1}(t_0, t_1)\int_{t0}^{t1} \phi^T(t, t_0) C^T(t) \underline{\hat{Y}_{\alpha}}(t) dt \qquad \text{(III.3.4)}$$

where the output $\hat{Y}(t)$ is adjusted for the direct control term and defined as follows:

$$\hat{Y}(t) = Y(t) - C(t)\phi(t, t_0)\int_{t0}^{t} \phi^T(t_0, \tau) B(\tau) u(\tau) d\tau - D(t)u(t) \qquad \text{(III.3.5)}$$

and the observability gramians remain unchanged

$$V(t_0, t_1) = \int_{t0}^{t1} \phi^T(t_0, \tau) C^T(\tau) C(\tau) \phi\ (t_0, \tau) d\tau \qquad \text{(III.3.6)}$$

The proof for 3.2.(ii) is identical to the proof of 3.1.(ii).

Note that theorem 3.2.(ii) is similar to theorem 3.1.(ii). A quick observation of theorem 3.2.(ii) reveals that the estimated membership function $\hat{\mu}_0(X - \overline{X})$ must be a subset of the prescribed membership function at the initial time $\mu^*_1(X - \overline{X}_0)$ for the system to be observable in the sense of $\mu^*_1(\cdot)$

3.3.1 Example of observability.

Consider the inverted pendulum example. The fundamental observability test satisfies the first requirement of theorem 3.2, if the observability matrix, calculated below, has rank =*n*.

For comparison purpose, consider three different measurement settings which are represented by their output matrices C_1=[1 0], C_2=[0 1] and C_3=[1 1] respectively. For the first measurement setting, the output *Y*(t), is just the direct measurement of the angle

of the pendulum. For the second setting, the output is the measurement of the angular velocity. For third setting, the output is a linear combination of the previous two outputs.

The general formula for computing the observability matrix is repeated below for convenience.

$$OB = \begin{bmatrix} C \\ CA \\ \mathrm{M} \\ CA^{n-1} \end{bmatrix} \tag{III.3.7}$$

for the first setting, the observability matrix OB_1 is computed as follows

$$\begin{aligned} C_1 A &= \begin{bmatrix} 0 & 1 \end{bmatrix} \\ OB_1 &= \begin{bmatrix} 1 & 0 \\ 0 & 1 \end{bmatrix} \end{aligned} \tag{III.3.8}$$

The rank of OB_1 is 2, and the system is observable under the fundamental test of general observability. Similarly for the second and third setting, their corresponding observability matrices OB_2 and OB_3 are

$$\begin{aligned} OB_2 &= \begin{bmatrix} 0 & 1 \\ -\dfrac{3g}{2l} & 0 \end{bmatrix} \\ OB_3 &= \begin{bmatrix} 1 & 1 \\ -\dfrac{3g}{2l} & 1 \end{bmatrix} \end{aligned} \tag{III.3.9}$$

Both have rank equal to 2. Assuming a vague knowledge of the initial conditions, an assortment of prescribed membership functions can be chosen to represent an expert guess at the initial conditions. The first and the second guesses show prescribed membership functions that have the same size and shape as the membership function at time t but their support and core are centered at different initial guess values. The third

guess show a set of membership functions that represent "guesses" more realistically. Their core region covers a greater range of values, expressing the uncertainty that any of these values are equally likely to be the actual initial condition.

The calculation of the initial state membership functions follows the procedure discussed in chapter 2 with equations (III.3.4) - (III.3.6) applied. The membership functions propagation which includes the input and output history that is needed in the calculation are taken from the previous example in section 3.2.1. The MATLAB program that performs this calculation can be founded in appendix A (obf). The figures below show the calculated initial membership functions superimposed on the same plot with the prescribed membership functions, as in the previous section.

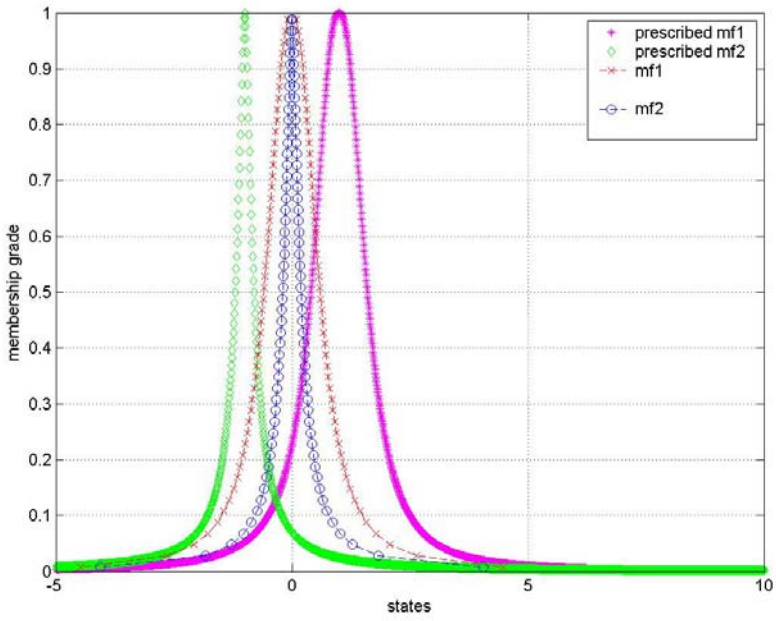

Figure 3.5(a) Demonstrating observability in the sense of the prescribed membership function type 1.

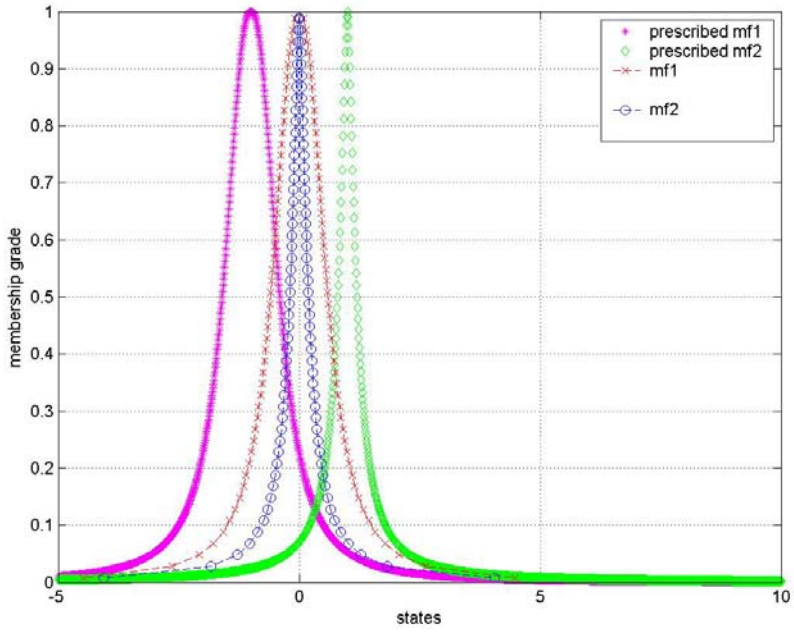

Figure 3.5(b) Demonstrating observability in the sense of the prescribed membership function type 2.

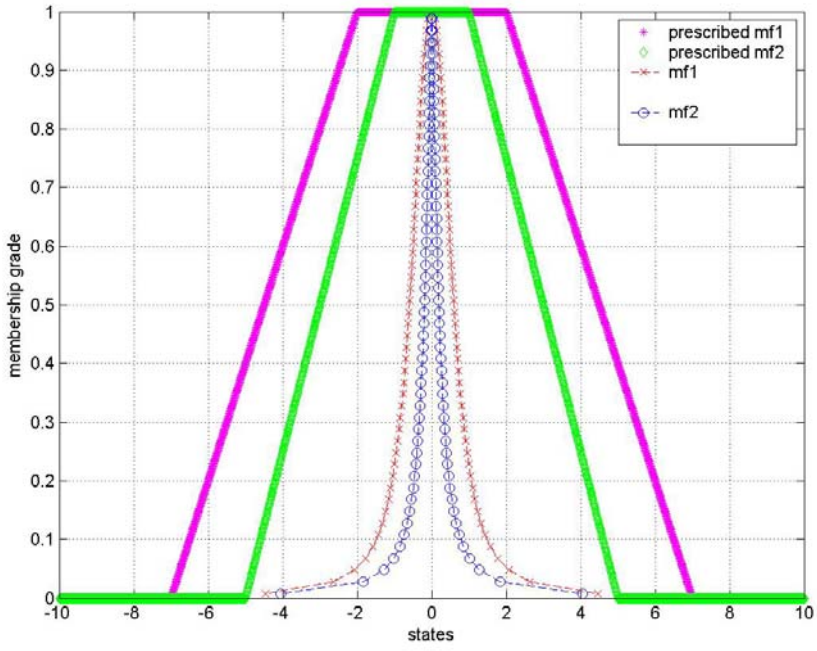

Figure 3.5(c) Demonstrating observability in the sense of the prescribed membership function type 3.

Evidently, only the prescribed membership function in the third guess is observable in the fuzzy sense. The first two guesses have narrow core regions which are focused inaccurately. This results in violation of the second condition of theorem 3.2. Hence, the observability of the membership function depends on the choice of the "guess" at the initial membership function. The guess needs to be generous, in a sense that it should cover sufficient space to contain the calculated initial membership function.

CHAPTER 4

APPLICATION TO A MECHANICAL MANIPULATOR

This chapter applies the concepts and theorems from the previous two chapters to a more complex physical system than the inverted pendulum, namely, a mechanical manipulator. This particular mechanical manipulator is a grinder that has two degree of freedom. The modeling process is discussed. A control design that linearizes the non-linear dynamic is implemented through simulations using SIMULINK. It is shown that the linearized system is controllable and observable. However, to complete the control, an observer subsystem must be built to provide full states feedback. The membership functions propagation procedure is applied to show that the linearized system is also controllable and observable in the fuzzy sense.

4.1 Robotic grinder

Grinding is the general name for the process of removing metal from the surface of a cast or machined work piece. A typical application of grinding is the surface finishing of nickel-bronze propeller blades. This application is suitable for a robot because there are many injuries related to the manual grinding operation. In addition, nickel is a hazardous material and manual grinding is exhaustive, which causes low productivity overall. Therefore, a robotic grinder improves productivity and create safer manufacturing environment.

The robotic grinder consists of two motors, which control motions of its waist and shoulder. In addition, a grinder, represented by a spinning disk, is attached at the end tip

of the robotic arm. However, the rate of spin of the disk is assumed to be constant. The following is the figure of the robotic grinder.

ψ - Waist angle	*L - Length of the shaft*
θ-Shoulder angle	*R - Radius of the disk*
Γ_1-Torque at waist	*ω_1- Constant spin rate of the disk*
Γ_2-Torque at shoulder	*X-Y-Z Reference coordinates of waist*
m_1- Mass of the disk	*x-y-z Reference coordinates of shoulder*
m_2 - Mass of the shaft	

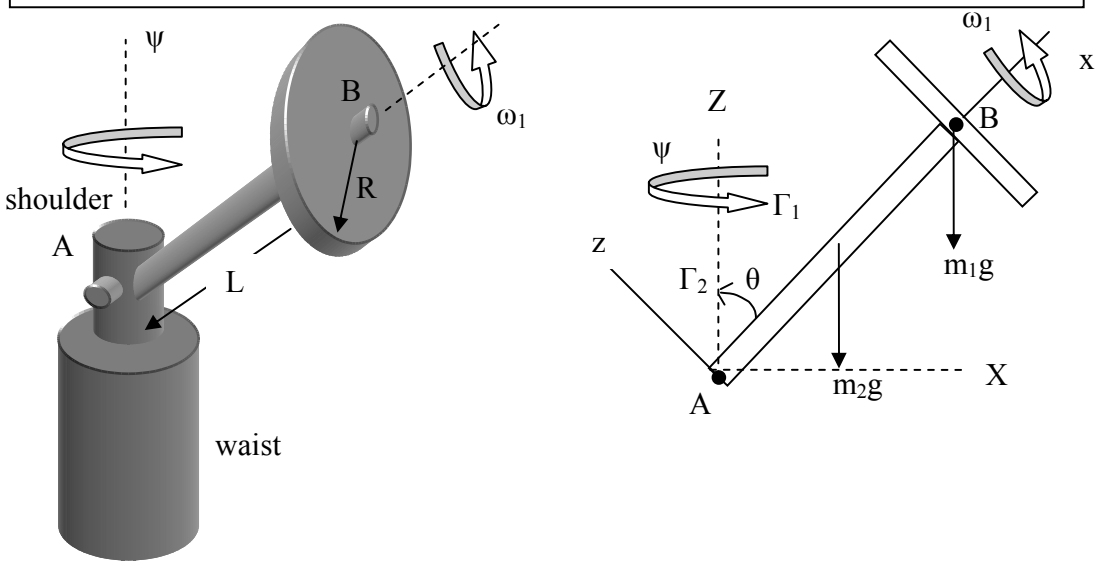

Figure 4.1: Robotic grinder

The waist angle ψ is controlled by torque from motor 1 and the shoulder angle θ is controlled by torque from motor 2. The torqueses are indicated by Γ_1 and Γ_2 respectively.

The disk spins about its axis at the constant rate ω_1. Two optical encoders are placed at the waist and the shoulder to measure the angle ψ and θ as output.

4.2 Equation of motion for the robotic grinder.

As done in chapter 2 for the inverted pendulum, the equation of motions is a set of differential equations that describe the states of the system which can be developed through the Lagrangian procedure. First, two generalized coordinate must be determined for this two-degree-of freedom system. The most suitable coordinates are the two angles, θ and ψ, because they are the two variables that need to be controlled. The inertia of the vertical shaft along with friction at contact point A and B are assumed negligible.

From the modeling process of an inverted pendulum in chapter 2, it is shown that the generalized forces are the force components in the directions of the generalized coordinate. In our cases, when the generalized coordinates are angles ψ and θ, the respective generalized forces are the two torqueses Γ_1 and Γ_2 respectively.

$$Q_1 = \Gamma_1 \tag{IV.2.1}$$

$$Q_2 = \Gamma_2 \tag{IV.2.2}$$

Taking point A as fixed relative to the disk, the kinetic energy of the waist and the shouder, which are the disk and the shaft AB, may be calculated as

$$T = \frac{1}{2}(\overline{H}_A \cdot \overline{\varpi})_{disk} + \frac{1}{2}(\overline{H}_A \cdot \overline{\varpi})_{shaft} \tag{IV.2.3}$$

where $\overline{H}_A$ and $\overline{\varpi}$ denotes the angular momentum and angular velocity of a body relative to point A. The x-y-z coordinates shown in Figure 4.1 has been chosen as the reference

frame. The chosen reference frame are also principal axes for both bodies, this means the product of inertia terms are zero and the kinetic energy reduces to

$$T = \frac{1}{2}(I_{xx}\omega_x{}^2 + I_{yy}\omega_y{}^2 + I_{zz}\omega_z{}^2)_{disk} + \frac{1}{2}(I_{xx}\omega_x{}^2 + I_{yy}\omega_y{}^2 + I_{zz}\omega_z{}^2)_{shaft} \quad \text{(IV.2.4)}$$

where I_{xx},I_{yy}, and I_{zz} are the moments of inertia about the x-y-z axes. ω_x, ω_y and ω_z are the angular velocity about the x-y-z axes.

The angular velocity of the disk is the vector sum of the precision rate $\dot{\psi}$, the nutation rate $\dot{\theta}$, and the spin rate ω_1, all of which must be resolved into xyz components

$$\bar{\omega}_{disk} = \dot{\psi}\bar{K} + \dot{\theta}(-\bar{j}) + \omega_1(-\bar{i}) = -\left[(\dot{\psi}\cos\theta + \omega_1)\bar{i} - \dot{\theta}\bar{j} + (\dot{\psi}\sin\theta)\bar{k}\right] \quad \text{(IV.2.5)}$$

The shaft is not spinning, so

$$\bar{\omega}_{shaft} = -(\dot{\psi}\cos\theta)\bar{i} - \dot{\theta}\bar{j} + (\dot{\psi}\sin\theta)\bar{k} \quad \text{(IV.2.6)}$$

The moments of inertia of the disk may be obtained from the tabulated properties [5].

$$(I_{xx})_{disk} = \frac{1}{2}m_1R^2 \quad \text{(IV.2.7)}$$

The moment of inertia of the shaft may be obtained using the parallel axis theorems (II.2.8) to translate the moment of inertia from its center of gravity at half length to the pivot point A.

$$(I'_{yy})_{shaft} = I_{yy} + m(X^2{}_o + Z^2{}_o) \quad \text{(IV.2.8)}$$

The untranslated I_{yy} moment of inertia is the sum of the disk inertia and the shaft

$$I_{yy} = \frac{1}{4}m_1R^2 + \frac{1}{12}m_2L^2 \quad \text{(IV.2.9)}$$

with the translational terms $m(X^2{}_o + Z^2{}_o)$ equals to the translated distance (in x direction since there is no translation in z) of the disk and shaft times their respective

$$m(X^2{}_o + Z^2{}_o) = m_1 L^2 + \frac{1}{4} m_2 L^2 \tag{IV.2.10}$$

combining (IV.2.9) and (IV.2.10) gives

$$\left(I'_{yy}\right)_{shaft} = \frac{1}{4} m_1 R^2 + (m_1 + \frac{1}{3} m_2) L^2 \tag{IV.2.11}$$

Substituting the angular velocities and moments of inertia equations (IV.2.5) through (IV.2.11)into equation (IV.2.4), the result is

$$\begin{aligned} T = {} & \frac{1}{2}(\frac{1}{2} m_1 R^2)(\dot{\psi}\cos\theta + \omega_1)^2 + \frac{1}{2}(\frac{1}{4} m_1 R^2 + m_1 L^2)\left[\dot{\theta}^2 + (\dot{\psi}\sin\theta)^2\right] \\ & + \frac{1}{2}(\frac{1}{3} m_2 L^2)\left[\dot{\theta}^2 + (\dot{\psi}\sin\theta)^2\right] \end{aligned} \tag{IV.2.12}$$

Next, the potential energy is calculated. The center of gravity of the shaft is at half length with point A being the reference point. The potential energy of the systems contributed by two masses is

$$\begin{aligned} V &= m_1 g(-L\cos\theta) + m_2 g(-\frac{L}{2}\cos\theta) \\ &= -(m_1 + \frac{1}{2} m_2) g L \cos\theta \end{aligned} \tag{IV.2.13}$$

Taking the partial derivatives with respect to ψ, θ, $\dot{\psi}$, and $\dot{\theta}$ yields

$$\frac{d}{dt}\left(\frac{\partial T}{\partial \dot{\psi}}\right) = \frac{d}{dt}\left[I_1(\dot{\psi}\cos\theta + \omega_1)\cos\theta + I_2\psi\sin^2\theta\right]$$

$$= I_1(\ddot{\psi}\cos^2\theta - 2\dot{\psi}\dot{\theta}\cos\theta\sin\theta - \omega_1\dot{\theta}\sin\theta) + I_2\dot{\psi}\sin^2\theta + 2I_2\dot{\psi}\dot{\theta}\sin\theta\cos\theta$$

$$\frac{d}{dt}\left(\frac{\partial T}{\partial \dot{\theta}}\right) = \frac{d}{dt}(I_2\dot{\theta}) = I_2\ddot{\theta}$$

$$\frac{d}{dt}\left(\frac{\partial T}{\partial \psi}\right) = \frac{\partial V}{\partial \psi} = 0$$

$$\frac{\partial T}{\partial \theta} = I_1(\dot{\psi}\cos\theta + \omega_1)(-\dot{\psi}\sin\theta) + (I_2(\dot{\psi}^2\sin\theta\cos\theta) \qquad \text{(IV.2.14)}$$

$$\frac{\partial V}{\partial \theta} = (m_1 + \frac{1}{2}m_2)gL\sin\theta$$

Finally, the equations of motions is obtained by substituting all of the above and equations (IV.2.1) and (IV.2.2) into the Lagrange equations:

$$\frac{d}{dt}\left(\frac{\partial T}{\partial \dot{\psi}}\right) - \frac{\partial T}{\partial \psi} + \frac{\partial V}{\partial \psi} = Q_1$$

$$(I_1\cos^2\theta + I_2\sin^2\theta)\ddot{\psi} - 2(I_1 - I_2)\dot{\psi}\dot{\theta}\sin\theta\cos\theta - I_1\omega_1\dot{\theta}\sin\theta) = \Gamma_1 \qquad \text{(IV.2.15)}$$

$$\frac{d}{dt}\left(\frac{\partial T}{\partial \dot{\theta}}\right) - \frac{\partial T}{\partial \theta} + \frac{\partial V}{\partial \theta} = Q_2$$

$$I_2\ddot{\theta} + (I_1 - I_2)\dot{\psi}^2\sin\theta\cos\theta + I_1\omega_1\dot{\psi}\sin\theta + (m_1 + \frac{1}{2}m_2)gL\sin\theta = \Gamma_2 \qquad \text{(IV.2.16)}$$

Notice that there are nonlinear terms in both of the equations of motion (IV.2.15) and (IV.2.16). However, both equations may still be represented in the matrix form, which is

$$\begin{bmatrix} I_1\cos^2\theta + I_2\sin^2\theta & 0 \\ 0 & I_2 \end{bmatrix}\begin{bmatrix} \ddot{\psi} \\ \ddot{\theta} \end{bmatrix} +$$
$$\begin{bmatrix} -2(I_1 - I_2)\dot{\theta}\sin\theta\cos\theta & -I_1\omega_1\sin\theta \\ (I_1 - I_2)\dot{\psi}\sin\theta\cos\theta + I_1\omega_1\sin\theta & 0 \end{bmatrix}\begin{bmatrix} \dot{\psi} \\ \dot{\theta} \end{bmatrix} + \qquad \text{(IV.2.13)}$$
$$\begin{bmatrix} 0 \\ (m_1 + \frac{1}{2}m_2)gL\sin\theta \end{bmatrix} = \begin{bmatrix} \Gamma_1 \\ \Gamma_2 \end{bmatrix}$$

4.3. The computed torque method

The apparent non-linearity and coupling in the equation of motions between the two generalized coordinates, θ and ψ, substantially complicate the design of a suitable

controller. There are two solutions: the first is to linearize the equation of motions about some equilibrium angles, obtain the state space representation of the linearized system, and place the controller's and observer's poles using the pole placement techniques. The second is to use the computed torque method (CTM). CTM primarily rely on exact cancellation of non-linear terms in order to obtain linear input-output behavior. In order to explain the CTM, the equation of motions can be written in a general form as:

$$M_{(q)}\ddot{q} + N_{(q,\dot{q})} = \Gamma \tag{IV.3.1}$$

where *q,* is the generalized coordinates. $M_{(q)}$ and $N_{(q,\dot{q})}$ are the mass matrix and the non-linear terms (which includes the centrifugal and coriolis terms) which are the first two terms in (IV.2.13) respectively. Γ is the computed torque, which can be expressed as the following:

$$\Gamma = \hat{M}(q)u + \hat{N}(q,\dot{q}) \tag{IV.3.2}$$

where, $\hat{M}(q)$ is the estimated inertia matrix and $\hat{N}(q,\dot{q})$ is the estimated centrifugal and coriolis terms and *u* is the fictitious input. Combining equating (IV.3.1) and (IV.3.2) gives:

$$M_{(q)}\ddot{q} + N_{(q,\dot{q})} = \hat{M}_{(q)}u + \hat{N}_{(q,\dot{q})}$$

This leads to the underlying idea of CTM: the estimated inertia and non linear matrix cancel out the plant's actual matrix and simplify the problem to:

$$\ddot{q} = u$$

in our case, this simplification equals

$$\ddot{q} = \begin{bmatrix} \ddot{\psi} \\ \ddot{\theta} \end{bmatrix} = \begin{bmatrix} u_1 \\ u_2 \end{bmatrix} \tag{IV.3.3}$$

The following block diagram shows the integration of CTM into the robot system

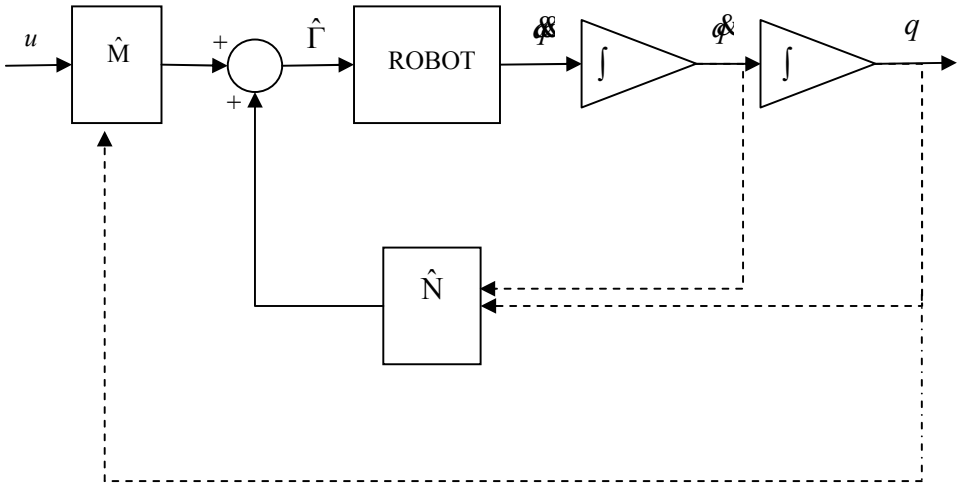

Figure 4.2.Schematic block diagram of the Computed Torque Method control scheme

4.4 Fundamental tests for controllability and observability

Now that the system is transformed to a simple linear time invariant system, the state space representation of the system can be derived from (IV.3.3) as

$$\psi = X_1 \quad \theta = X_3$$
$$\dot{\psi} = X_2 \quad \dot{\theta} = X_4$$
$$\ddot{\psi} = u_1 \quad \ddot{\theta} = u_2$$

$$\begin{bmatrix} \dot{\psi} \\ \ddot{\psi} \\ \dot{\theta} \\ \ddot{\theta} \end{bmatrix} = \begin{bmatrix} 0 & 1 & 0 & 0 \\ 0 & 0 & 0 & 0 \\ 0 & 0 & 0 & 1 \\ 0 & 0 & 0 & 0 \end{bmatrix} \begin{bmatrix} \varphi \\ \dot{\varphi} \\ \theta \\ \dot{\theta} \end{bmatrix} + \begin{bmatrix} 0 & 0 \\ 1 & 0 \\ 0 & 0 \\ 0 & 1 \end{bmatrix} \begin{bmatrix} u_1 \\ u_2 \end{bmatrix}$$

$$\mathrm{y} = \begin{bmatrix} 1 & 0 & 0 & 0 \\ 0 & 0 & 1 & 0 \end{bmatrix} \begin{bmatrix} \psi \\ \dot{\psi} \\ \theta \\ \dot{\theta} \end{bmatrix} \qquad \text{(IV.4.1)}$$

which represents a completely linearized and decoupled fourth order system. Furthermore, the resulting system is controllable and observable in the general sense, as its controllability and observability matrices are full ranked. The controllability matrix is computed as follows:

$$
\begin{aligned}
CO &= \left[B \;\; AB \;\; A^2B \;\; A^3B \right] \\
AB &= \begin{bmatrix} 1 & 0 \\ 0 & 0 \\ 0 & 1 \\ 0 & 0 \end{bmatrix} \\
A^2B = A^3B &= \begin{bmatrix} 0 & 0 \\ 0 & 0 \\ 0 & 0 \\ 0 & 0 \end{bmatrix} \\
CO &= \begin{bmatrix} 0 & 0 & 1 & 0 & 0 & 0 & 0 & 0 \\ 1 & 0 & 0 & 0 & 0 & 0 & 0 & 0 \\ 0 & 0 & 0 & 1 & 0 & 0 & 0 & 0 \\ 0 & 1 & 0 & 0 & 0 & 0 & 0 & 0 \end{bmatrix}
\end{aligned}
\qquad \text{(IV.4.2)}
$$

The observability matrix is computed as follows:

$$OB = \begin{bmatrix} C \\ CA \\ \text{M} \\ CA^{n-1} \end{bmatrix}$$

$$CA = \begin{bmatrix} 0 & 1 & 0 & 0 \\ 0 & 0 & 0 & 1 \end{bmatrix}$$

$$CA^2 = CA^3 = \begin{bmatrix} 0 & 0 & 0 & 0 \\ 0 & 0 & 0 & 0 \end{bmatrix}$$

$$OB = \begin{bmatrix} 1 & 0 & 0 & 0 \\ 0 & 0 & 1 & 0 \\ 0 & 1 & 0 & 0 \\ 0 & 0 & 0 & 1 \\ 0 & 0 & 0 & 0 \\ 0 & 0 & 0 & 0 \\ 0 & 0 & 0 & 0 \\ 0 & 0 & 0 & 0 \end{bmatrix} \qquad \text{(IV.4.3)}$$

This means that the system can be transferred to any desired location. The control can be

$$u(t) = -B^T(t)\phi^T(t_0,t)W^{-1}(t_0,t_1)[X_0 - \phi(t_0,t_1)\overline{X}_1] \qquad \text{(IV.4.4)}$$

with W as the controllability gramians. X_0 and $\overline{X}_1$ are the initial and desired states respectively. Note that (IV.4.4) is also called the *mimimum-energy control* [6]. Also, given an input and an output history, the unobservable states can be calculated by an observer subsystem that is discussed in the next section.

4.5 The observer subsystem.

In our robot system, we assume that the only measurable variables are angles, ψ and θ. Both angles are to be measured by using two optical encoders attached to each of

the corresponding motors. Other variables, such as the two angular velocities, are not measurable. However, the angular velocities are required in calculating the control input, the estimated non-linear matrix, and the robot dynamic. These requirements may be seen in Figure 4.2 by following the dotted arrows. Figure 4.2 also shows that the calculations of angular velocities come from integrating angular accelerations. However, in our robot model, which tries to mimic real system, integrating angular accelerations is not valid because we assume that the only measurable variables are the angles. Therefore, a Luenberger observer is needed to estimate angular velocities. The observer takes two inputs, which are the input *u*(t) and the plant's output *Y*(t).

A schematic of a Luenberger observer is shown in figure 4.3. Let $\hat{X}(t)$ be the estimated states, the observer dynamic is as follows

$$\dot{\hat{X}}(t) = A\hat{X}(t) + Bu(t) - L\tilde{Y}(t) \qquad \text{(IV.5.1)}$$

where *L* is the observer gain matrix that has four rows and two columns. $\tilde{Y}(t)$ is the estimation error defined as the difference between the real output and the estimated output $\tilde{Y}(t) = Y(t) - \hat{Y}(t)$, with *Y(t)=CX(t)* and $\hat{Y}(t) = C\hat{X}(t)$. Similarly, the state estimation error is

$$\tilde{X}(t) = X(t) - \hat{X}(t) \qquad \text{(IV.5.2)}$$

Differentiation of (IV.5.2) and substitution of (IV.5.1) and the state equations yields

$$\begin{aligned}
\dot{\tilde{X}}(t) &= \dot{X}(t) - \dot{\hat{X}}(t) \\
\dot{\tilde{X}}(t) &= AX(t) + Bu(t) - \hat{X}(t) - Bu(t) + L\tilde{Y}(t) \\
\dot{\tilde{X}}(t) &= A(X(t) - \hat{X}(t)) + LC(X(t) - \hat{X}(t)) \\
\dot{\tilde{X}}(t) &= (A + LC)\tilde{X}(t)
\end{aligned} \qquad \text{(IV.5.3)}$$

The solution to this differential equation is a familiar $\tilde{X}(t) = \exp[(A + LC)t]\tilde{X}(0)$, which is known to approach zero asymptotically if the eigenvalues of the matrix *(A+LC)* lie in the left half plane.

Basically, the observer is constructed based on the linearized system from the CTM, shown in the previous section. Therefore, the state space representation matrix in equation (IV.4.1) may be used to construct the observer. A block diagram representing the robot system with an integrated observer subsystem may be created:

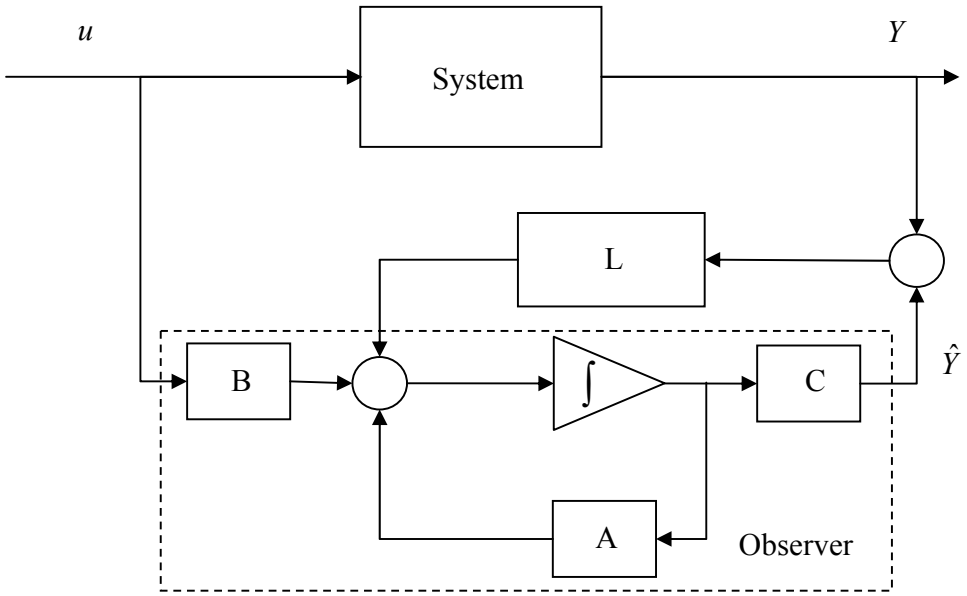

Figure 4.3.Observer block diagram

The concept of observer shown in Figure 4.3 may be included into the system in Figure 4.2. This addition will not affect the closed loop transfer function because observer dynamics are canceled when performing calculation of closed loop transfer function with the observer included. Figure 4.4 shows block diagram of the robot plant with both controller and observer introduced.

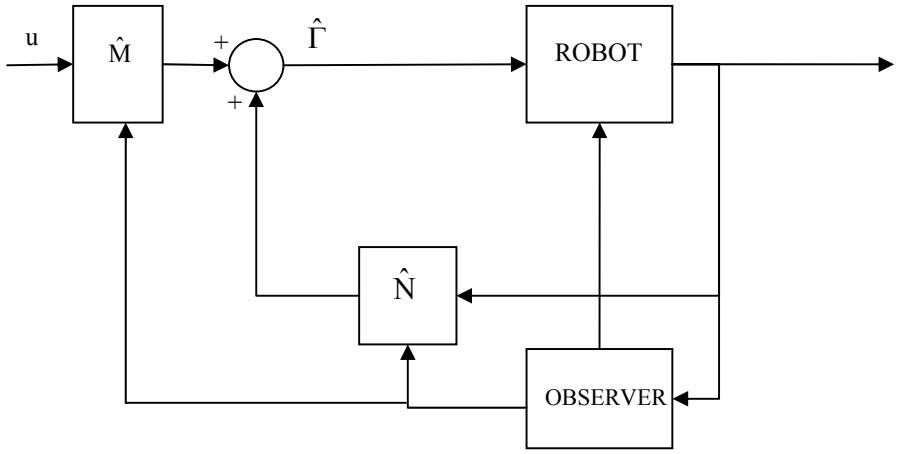

Figure 4.4: The complete system

4.5.1 Determining the luenberger observer gain

Even though observer dynamics are cancelled in the closed loop transfer function, the observer gain, denoted *L* in figure 4.3 still need to be determined. Although there is no absolute guideline for choosing the observer gain, a good rule of thumb is to pick a fast observer. This is to avoid aliasing in accordance with the Nyquist criterion; the sampling frequency should be atleast twice the highest frequency being sampled.

The sampling frequency directly affects the observer's poles. Therefore, the procedure for calculating the gain proceeds in a similar manner to the controller pole placement. In fact, the same procedure for placing the controller poles can be used on the matrices pair A^T and C^T instead of A and B for the observer poles.

4.6 Simulation verification for controllability.

MATLAB programs were written to perform the membership functions propagation of the robotic grinder. The grinder has the following dimension.

Table 4.2 Dimension of the robotic grinder

Mass of the disk, m_1	0.3 kg
Mass of the shaft m_2	0.6 kg
Length of the shaft L	0.75 m
Radius of the disk R	0.25 m
Constant spin rate of the disk ω_1	1 rad/s

The programs and their accompanying SIMULINK system can be found in the appendix A and B(NTR_W2, NTRT_W2 and ROBO_W2). A set of initial membership functions that corresponds to a near stationary configuration is shown below.

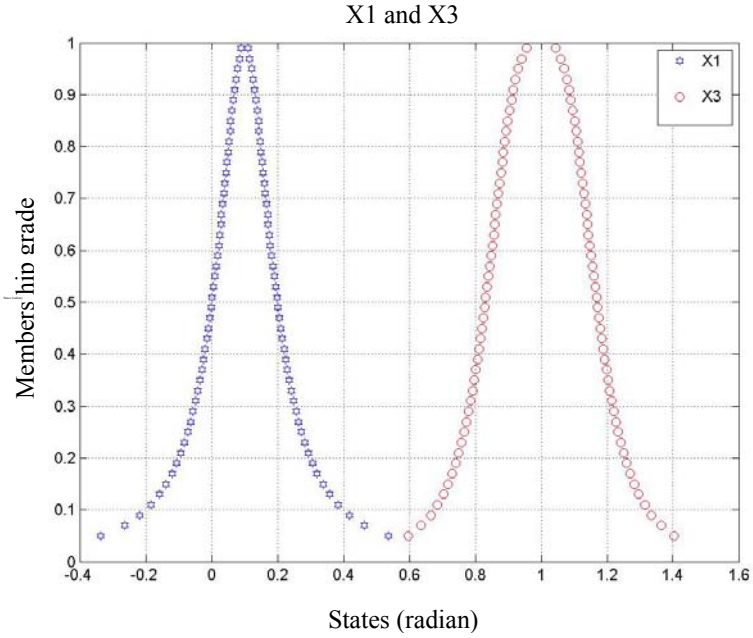

Figure 4.5(a) Initial membership functions.

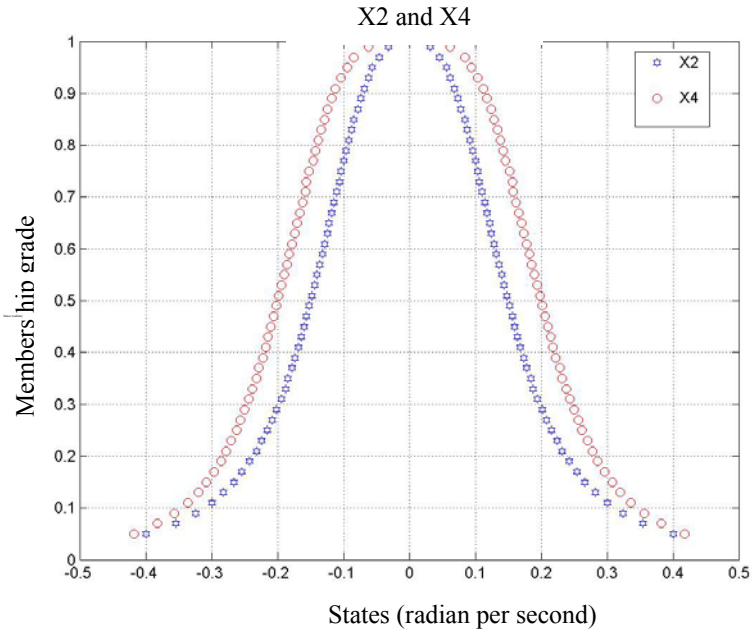

Figure 4.5(b) Initial membership functions.

The states are to be transferred to the following desired set of conditions

$$\psi = X_1 = 9 \text{ rad}$$
$$\dot{\psi} = X_2 = 11 \text{ rad/sec}$$
$$\theta = X_3 = -10 \text{ rad}$$
$$\dot{\theta} = X_4 = 12 \text{ rad/sec}$$

where the corresponding target membership functions that define the acceptable region around the desired states are shown below.

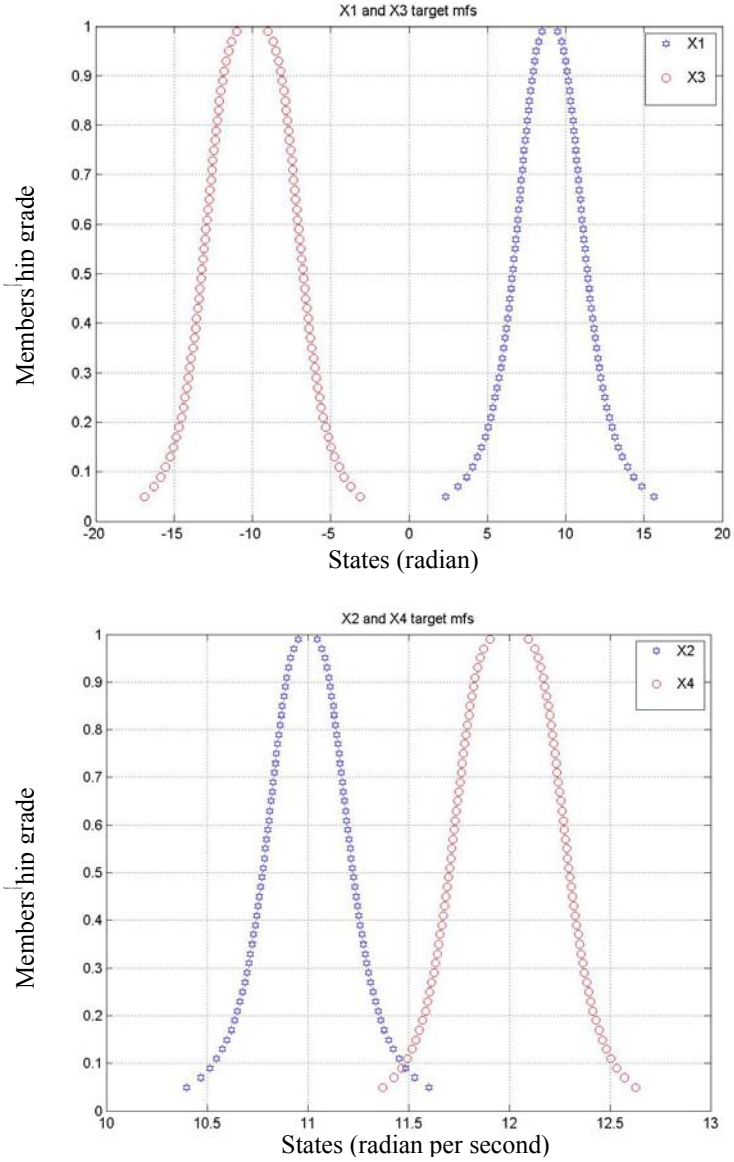

Figure 4.6 Target membership functions.

The propagation history, from the initial time of t=0 second to the final time t=10 second, can be found in appendix C (Propagation 1). According to figure 4.7 showing the target membership functions superimposed on the final membership functions, the system is controllable in the fuzzy sense.

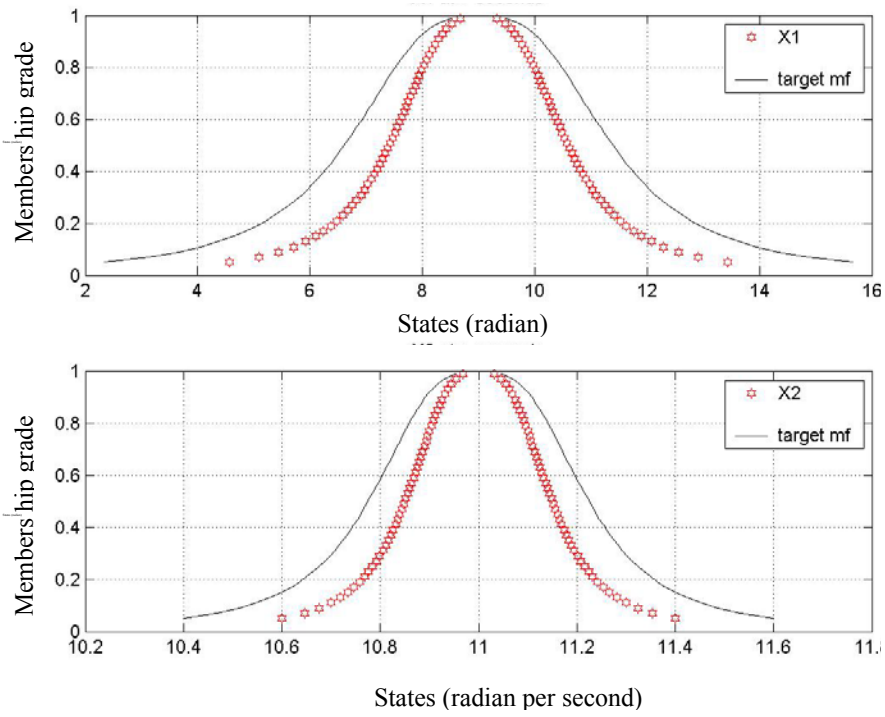

Figure 4.7(a) Membership functions at the final time

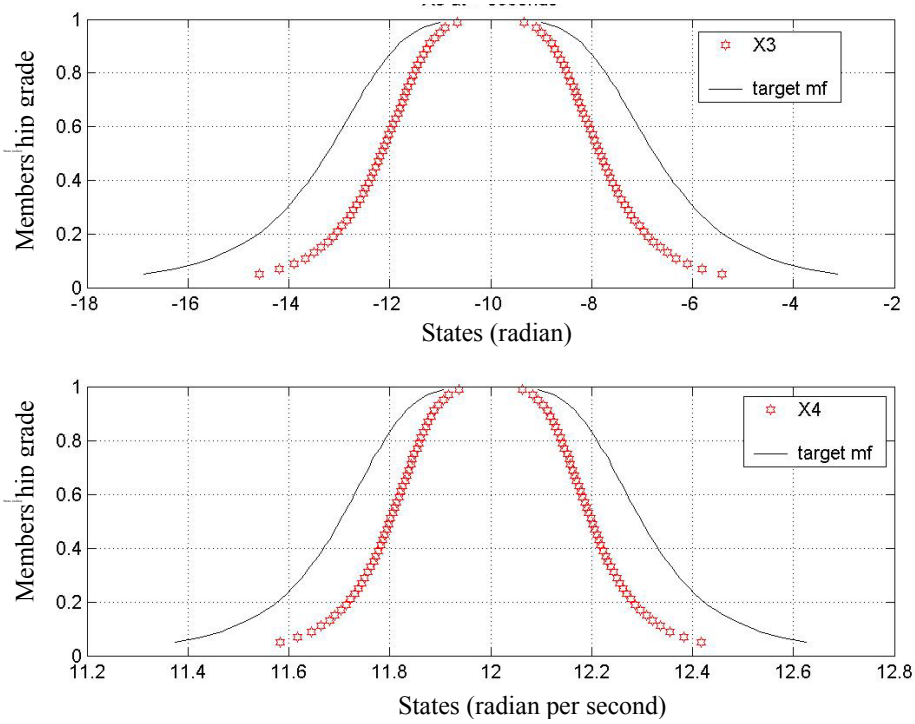

Figure 4.7(b) Membership functions at the final time.

It is evident that controllability in the fuzzy sense depends on the size and shape of the prescribed target membership function. One question that may arise is how such membership functions could be selected? The answer is; there is no strict rule as long as the selected membership functions are large and wide enough to contain all possible states as stated in theorem 3.1.ii.

A possible procedure for selecting such prescribed membership functions is as follows. First, pick an initial prescribed membership function for the states at time t_0, denoted $\mu^*_1(X_0)$ that contain the initial membership function, $\hat{\mu}_0(X_0)$ such that 3.1.ii is true for $t=t_0$. Second, perform the membership propagation procedure on $\mu^*_1(X_0)$, using (III.2.4-6) to bring its core region to the desired set of conditions which would yield the prescribed target membership function $\mu^*_1(X_1)$ for the states at time t_1.

This procedure is guaranteed to be valid because a close examination on (III.2.6), repeated here for convenient, would show that the membership function propagation is a linear transformation

$$\overline{X}_i^{\alpha}(t) = \phi(t,0) \cdot \overline{X}_i^{\alpha}(0) + \int_0^t \phi(t,\tau) \cdot B \cdot u(\tau) d\tau$$

$$\underline{X}_i^{\alpha}(t) = \phi(t,0) \cdot \underline{X}_i^{\alpha}(0) + \int_0^t \phi(t,\tau) \cdot B \cdot u(\tau) d\tau \qquad \text{(III.2.6)}$$

The first term of (III.2.6) is a matrix multiplication between the state transition matrix and the alpha cuts of the initial membership function. Let $T(q)$ denotes a multiplication between a matrix *T* and a vector *q*, for every constant *c* and *d*, it can be shown that

$$T(cx+dy)=c(T(x))+d(T(y)) \qquad \text{(IV.6.1)}$$

and therefore the operation is linear. The second term of (III.2.6) is just addition of two vectors. Hence, for a linear transformation, it is required that if x is transformed to x', then 2x must be transformed to 2x'. In our case, $\mu^*_1(X_0)$ represents a larger membership function than $\hat{\mu}_0(X_0)$ for all *X*. Therefore, the linear transformation that transfers $\hat{\mu}_0(X_0)$ to $\hat{\mu}_0(X_1)$ must also transfer $\mu^*_1(X_0)$ to $\mu^*_1(X_1) \geq \hat{\mu}_0(X_0)$.

4.7 Trajectory tracking using a proportional-derivative controller.

The purpose of this and the next section is to study the membership functions propagations under a traditional PD control. This section explains the goal and development of such controller. Simulation results show the performance of a PD

controller applied to the robotic grinder that has crisp states. The same controller is then applied to the robotic grinder with fuzzy states, computed through the membership functions propagation procedure. The results are shown in the next section.

In the previous sections, the open loop input (III.2.4) transfers the states to the desired location within a desired time interval. However, that is where the control ends. Neither the transient nor the steady state behavior or the issue of the system stability is addressed, which means there is no guarantee that the system stays at the desired states after the final time. Such control is impractical and there are better alternatives to accomplish a task such as trajectory tracking. One of which is to use a widely popular Proportional Derivative (PD) control law.

A PD controller is a combination of the proportional and derivative controller. The input of the proportional controller is an error signal between the actual plant output and a reference input (the desired states). The controller then outputs a control signal that is proportional to the error. The down side of this method is a possible large overshoot that can be reduced by a derivative controller. The output from a derivative controller is a constant gain that multiplies the rate of change of the error signal. In other words, the controller now acquires the ability to recognize how fast the plant output is approaching the set point and adjust its output accordingly.

Typical performance measures of a system are rise time, percent overshoot and settling time. For our system, the performance criterions are as follows:

From a stationary configuration, the states should be maintained at ψ=10 radian and θ = 20 radian with

Rise time < 1 s

Settling time < 2 s

Percent overshoot < 8%

Rise time measures the swiftness of the system's response. Specifically, it is defined as the time the trajectory takes to rise from 10% to 90%. Settling time and percent overshoot measures the system's ability to remain close to the set point. Percent overshoot is calculated by taking the percentage of the difference between the maximum (or minimum) of the trajectory and the set point as follows

$$P.O. = \frac{Peak - SetPo\,\text{int}}{SetPo\,\text{int}} \times 100\% \qquad \text{(IV.7.1)}$$

Settling time is defined as the time required for the system to remain within 8% of the set point.

A PD control law can be chosen for this controller such that the fictitious input u may be expressed as followed.

$$u = \ddot{q}_d - K_d \dot{e} - K_p e \qquad \text{(IV.7.2)}$$

$$\dot{e} = (\dot{q}_d - \dot{q})$$
$$e = (q_d - q)$$

q_d is the desired trajectories, e is the error signal and K_d and K_p are the proportional and the derivative gain. Equating the above equation with (IV.3.3) gives.

$$\ddot{q} = \ddot{q}_d - K_v \dot{e} - K_p e$$

$$\ddot{q} - \ddot{q}_d = -K_v \dot{e} - K_p e$$

$$\ddot{e} + K_d \dot{e} + K_p e = 0 \qquad \text{(IV.7.3)}$$

Comparing (IV.7.3) with the standard second order equation:

$$s^2 + 2\xi\omega_n s + \omega_n{}^2 = 0 \qquad \text{(IV.7.4)}$$

where ξ and ω_n are the damping ratio and the natural frequency of the system. The gains can be determined by matching coefficient

$$\begin{aligned} K_d &= 2\xi\omega_n \\ K_p &= \omega_n{}^2 \end{aligned} \qquad \text{(IV.7.5)}$$

Trajectory tracking is accomplished if K_p and K_d are chosen such that the error terms in equation (IV.7.3) asymptotically approach zero. This could be viewed as a regulation problem where the regulated variables are the error signals instead of the states. We want to force the error signals to zero, which may be achieved if the roots of equation (IV.7.3) have negative real parts. Two design parameters, namely ξ (damping ratio) and ω_n (natural frequency) need to be chosen. ξ is typically 0.707**,** which leaves ω_n as the only free variable. Larger ω_n provides faster response; causes larger percent overshoot and requires more control effort. Therefore, ω_n is chosen just so that the time responses requirements are satisfied**.**

Two simulation trails were performed with different ω_n. Both choices of ω_n satisfied all performance criterions. The error is reduced to zero and the states converge at the set point. Since there is no practical restriction such as physical limitations of an actuator, ω_n=10 rad/sec as in trail 1 is selected because of its faster response, which is deemed desirable. Important parameters of the simulation is summarized below

Table 4.3 Specified set point and performance criterions for the robotic grinder

Trail	**1**	**2**
Desired trajectory [φ θ]	[10 30]	[10 30]
Wn (rad/s)	10	5
ζ	0.707	0.707
Kd	14.142	7.07
Kp	100	25
Percent Overshoot	6	3.55
Rise Time (s)	0.271	0.548
Settling Time (s)	0.596	1.251

The time responses from both trails are shown below. Appendix A and B (NTR31.m, B.7) shows the respective MATLAB and SIMULINK programs that generate these responses.

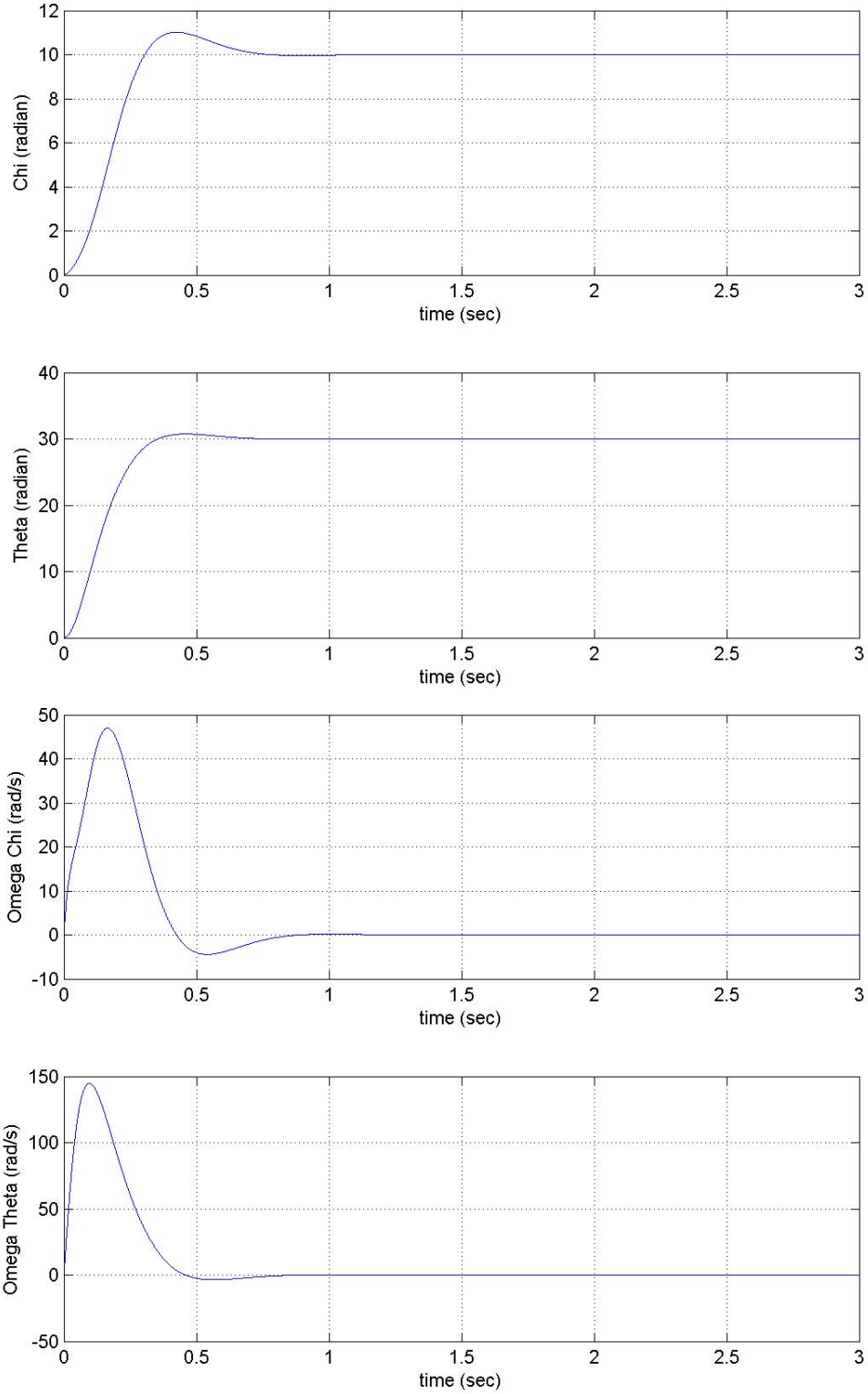

Figure 4.8 Time response of trial 1.

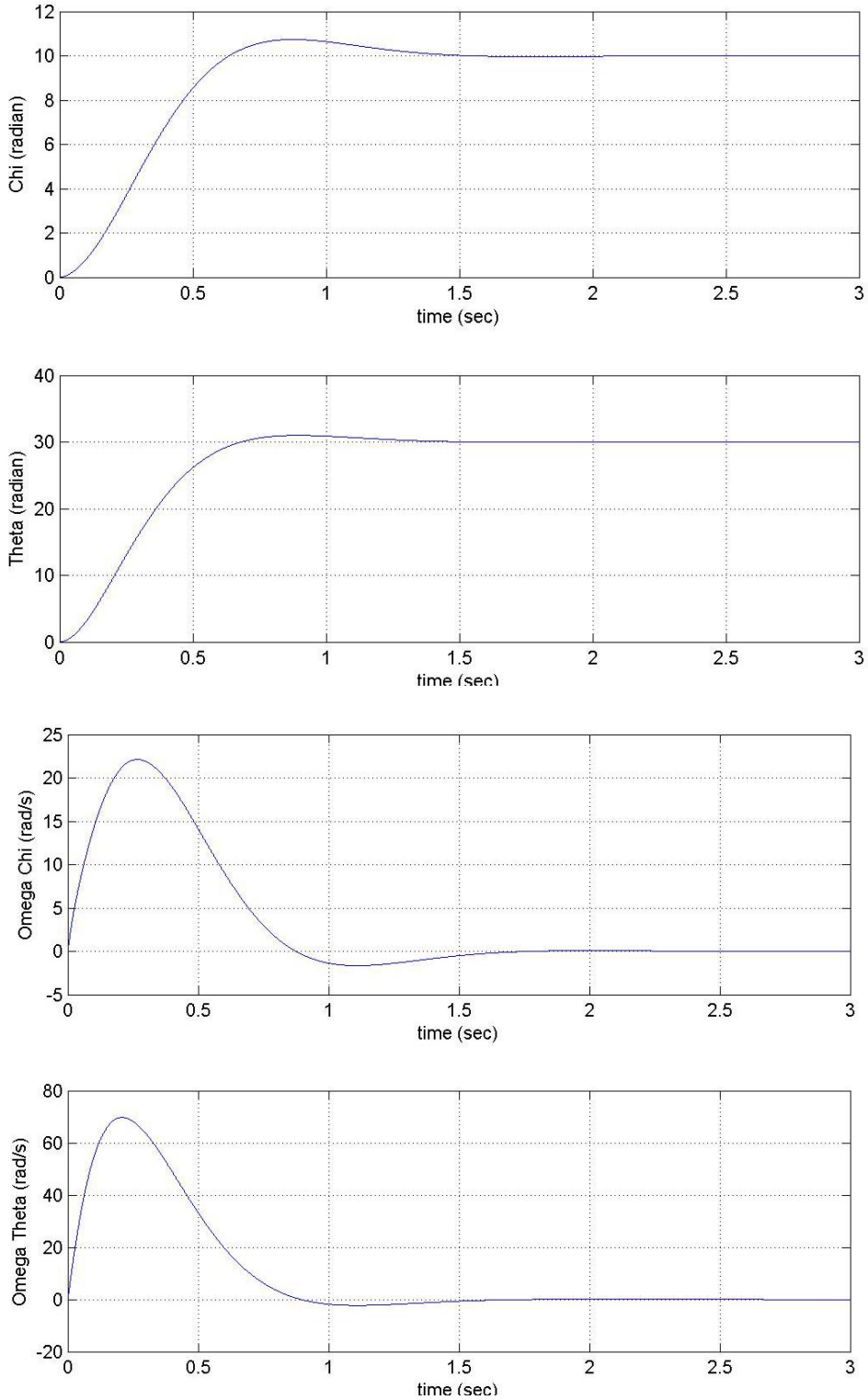

Figure 4.9 Time response of trial 2.

4.8 Fuzzy controllability under different controls design.

This section highlights an interesting observation: it is observed that the final shapes of the propagated membership functions are independent of the choice of control signals. The PD control scheme proposed in the previous section is applied to the robotic grinder with fuzzy states. Membership functions propagations procedure is used to produce a set of propagated membership function under the PD control. It is shown that this set is identical to another set of propagated membership function that is produced by the control function IV.4.4 or the minimum-energy control.

By the definition of controllability, the input that transfers the initial states X_0 to a desired location X_d does not need to be unique; instead, the importance is placed on its existence. In the context of general controllability (crisp states), if there exist one such input, chances are that there exist many other inputs that also transfer the states from X_0 *to* X_d because the path is not specified. The minimum-energy control is only one choice among many. The input given by the feedback control design system above is also an alternative.

However, when controllability in the fuzzy sense is considered; such may not be the case. Since fuzzy controllability is directly related to the set of prescribed membership functions, they too, must be taken under consideration. Intuitively, it is not obvious from III.2.6 that two sets of membership functions at a final time t_f is the same, if they result from the same system but controlled by two different choices of input that are intended to produce the same X_d from the same X_0.

A quick insight might jump to a conclusion that an input choice that is valid in a sense of one set of prescribed membership functions may not be valid in a sense of

another set of prescribed membership function and vice versa. An argument for this conclusion is as follows: the different input steers the states vector along different paths. As such, the states uncertainty of these two trails vary because the states themselves are at different location. Hence, the membership functions representing the states uncertainty must also have different shapes at time t_f, even though their core region are placed to the same X_d location.

The insight above is proven wrong by series of simulations that is presented below. The argument is flawed because it overlooks the linearity property of (III.2.6). As long as the same input is applied to all of the alpha cuts, the property holds. Although the intermediates trajectory path are different, linearity of the propagation dictates that if X is transferred to X_d then, cX (let cX be X^{α}) is transferred to cX_d ($X_d{}^{\alpha}$). This applies to all the alpha cuts and the final membership functions are identical as long as the input transfers the states to the same X_d.

Proposition 1: If there exist different sets of control signals u_1(t), u_2(t),…u_n(t) that transfer the system defined by (III.2.3) from the same set of initial states to the same set of desired states, then the membership functions at the desired states resulting from any control choices are identical. This implies that any set of prescribed target membership functions that is valid for u_1(t) is also valid for u_2(t),…u_n(t) and vice versa.

Two simulations demonstrate this through different input signals.

The first trail uses the minimum-energy control as given in IV.4.4 and is similar to results in 4.6. The obvious alternative to the first is to use the input resulting from the controller designed in the previous section. In both cases, the same control that is computed for the core region to reach X_d is applied to the entire membership function.

The MATLAB and SIMULINK programs used in simulations can be found in appendix A(NTR31, NTR33 and NTR_W2) and B (B.7 and B.8). Membership propagation history can be found in appendix C (Propagation 2 for the first control choice, Propagation 3 for the second control choice). The initial conditions are chosen to be at the origin. The desired trajectory is at $\psi = 100\,\text{rad}$ and $\theta = 30\,\text{rad}$ at time 3 seconds with zero angular velocity. The initial membership functions are shown below

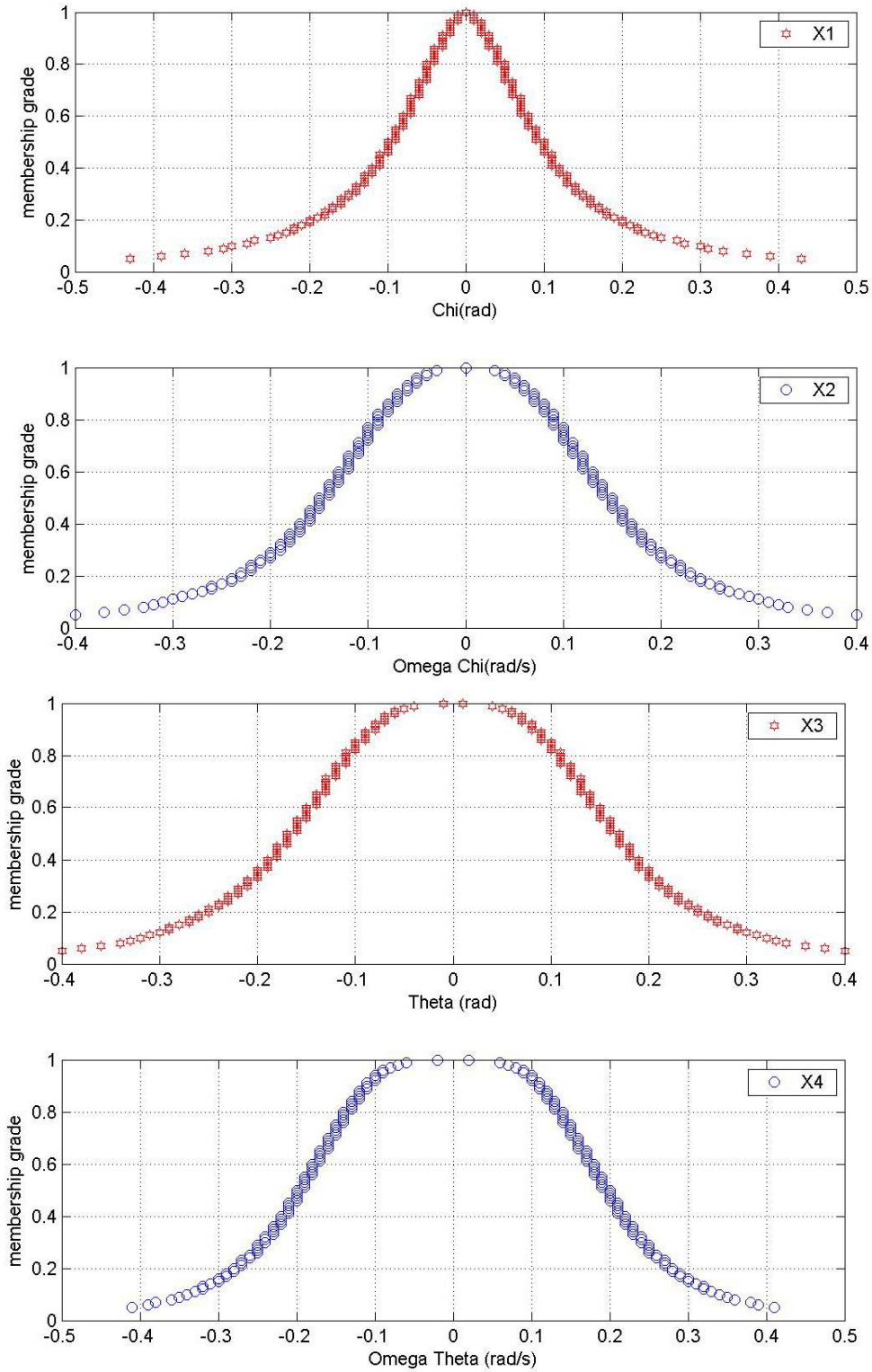

Figure 4.10 Initial membership functions.

The first choice of control signal produces the following result at time 3 seconds.

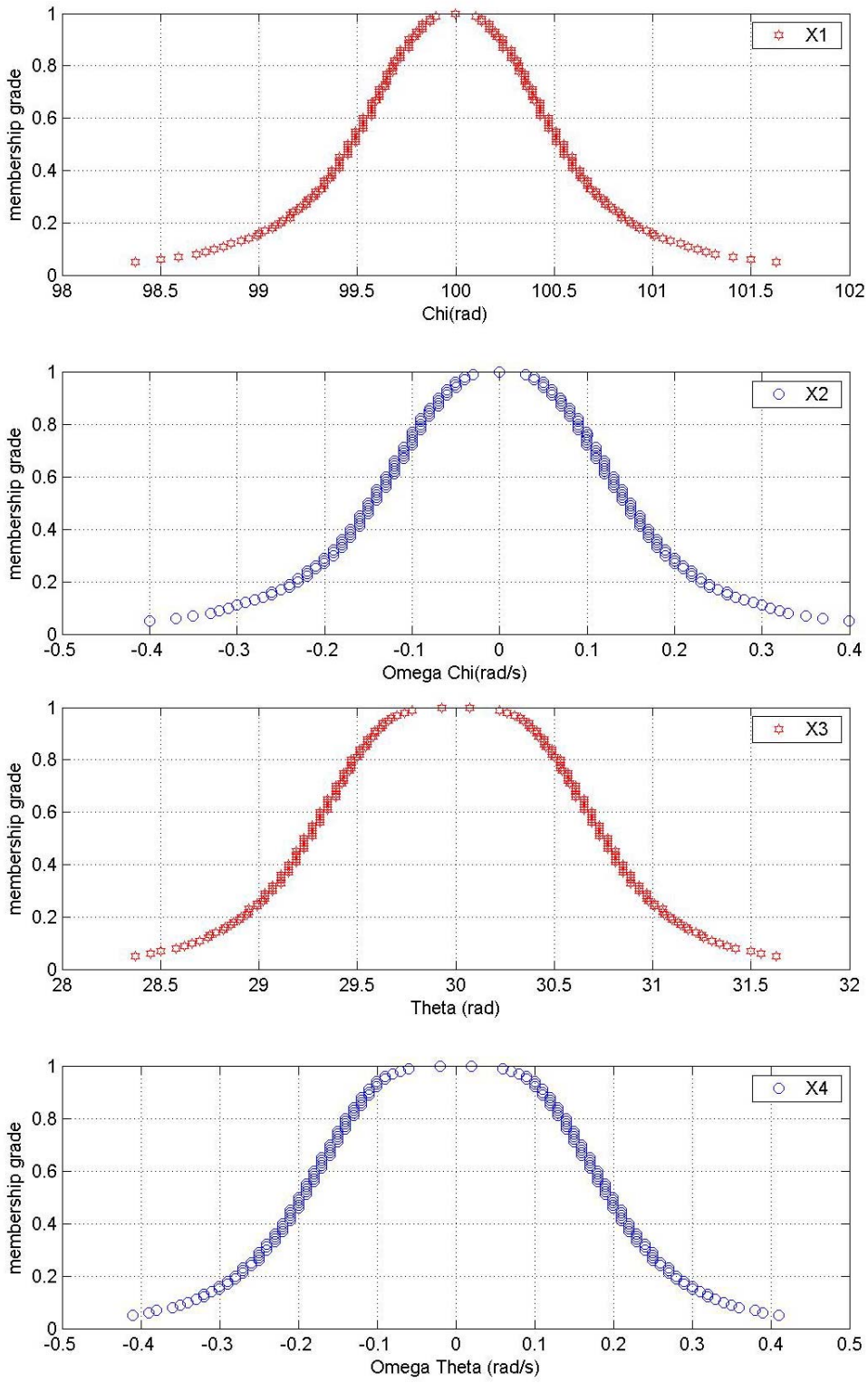

Figure 4.11 Membership functions [minimum-energy control] at time 3 seconds.

The second choice of control signal produces the following result at time 3 seconds.

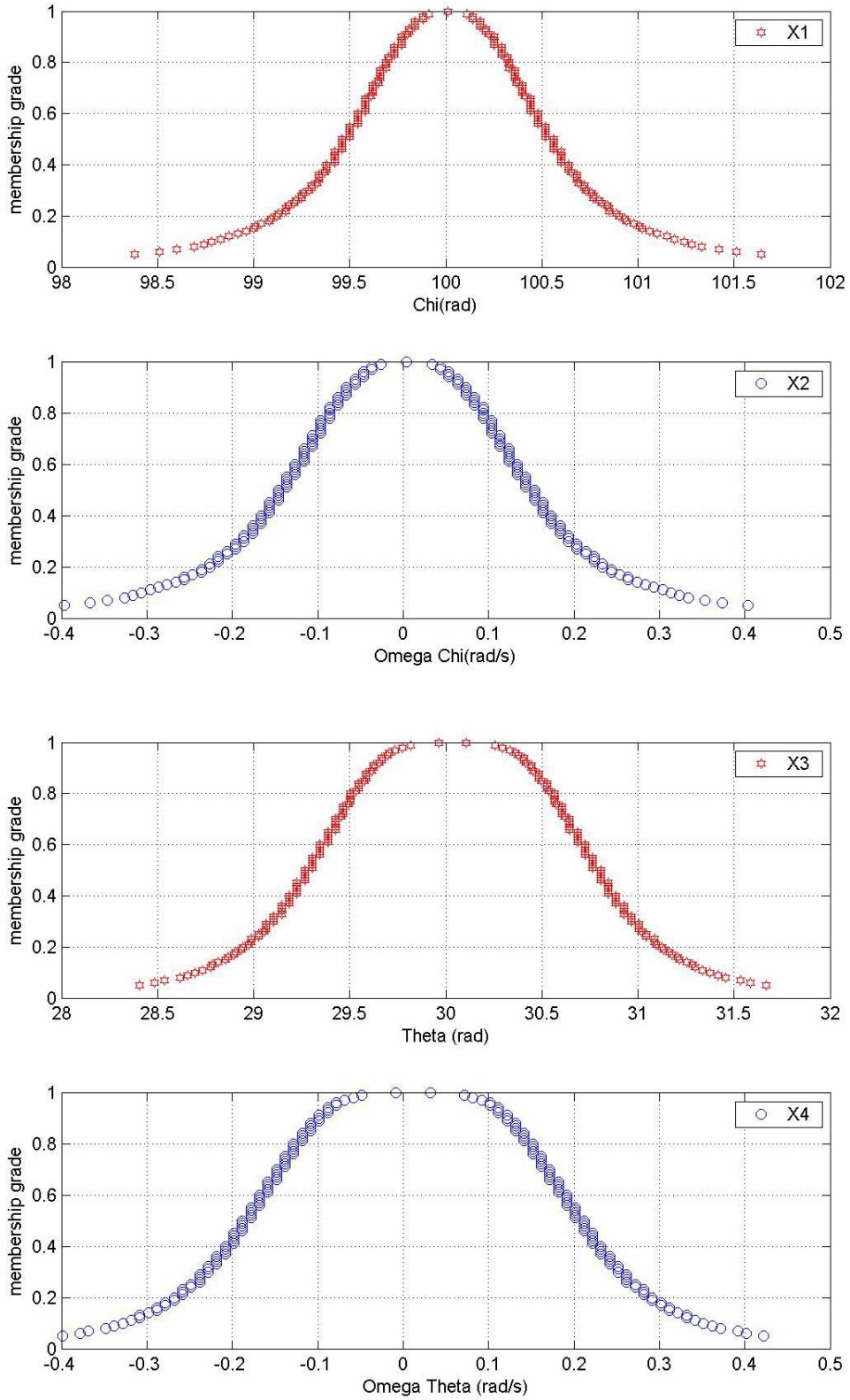

Figure 4.12 Membership functions [CTM with w_n at 10 rad/sec] at time 3 seconds.

Evidently, the two sets of membership function at 3 seconds are identical, despite the different intermediate trajectory as shown in their propagation history. The implication on controllability is that any prescribed target membership function that is valid for the first choice of control input would also be valid for the second choice of control input as well. For verification, another simulation is performed for the CTM design with w_n at 5 rad/sec. Due to lower controller frequency; the total simulated time is extended to 4 seconds (from 3 seconds) to assure steady states. At the 4 seconds, the final membership functions are identical to the previous two cases (with different intermediate trajectory, refer to propagation 4 in appendix C) which firmly prove the proposition above.

CHAPTER 5

CONCLUSIONS AND RECOMMENDATIONS

This chapter provides a conclusion of the work presented in this document. It highlights the major contributions and concludes with suggestions for further research.

5.1 Conclusions

The main objective of this work is to present membership functions propagation as a new tool for capturing the dynamical aspects of uncertainty in physical systems. Membership function is the central idea in fuzzy sets theory that represents uncertainty in the possibility aspect. Many existing theories discuss rules that govern static interactions of membership functions however, none of them discuss how or even if the membership functions evolve through time at all. In practicality, it is easy to see that this view alone portrays an incomplete account of uncertainty as they do certainly propagate with regards to the respective systems. This is where the major contribution of this work lies; it fulfills the absent account of how membership functions propagate through time.

The underlying supposition of this work is as follows; for linear systems, state uncertainty as represented by the membership functions undergoes the same linear transformation as the crisp states. That is, the solution to the state equations applies to the membership functions in their alpha cuts representation just as well, as seen by equation II.5.5. Because any set of state variables fully describes the behavior of the system and the membership function associated with each state variable receives the same linear transformations, the implication then ensues that the shape of the propagated

membership function reflects the behavior of the system's uncertainty as seen by the comparison of two different systems in section 2.6 and 2.7.

Upon consideration of the two traditional concepts in control; controllability and observability, it is proposed that additional requirements are needed to address these two concepts in the context of membership functions propagation. Since the possible states are spread over a range of value with varying membership grades, it is no longer sufficient to speak of the desired trajectory merely as crisp points. They too, must be represented by a set of separated membership functions, one for each state called the target membership functions, when the question of controllability is addressed. Of course, the system is controllable in the fuzzy sense only if the propagated membership functions are subset of their target membership functions. As for observability, the estimated set of initial conditions also becomes a set of estimated membership functions, where each initial alpha cuts is calculated using equation III.3.4 applied to the known current states. Therefore, the observable task is accomplished if and only if the estimated set of initial membership functions are subset of an acceptable initial bound similarly represented by another larger set of membership functions.

As seen, subsethood becomes the key concept when tackling either controllability or observability in the fuzzy sense. The proposed conditions for both concepts suggest that the propagated membership functions, in controllability, and the estimated initial membership functions are contained within their respective bounds. Literally 3.1.(ii) and 3.2.(ii) translate to the bounds having higher membership grades. This, in turn, is the same as declaring that if the bound at a particular state has a membership value of zero, then it is not possible that the actual trajectory lies in that state. More importantly, the

subsethood condition dictates that the fuzzy controllability and observability are valid in the sense of specific prescribed bounds only. The possibility of having a generally fuzzy controllable or fuzzy observable system is ruled out because the shape of the actual membership function may changes and a set of prescribed bounds that is valid for one set of actual membership function may not be valid for another.

Finally, it is shown in chapter 4 that although the membership functions propagation is designated for linear system, its application fits equally well for a non-linear system under control from the computed torque method (CTM). Chapter 4 also demonstrates another proposition that may be counter intuitive at first. The proposition claims that in the final shape of the propagated membership functions depend only on the initial membership functions shape and the final desired trajectory alone. It is independent of the choices of control signals. As in all previously proposed theories, this proposition is supported by MATLAB and SIMULINK simulations results which can be found in the appendix.

5.2 Recommendations for future work.

This work resulted in successful demonstration of the membership functions propagation as a tool for describing dynamic uncertainty in a sense that it describes how uncertainty evolve through time. However, there are other opportunities that deserve further investigation.

In chapter 3, definitions and criteria for controllability and observability in the fuzzy sense are established. Controllability and observability in the fuzzy sense differ from their classical counterparts by the subsethood requirement which command a

perscribed target membership function to contain the propagated membership function in controllability and the estimated initial membership function in observability. While this is a sufficient framework for controllability and observability in the fuzzy sense, it effectively allows only two possible answers to the controllability and observability question. That is, either the system is controllable or observable in the sense of a particular prescribed target membership function, or it is not. In this way, this approach provides a crisp solution to a question that is stated in a fuzzy sense.

Is there a way to provide a fuzzy answer to the same question? Clearly, this is of great interest: the expression of controllability or observability in the fuzzy sense to a degree. They could be called fuzzy controllability and fuzzy observability. Since this work sufficiently established controllability and observability in the fuzzy sense, one way to develop fuzzy controllability and observability is to extend on the concepts proposed by this work.

One possible extension for fuzzy controllability is as follow: the degree of controllability can be viewed as the degree of subsethood of the fuzzy set *B*, which is represented by the target prescribed membership function in question, in set the fuzzy *A*, which is represented by another membership function. The system is controllable in the sense of the membership function that represents the fuzzy set *A*.

Let $\mu^*_1(\cdot)$ be a target prescribed membership function defined over the set of state at time t_1 denoted X_1 and $X, \overline{X}_1 \in X_1$. Furthermore, let $\hat{\mu}_1(\cdot)$ be the membership function describing the state at time t_1. Suppose the subset hood condition

$$\exists \overline{X}_1 \text{ such that } \mu^*_1(X - \overline{X}_1) \geq \hat{\mu}_1(X - \overline{X}_1) \quad \forall X \in X_1 \qquad \text{(V.2.1)}$$

is not satisfied, that is, $\exists X \in X_1$ in which $\mu^*_1(X - \overline{X}_1) < \hat{\mu}_1(X - \overline{X}_1)$ then one could find another target prescribed membership function $\tilde{\mu}_1(\cdot)$ such that

$$\exists \overline{X}_1 \text{ such that } \quad \tilde{\mu}_1(X - \overline{X}_1) \geq \hat{\mu}_1(X - \overline{X}_1) \quad \forall X \in X_1 \qquad \text{(V.2.2)}$$

The next step in answering the question " To what degree that the system is controllable in the sense of $\mu^*_1(\cdot)$?" would be to calculate the degree of subsethood of $\mu^*_1(\cdot)$ in $\tilde{\mu}_1(\cdot)$ by following the formula

$$S(B, A) = \frac{|B \cap A|}{|B|} \qquad \text{(V.2.3)}$$

where the fuzzy set *B* and the fuzzy set *A* are represented by the membership functions $\mu^*_1(\cdot)$ and $\tilde{\mu}_1(\cdot)$ respectively. The degree of subsethood of *B* in *A*, *S(B,A)*, is the that the system is controllable in the sense of $\mu^*_1(\cdot)$. Similarly, a parallel approach can be developed for fuzzy observability.

All simulations results that are presented as support to the theories in this work have been for a continuous, linear time invariant systems. Although it is not expected that the transition from continuous to discrete systems would drastically alter the synopsis provided by the theory, it would still be of great interest to study results from simulated discrete systems. In a similar manner, the proposed theory also holds for time variant systems which still lack simulation evidences. Therefore simulation results that support the theory for such systems would be particularly interesting.

The recommendations above share one common feature; their results are expected to follow the predictions given by the membership functions propagation process. To create a genuine contribution, it is necessary to provide a novel result. This can be achieved by examining the underlying supposition of this work; linearity. The system

under consideration must be linear, or capable of being reduced to linear system. Unfortunately, such capability may become a luxury that rarely presents itself as many practical systems are inherently non-linear. Therefore, the first recommendation is to develop a parallel theory that describes non-linear dynamic uncertainty.

Such development pledges difficulty. Non-linear dynamic are generally less understood and consequently, to unearth a unifying statement that address the dynamic uncertainty of non-linear system is no trivial task. In addition, all benefits that stem from linearity of the system vanish. And in their places, a collection of traditional non-linear issues provide opportunities for further research and therefore, the development of a non-linear dynamic account of uncertainty will truly be ground breaking.

Lastly, this final recommendation may be viewed as ambitious and imaginative. As mentioned in the first paragraph of Chapter 1, uncertainty is prevalent in daily lives. Similarly, uncertainty propagation is also prevalent. The most conspicuous example of such propagation is in verbal communication which is inherently inferential. Cognitive inference is a powerful process. It enables us to easily extract content from incomplete input but it is also a source of uncertainty. Human beings make inferences based on mental models [7] which are internal representations of what really exist in the real world. Surely, different people have varying mental models, based on their differing interpretation of the real world. As information propagates, its content is inferred through various mental models and finally the original meaning is concealed in tiny fraction of the whole package; this is the generation of rumor.

Example of such process is as follows:

Original messages,: Tom argued that Bob's policy would significantly decrease our company's market share. I think Tom is right, he is a smart guy. We need a smart guy to be a marketing director.

Transmission 1: Tom pointed out flaws in Bob's policy; he should be a marketing director.

Transmission 2: Tom says that Bob is wrong and he should replace Bob as marketing director.

Transmission 3: Tom desperately wants to replace Bob; he thinks Bob unfit for the job.

Transmission 4: Tom tries to topple Bob down from the director's chair.

As shown, rumor propagates as there are always rooms for interpretation in spreading the words of mouth. Therefore, the last recommendation is that the fuzzy theory could expand into this realm. Specifically, propagation of uncertainty is certainly not limited to physical systems alone. In fact, it is a widespread characteristic that is fundamental to any processes that involve human interactions. An improved understanding in this subject will most likely benefits many disciplines such as information systems, intelligent systems, and machine-human interface, etc.

Keeping in mind that the major difference now becomes the fact that the system under consideration is no longer a mindless physical system, but human being whose behaviors are fuzzy by nature, there must be various tasks fit for the application of fuzzy theory. While many tasks are irrelevant to this work, there are multiple architectures that cognitive scientists, behaviorist, computer scientist and sociologist employ to model human behavior such as script and production system [7]. From the author's point of view, mergers between fuzzy theory and the said architectures are possible, novel and

innovative. Such is a multidisciplinary effort that forges ideas from different fields which could hopefully provide meaningful contributions and advancements to science.

APPENDIX A

MATLAB PROGRAMS

CUTOFF.m

```
% Author: Attapong Terdpravat
% January 08,2004.
% This function returns the min and max of each alpha cuts.

function[rmin,rmax]=cutoff(acut,mem,T)
%acut*the alpha value
%mem *membership grade of T to be cut.
%T   *the universal set in which mem is defined.

acount=0;%var to count how many point above each cut

for i = 1:1:length(mem)
  if (mem(i) >= acut)
        acount=acount+1;
          d(acount)=T(i);

    end%if
end%i for

rmin=min(d);
rmax=max(d);
```

NTEST12.m

```
% Author: Attapong Terdpravat
% May 05,2004.
% This program demonstrates mfs propagation
% 1) creates membership functions
% 2) takes alpha cuts, using another program “cutoff”.
% 3) defines systems in the state space representation.
% 4) input is set to zero.
% 5) simulated using the lsim function.
clear all
%1)
left1=0;
left2=1.5;
right1=6;
right2=4.5;
ofs = 3; % the initial condition of mf1
ofs2= 3;% the initial condition of mf2

T = (0:0.03:6);

% shape parameter for the generic bell membership function

X10 = trimf(T,[left1,ofs,right1]);
```

```
X20 =trimf(T,[left2,ofs2,right2]);

a_increment=0.02;
tolerance=0.1*a_increment;

%taking the alpha cut
acut=(0.02:a_increment:1)';
acut=acut-1*tolerance;

%2)
%calling cut off here

for k=1:1:length(acut)
   [min1(k),max1(k)] =cutoff(acut(k),X10,T);
   %added line below to get a cut of X20
   [min2(k),max2(k)] =cutoff(acut(k),X20,T);
end
%----------------
%3)
syms s t1
 m=1;
 l = 10;
 g = 9.8;
 A = [0 1;-1.5*(g/l) 0];
 B = [0;3/(m*l^2)];
 C=[1 0;0 1];
 D=[0;0];
sys=ss(A,B,C,D);
%--initial and desired condition
  x0=[ofs;ofs2];
  xd = [1;10];

%---state transition matrix and itstranspose
 stm=ilaplace(inv(s*eye(2)-A));
 stmtp=transpose(stm);
%--- must note
%    t=t1-t
%--controllability grammian
tt=10;
t=tt;
t_incre=0.1;
Wc=int(stm*B*B'*stmtp,0,tt);
Wc_val = eval(Wc);
stm_val=eval(stm);
%----------------
%4)
 t2 = [0:t_incre:tt];
```

```
  for i=1:1:length(t2)
      t=tt-t2(i);% t=t1-t;
        u(i)=0;

end%for

%---simulation---%
 t = t2;
 for i=1:1:length(acut)
     lower_x(:,i)=[min1(i);min2(i)];
     upper_x(:,i)=[max1(i);max2(i)];
     %s for simulated
     s_lower{i}=lsim(sys,u,t,lower_x(:,i));
     s_upper{i}=lsim(sys,u,t,upper_x(:,i));
end

%-------------------------END OF NTEST12.m----------------%
```

NT2.m

```
% Author: Attapong Terdpravat
% May 05,2004.
% This program plots results for NTEST11S,NTEST12,MPP.
% 1)get time index
% 2)transform data
% 3)plot.


%1)
clf

t3=input('enter time (no smaller than 0.1 decimal digit)(0-
10)')

t_index = round(t3/t_incre+1);

%2)

for i=1:1:length(acut)
    x1out_lower(i)=s_lower{i}(t_index,1);
    x1out_upper(i)=s_upper{i}(t_index,1);
    x2out_lower(i)=s_lower{i}(t_index,2);
    x2out_upper(i)=s_upper{i}(t_index,2);
end
%
 X1t = [x1out_lower;x1out_upper];
 X2t = [x2out_lower;x2out_upper];
```

```
%3)
 plot(X1t,acut,'xr--',X2t,acut,'ob--')
 grid
 xlabel('states')
 ylabel('membership grade')
 legend('x1','','x2')

%-------------------------END OF NT2.m---------------%
```

MPP.m

```
% Author: Attapong Terdpravat
% May 06,2004.
% This program demonstrates mfs propagation.
% 1) creates membership functions
% 2) takes alpha cuts, using another program “cutoff”.
% 3) defines systems in the state space representation.
% 4) input is set to zero.
% 5) simulated using the lsim function.

%1)
clear all

ofs = 1.5; % the initial condition of mf1
ofs2= 1.5;% the initial condition of mf2
T =(-
max(abs(ofs),abs(ofs2))*10:0.01:max(abs(ofs),abs(ofs2))*10)
;

% shape parameter for the Triangular membership function

 X10 = trapmf(T, [0.5 1 ofs 2]);
 X20 = trapmf(T, [-1  ofs2 4 6.5]);

a_increment=0.02;
tolerance=0.1*a_increment;

%taking the alpha cut
acut=(0.05:a_increment:1)';
acut=acut-1*tolerance;

%2)
 for k=1:1:length(acut)
   [min1(k),max1(k)] =cutoff(acut(k),X10,T);
   %added line below to get a cut of X20
   [min2(k),max2(k)] =cutoff(acut(k),X20,T);
end
%-------------------
tt=10;
```

```
t=tt;
t_incre=0.1;
T=(0:t_incre:tt);
%------------------
%3)
syms s
 m=1;
 l = 10;
 g = 9.8;
 A = [0 1;-1.5*(g/l) 0];
 B = [0;3/(m*l^2)];
 C=[1 0;0 1];
 D=[0;0];
%gain matrix
P=[-1.5 -1];
K = PLACE(A,B,P);
Abar=A-B*K;
sys=ss(Abar,B,C,D);

syms s t;
I = eye(length(A));
ev = eig(Abar)
stm =ilaplace(inv(s*I-Abar));

%4)
%zero input
for i=1:1:length(T)
        u(i)=0;

end%for

%5)
for j=1:1:length(acut)
     lower_x(:,j)=[min1(j);min2(j)];
     upper_x(:,j)=[max1(j);max2(j)];
%s for simulated
     s_lower{j}=lsim(sys,u,T,lower_x(:,j));
     s_upper{j}=lsim(sys,u,T,upper_x(:,j));
end

%-------------------------END OF MPP.m--------------------%
```

NTEST11S.m

```
% Author: Attapong Terdpravat
% June 17,2004.
% This program demonstrates fuzzy controllability
% 1) creates membership functions
% 2) takes alpha cuts, using another program “cutoff”.
```

```
% 3) defines systems in the state space representation.
% 4) calculate input.
% 5) simulated using the lsim function.

%1)
 clear all

ofs = 0; % the initial condition of mf1
ofs2= 0;% the initial condition of mf2

T=(-5:0.01:5);
% shape parameter for the generic bell membership function
w = 0.6 ; %width of mf 1
sh =1.2; %sharpness of mf 1
w2 = 0.2 ; %width of mf 2
sh2 =0.8; %sharpness of mf 2

X10 = gbellmf(T,[w,sh,ofs]);
X20 =gbellmf(T,[w2,sh2,ofs2]);

a_increment=0.05;
tolerance=0.1*a_increment;

%taking the alpha cut
acut=(0.01:a_increment:1)';
acut=acut-1*tolerance;
%calling cut off here

%2)
for k=1:1:length(acut)
   [min1(k),max1(k)] =cutoff(acut(k),X10,T);
   %added line below to get a cut of X20
   [min2(k),max2(k)] =cutoff(acut(k),X20,T);
end
%---------------
%3)
syms s t1
 m=1;
 l = 1;
 g = 9.8;
 A = [0 1;-1.5*(g/l) 0];
 B = [0;3/(m*l^2)];
 C=[1 0;0 1];
 D=[0;0];
sys=ss(A,B,C,D);
%--initial and desired condition
  x0=[ofs;ofs2];
```

```
  xd = [30.1;10.1];

%---state transition matrix
 stm=ilaplace(inv(s*eye(2)-A));
 stmtp=transpose(stm);%stm' does not work
%--- must note
%    t=t1-t
%--controllability grammian
tt=1;
t=tt;
t_incre=0.1;
Wc=int(stm*B*B'*stmtp,0,tt);
Wc_val = eval(Wc);
stm_val=eval(stm);
%----------------
%4)
 t2 = [0:t_incre:tt];
  for i=1:1:length(t2)
      t=tt-t2(i);% t=t1-t;
        u(i)=eval(B'*stmtp*inv(Wc_val)*(xd-stm_val*x0));

end%for

%5)
%---simulation---%
 t = t2;
 for i=1:1:length(acut)
     lower_x(:,i)=[min1(i);min2(i)];
     upper_x(:,i)=[max1(i);max2(i)];
%s for simulated
     s_lower{i}=lsim(sys,u,t,lower_x(:,i));
     s_upper{i}=lsim(sys,u,t,upper_x(:,i));
end
%---------------------END OF NTEST11S.m-------------------%
```

OBF.m

```
% Author: Attapong Terdpravat
% January 8,2004
% This program calculates the initial condition.
% 1) Define system.
% 2) Simulate system.
% 3) Find observability Grammian
% 4) perform the numerical integration according to formula
clear all
syms s t1
m=1;
 l = 10;
 g = 9.8;
```

```
 A = [0 1;-1.5*(g/l) 0];
 B = [1;0];
 C=[1 1];
 D=[0];
sys=ss(A,B,C,D);

stm=ilaplace(inv(s*eye(2)-A));
 stmtp=transpose(stm);

t_incre=0.01;
tt=1;
t=[0:t_incre:tt];
x0=[21;0.5];

for j=1:1:length(t)
    u(j)=0;
end
[Y,T,X]=lsim(sys,u,t,x0);

 %--__--__--__--__--%--__--__--__--__--%
 %    for the final integral, integ as Y and time as X %
 %    pass it into nint (area under curve of integrand)%
 %--__--__--__--__--%--__--__--__--__--%

%observability grammian.
 V=int(stmtp*C'*C*stm,0,tt);
 Val=eval(V);
 Vi=inv(Val);

% produce integrand
for i =1:1:length(T)
    t=T(i);
    stmtp_val=eval(stmtp);
    integ(:,i)=stmtp_val*C'*Y(i);
end
 %--__--__--__--__--%--__--__--__--__--%
%   numberical integration              %
 %--__--__--__--__--%--__--__--__--__--%
n=length(T);
N=n-1;
M=(T(n)-T(1))/(3*N);

W(1)=1;
W(n)=1;

for i=2:1:n-1
    if  mod(i,2)==0
```

```
        % even then 4
        W(i)=4;
    else if mod(i,2)==1
            % odd then 2
            W(i)=2;
        end%if
    end%if
end%for

wy=M*W*integ' %product of numberical integration
Xov=Vi*wy'
%----------------------END OBF--------------------------%
```

NTR_W2.m

```
% Author: Attapong Terdpravat
% January 24,2004.
% Membership propagation for robotic grinder.
% 1) creates desired and initial condition
% 2) calculate gain.
% 3) calculate input
% 4) assign values to robot parameter
% 5) generate membership functions and get their alpha cuts
% 6) iteratively run simulink robo_w2 to simulate the robot
%    for each cuts. .
clear all

%===intial condition===%
chio= 0;
chidoto=0;
thetao=0;
thetadoto=0;%

chid=100;
chidotd=0;
thetad=30;
thetadotd=0;

x0=[chio;chidoto;thetao;thetadoto];
xd=[chid;chidotd;thetad;thetadotd];

%===system definition===%
syms s t1

A=[0 1 0 0;0 0 0 0;0 0 0 1;0 0 0 0];
B=[0 0;1 0;0 0;0 1];
C=[1 0 0 0; 0 0 1 0];
%C=[1 0 1 0];
D=[0];
```

```
% K=place(A',C',[-32;-33;-34+j;-34-j]);
K=place(A',C',[-123;-125;-124+j;-124-j]);
Lu=K';
sys=ss(A,B,C,D);
%---state transition matrix and its transpose
 stm=ilaplace(inv(s*eye(4)-A));
 % note here that transpose(stm) not equal to stm'
 stmtp=transpose(stm);

%--- must note
%    t=t1-t
%--controllability grammian
tt=3;
t=tt;
t_incre=0.0005;
% smaller stepsize allow more negative poles for K (line
40) which
% gives better observer responses.
Wc=int(stm*B*B'*stmtp,0,tt);
Wc_val = eval(Wc);
stm_val=eval(stm);
%----------------
 t2 = [0:t_incre:tt];
  for i=1:1:length(t2)
      t=tt-t2(i);% t=t1-t;
        open_u(:,i)=eval(B'*stmtp*inv(Wc_val)*(xd-
stm_val*x0));
end%for
%----------------
t=t2;
w1=1;
m1=0.3;%kg
m2=0.6;%kg
R=0.25;%m
L=0.75;%m
I1=0.5*m1*R^2;
I2=0.25*m1*R^2+(m1+(1/3)*m2)*L^2;
%-----------------------------------------------%
%---------generates four membership function---%
%-----------------------------------------%
a_increment=0.01;
tolerance=0.01*a_increment;
% shape parameter for the generic bell membership function
w =[0.1;0.15;0.17;0.2];
sh=10*w;
%-----------------------------------------------
T=(-2:a_increment:2);
```

```
%-----------------------------------------------
X10p = gbellmf(T,[w(1),sh(1),x0(1)]);
X20p = gbellmf(T,[w(2),sh(2),x0(2)]);
X30p = gbellmf(T,[w(3),sh(3),x0(3)]);
X40p = gbellmf(T,[w(4),sh(4),x0(4)]);

X10ptg = gbellmf(T,[1.5*w(1),sh(1),x0(1)]);
X20ptg = gbellmf(T,[1.5*w(2),sh(2),x0(2)]);
X30ptg = gbellmf(T,[1.5*w(3),sh(3),x0(3)]);
X40ptg = gbellmf(T,[1.5*w(4),sh(4),x0(4)]);


%taking the alpha cut
acut=(0.05:a_increment:max(X10p))';
acut=acut-1*tolerance;
%calling cut off here

for k=1:1:length(acut)
    %return [lower cut,upper cut]
   [min1(k),max1(k)] =cutoff(acut(k),X10p,T);
   [min2(k),max2(k)] =cutoff(acut(k),X20p,T);
   [min3(k),max3(k)] =cutoff(acut(k),X30p,T);
   [min4(k),max4(k)] =cutoff(acut(k),X40p,T);
 %target mf
   [min5(k),max5(k)] =cutoff(acut(k),X10ptg,T);
   [min6(k),max6(k)] =cutoff(acut(k),X20ptg,T);
   [min7(k),max7(k)] =cutoff(acut(k),X30ptg,T);
   [min8(k),max8(k)] =cutoff(acut(k),X40ptg,T);
end
X10=[min1',max1'];
X20=[min2',max2'];
X30=[min3',max3'];
X40=[min4',max4'];
%target mf
X10tg=[min5',max5'];
X20tg=[min6',max6'];
X30tg=[min7',max7'];
X40tg=[min8',max8'];
%-----------------------------------------------%
%  S   I  M   U  L  A  T  I  O  N %
%-----------------------------------------------%
% change simulation time paramter

% For each acut (loop from acut 1 to k)
%   -change initial conditions(4 of them) AND the output
dataname to workspace (four of them)
% this is for lower cut
```

```
%should open robo before running else it gives warning
open robo_w2

ttt=num2str(tt);
set_param('robo_w2','StopTime',ttt)
tfx=num2str(t_incre);
set_param('robo_w2','fixedstep',tfx)

for i =1:1:length(acut)
% change initial conditions
a=num2str(X10(i,1));
    set_param('robo_w2/Actin/chiic','value',[a]);
b=num2str(X20(i,1));
    set_param('robo_w2/Actin/chidic','value',[b]);
c=num2str(X30(i,1));
    set_param('robo_w2/Actin/thetaic','value',[c]);
d=num2str(X40(i,1));
    set_param('robo_w2/Actin/thetadic','value',[d]);
    %for the target mfs
e=num2str(X10tg(i,1));
    set_param('robo_w2/targin/chiic','value',[e]);
f=num2str(X20tg(i,1));
    set_param('robo_w2/targin/chidic','value',[f]);
g=num2str(X30tg(i,1));
    set_param('robo_w2/targin/thetaic','value',[g]);
h=num2str(X40tg(i,1));
    set_param('robo_w2/targin/thetadic','value',[h]);
%Y is the plant output and Y2 is the output from observer
[T,LX{i},LY{i},LY2{i},LY3{i}]=sim('robo_w2');

end
LX=0;
% repeat for upper cut
for j =1:1:length(acut)
% change initial conditions
a=num2str(X10(j,2));
    set_param('robo_w2/Actin/chiic','value',[a]);
b=num2str(X20(j,2));
    set_param('robo_w2/Actin/chidic','value',[b]);
c=num2str(X30(j,2));
    set_param('robo_w2/Actin/thetaic','value',[c]);
d=num2str(X40(j,2));
    set_param('robo_w2/Actin/thetadic','value',[d]);
     %for the target mfs
e=num2str(X10tg(j,2));
    set_param('robo_w2/targin/chiic','value',[e]);
f=num2str(X20tg(j,2));
```

```
    set_param('robo_w2/targin/chidic','value',[f]);
g=num2str(X30tg(j,2));
    set_param('robo_w2/targin/thetaic','value',[g]);
h=num2str(X40tg(j,2));
    set_param('robo_w2/targin/thetadic','value',[h]);
%Y is the plant output and Y2 is the output from observer
[T,UX{j},UY{j},UY2{j},UY3{j}]=sim('robo_w2');
end
UX=0;
%return  LX and UX to nil to save memory.
%-----------------------END NTR_W2-----------------------%
```

NTRT_W2.m

```
% Author: Attapong Terdpravat
% January 24,2004.
% This program plots simulation result from ntr_w2.

t_index = round(t3/t_incre+1);% t3/5
% t_index=length(T);
for k=1:1:length(acut)
    %lowercut is first col
    %upper cut is second col
     X1d(k,1)=LY{k}(t_index,1);
     X1d(k,2)=UY{k}(t_index,1);

     X2d(k,1)=LY{k}(t_index,2);
     X2d(k,2)=UY{k}(t_index,2);

     X3d(k,1)=LY{k}(t_index,3);
     X3d(k,2)=UY{k}(t_index,3);

     X4d(k,1)=LY{k}(t_index,4);
     X4d(k,2)=UY{k}(t_index,4);
     % from the observer
     X1ob(k,1)=LY2{k}(t_index,1);
     X1ob(k,2)=UY2{k}(t_index,1);

     X2ob(k,1)=LY2{k}(t_index,2);
     X2ob(k,2)=UY2{k}(t_index,2);

     X3ob(k,1)=LY2{k}(t_index,3);
     X3ob(k,2)=UY2{k}(t_index,3);

     X4ob(k,1)=LY2{k}(t_index,4);
     X4ob(k,2)=UY2{k}(t_index,4);

     % for the target mf
     X1tg(k,1)=LY3{k}(t_index,1);
```

```
     X1tg(k,2)=UY3{k}(t_index,1);

     X2tg(k,1)=LY3{k}(t_index,2);
     X2tg(k,2)=UY3{k}(t_index,2);

     X3tg(k,1)=LY3{k}(t_index,3);
     X3tg(k,2)=UY3{k}(t_index,3);

     X4tg(k,1)=LY3{k}(t_index,4);
     X4tg(k,2)=UY3{k}(t_index,4);
end
clf
td=num2str(t3);

subplot(2,1,1),
plot(X1d,acut,'rh')
    xlabel('Chi (radian)')
    ylabel('membership grade')
    legend('X1')
    grid

subplot(2,1,2),
plot(X2d,acut,'bo')
    xlabel('Omega Chi (rad/sec)')
    ylabel('membership grade')
    legend('X2')
    grid

figure

subplot(2,1,1),
plot(X3d,acut,'rh')
    xlabel('Theta (radian)')
    ylabel('membership grade')
    legend('X3')
    grid

subplot(2,1,2),
plot(X4d,acut,'bo')
     xlabel('Omega Theta (rad/sec)')
    ylabel('membership grade')
    legend('X4')
    grid
%----------------------END NTRT_W2-----------------------%
```

NTR31.m

```
% Author: Attapong Terdpravat
% January 26,2004.
```

```
% This program runs robo31.
% robo31 outputs its control to be used with robo33.
clear all

%should open robo before running else it gives warning
%===intial condition===%
chio= 0;
chidoto=0;
thetao=0;
thetadoto=0;%
x0=[chio;chidoto;thetao;thetadoto];
qd =[0 100 30];
qdo = [0 0 0];
qdoo = [0 0 0];
%===system definition===%
syms s t1

A=[0 1 0 0;0 0 0 0;0 0 0 1;0 0 0 0];
B=[0 0;1 0;0 0;0 1];
C=[1 0 0 0; 0 0 1 0];
%C=[1 0 1 0];
D=[0];
% K=place(A',C',[-32;-33;-34+j;-34-j]);
K=place(A',C',[-123;-125;-124+j;-124-j]);
% K=place(A',C',[-11;-10;-14+j;-14-j]);
Lu=K';
sys=ss(A,B,C,D);
%---------------------------
w1=1;
m1=0.3;%kg
m2=0.6;%kg
R=0.25;%m
L=0.75;%m
I1=0.5*m1*R^2;
I2=0.25*m1*R^2+(m1+(1/3)*m2)*L^2;
%---------generates four membership function---%
[T,X,Chi,Chid,Theta,Thetad]=sim('robo31');
clf
subplot(2,1,1)
plot(T,Chi)
grid
ylabel('Chi (radian)')
xlabel('time (sec)')
subplot(2,1,2)
plot(T,Theta)
grid
ylabel('Theta (radian)')
```

```
xlabel('time (sec)')

figure
subplot(2,1,1)
plot(T,Chid)
grid
ylabel('Omega Chi (rad/s)')
xlabel('time (sec)')
subplot(2,1,2)
plot(T,Thetad)
grid
ylabel('Omega Theta (rad/s)')
xlabel('time (sec)')
%----------------------END NTR31-----------------------%
```

NTR33.m

```
% Author: Attapong Terdpravat
% January 27,2004.
% This program runs robo33 with the uctm input from robo31.
clear all
load uctm.mat
uctm(1,:)=ans(2,:);
uctm(2,:)=ans(3,:);

open robo31
open robo33
tt=get_param('robo31','StopTime')
set_param('robo33','StopTime',tt)
bt=get_param('robo31','fixedstep')
t_incre=str2num(bt)
tsim=(0:t_incre:3);
%-----------------------------------------------%
%---------generates four membership function---%
%-----------------------------------------------%
x0=[0 0 0 0];
a_increment=0.01;
tolerance=0.01*a_increment;
% shape parameter for the generic bell membership function
w =[0.1;0.15;0.17;0.2];
sh=10*w;
%-----------------------------------------------
Ba=(-2:0.01:2);
%-----------------------------------------------
X10p = gbellmf(Ba,[w(1),sh(1),x0(1)]);
X20p = gbellmf(Ba,[w(2),sh(2),x0(2)]);
X30p = gbellmf(Ba,[w(3),sh(3),x0(3)]);
X40p = gbellmf(Ba,[w(4),sh(4),x0(4)]);
```

```
%taking the alpha cut
acut=(0.05:a_increment:max(X10p))';
acut=acut-1*tolerance;
%calling cut off here

for k=1:1:length(acut)
    %return [lower cut,upper cut]
   [min1(k),max1(k)] =cutoff(acut(k),X10p,Ba);
   [min2(k),max2(k)] =cutoff(acut(k),X20p,Ba);
   [min3(k),max3(k)] =cutoff(acut(k),X30p,Ba);
   [min4(k),max4(k)] =cutoff(acut(k),X40p,Ba);

end
X10=[min1',max1'];
X20=[min2',max2'];
X30=[min3',max3'];
X40=[min4',max4'];
%===system definition===%
syms s t1

A=[0 1 0 0;0 0 0 0;0 0 0 1;0 0 0 0];
B=[0 0;1 0;0 0;0 1];
C=[1 0 0 0; 0 0 1 0];
%C=[1 0 1 0];
D=[0];
% K=place(A',C',[-32;-33;-34+j;-34-j]);
K=place(A',C',[-123;-125;-124+j;-124-j]);
Lu=K';
%==============
w1=1;
m1=0.3;%kg
m2=0.6;%kg
R=0.25;%m
L=0.75;%m
I1=0.5*m1*R^2;
I2=0.25*m1*R^2+(m1+(1/3)*m2)*L^2;
%----S I M U L A T I O N---%
open robo33
tfx=num2str(t_incre);
set_param('robo33','fixedstep',tfx)

for i =1:1:length(acut)
% change initial conditions
a=num2str(X10(i,1));
    set_param('robo33/Actin/chiic','value',[a]);
b=num2str(X20(i,1));
```

```
    set_param('robo33/Actin/chidic','value',[b]);
c=num2str(X30(i,1));
    set_param('robo33/Actin/thetaic','value',[c]);
d=num2str(X40(i,1));
    set_param('robo33/Actin/thetadic','value',[d]);
    %for the target mfs
[T,LX{i},LY{i}]=sim('robo33');
end

% repeat for upper cut
for j =1:1:length(acut)
% change initial conditions
a=num2str(X10(j,2));
    set_param('robo33/Actin/chiic','value',[a]);
b=num2str(X20(j,2));
    set_param('robo33/Actin/chidic','value',[b]);
c=num2str(X30(j,2));
    set_param('robo33/Actin/thetaic','value',[c]);
d=num2str(X40(j,2));
    set_param('robo33/Actin/thetadic','value',[d]);
     %for the target mfs
[T,UX{j},UY{j}]=sim('robo33');
end
%return  LX and UX to nil to save memory.
%----------------------END NTR33 ------------------------%
```

APPENDIX B

SIMULINK PROGRAMS

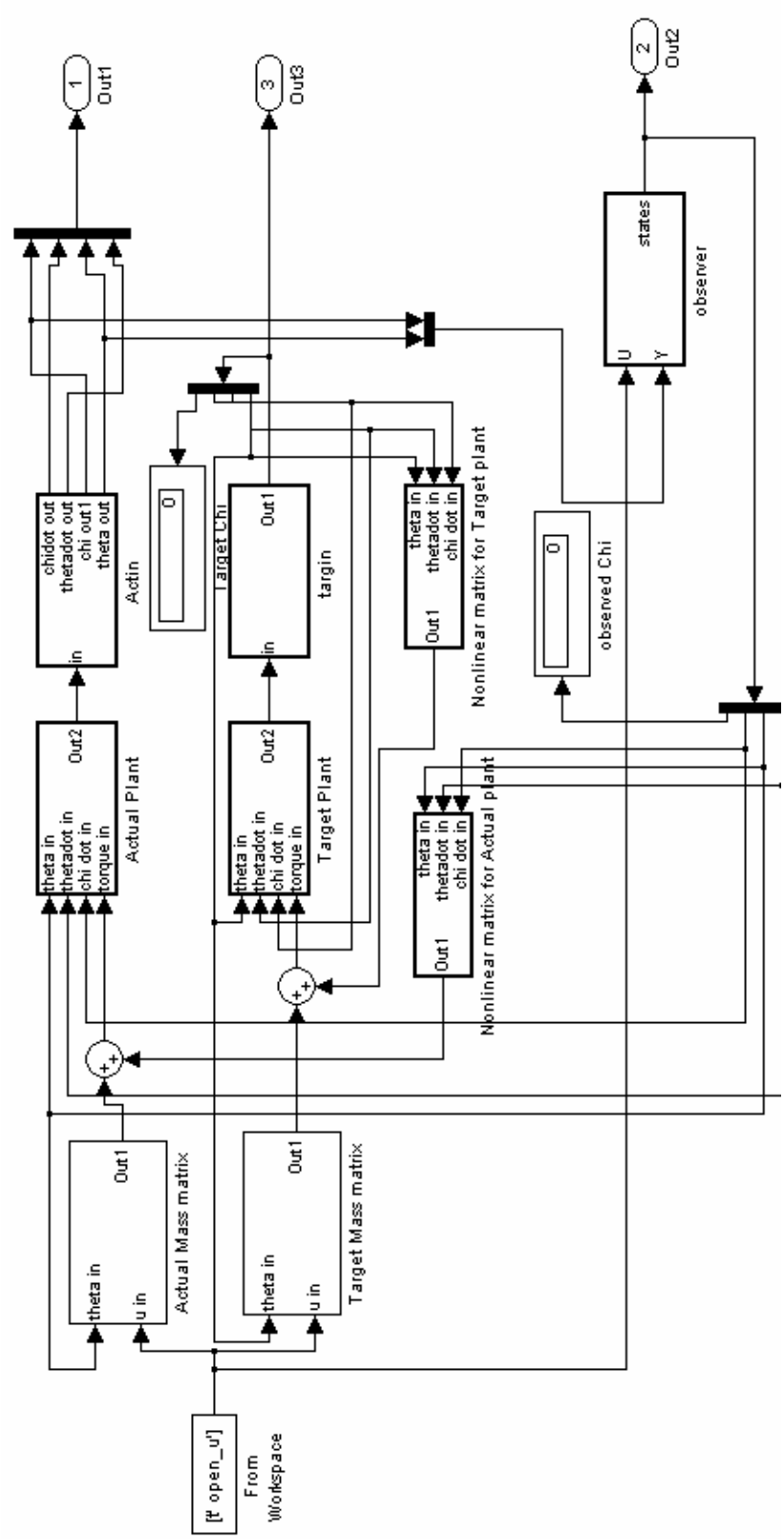

B.1 Robo_W2 used in section 4.6.

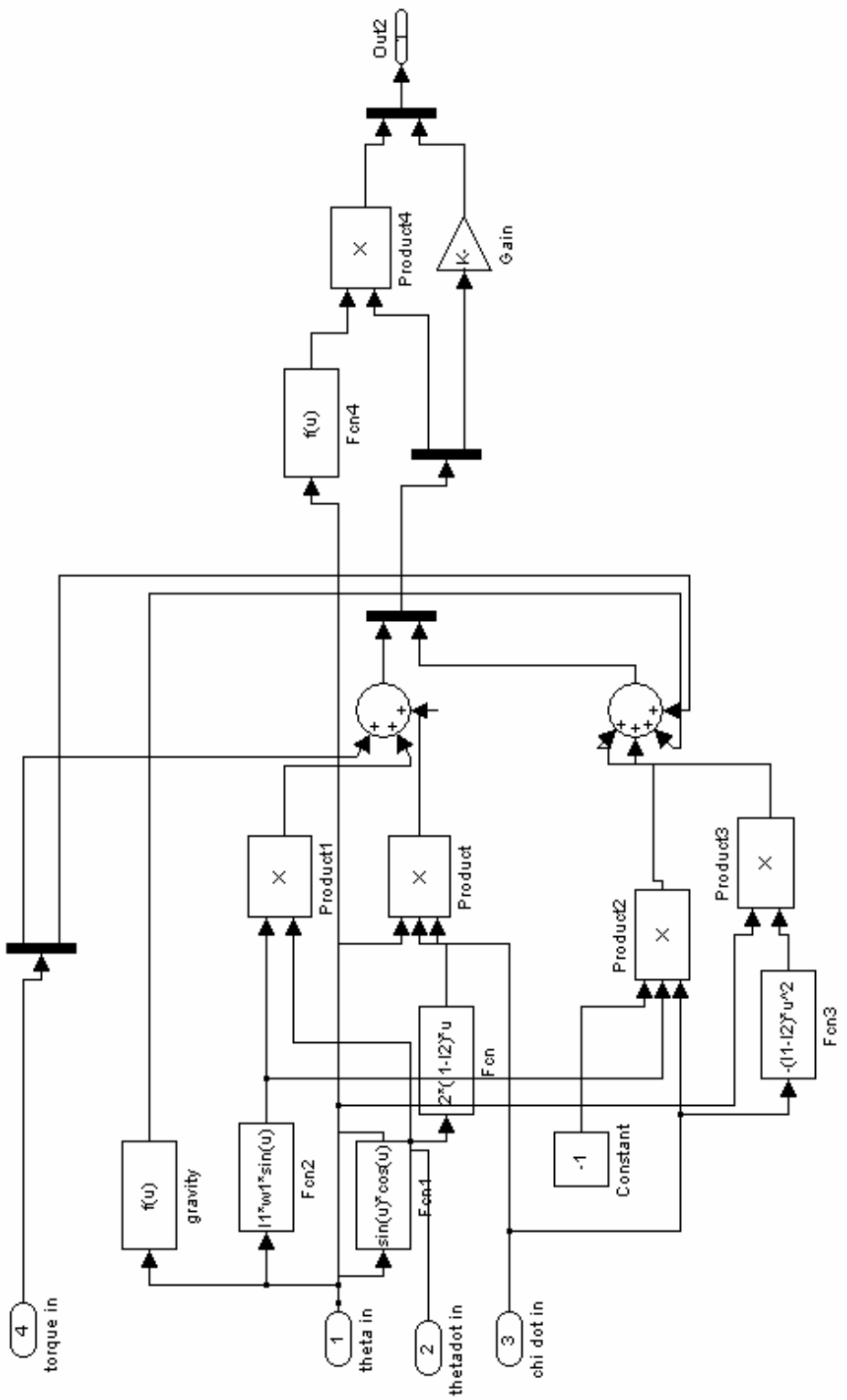

B.2 Plant subsystem

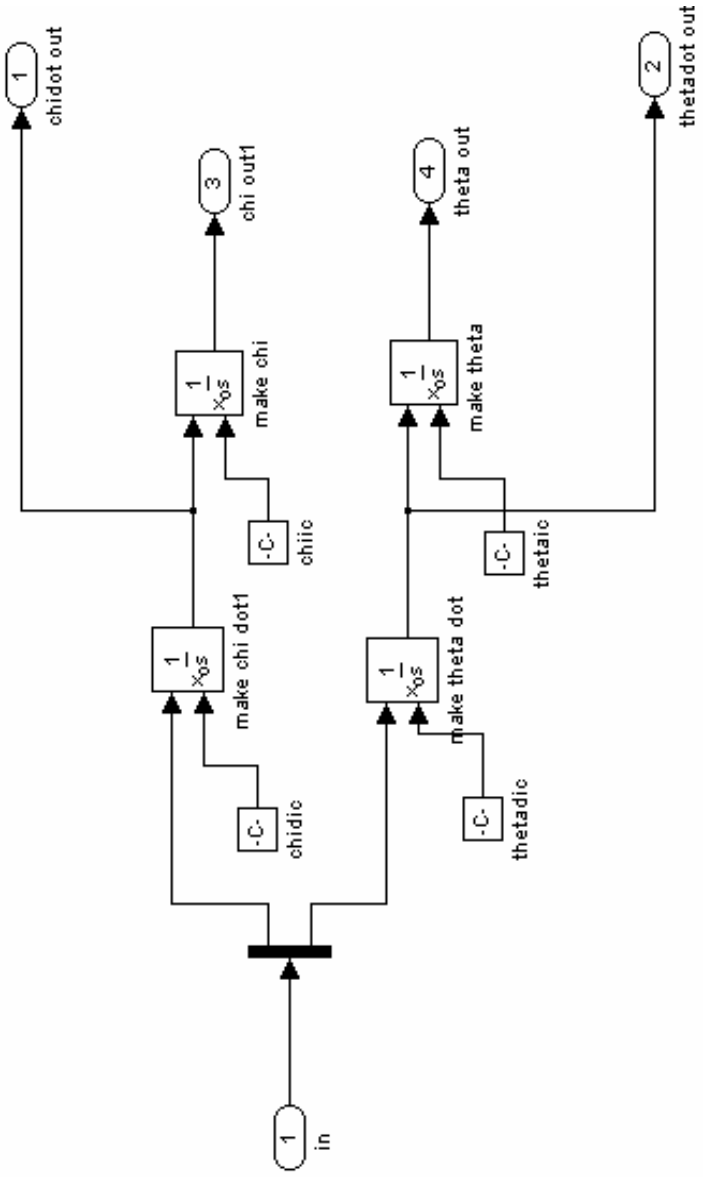

B.3 Integration block (Actin)

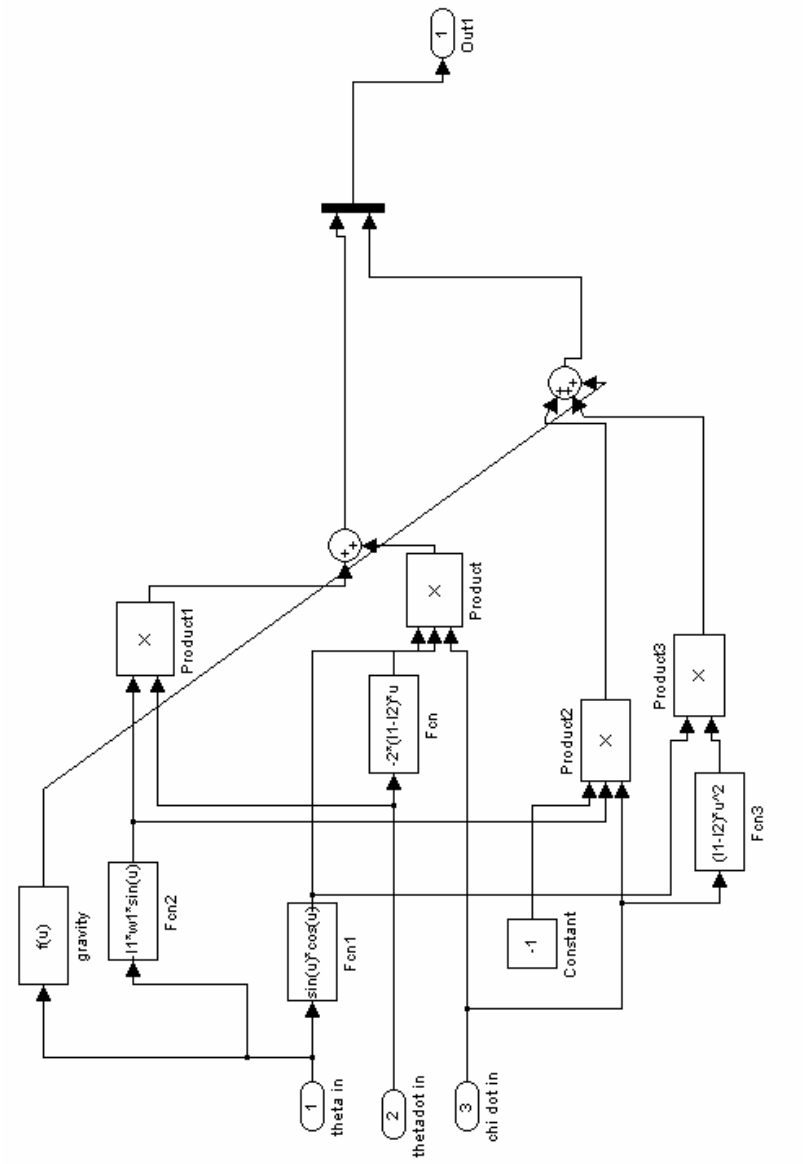

B.4 Nonlinear matrix subsystem for CTM

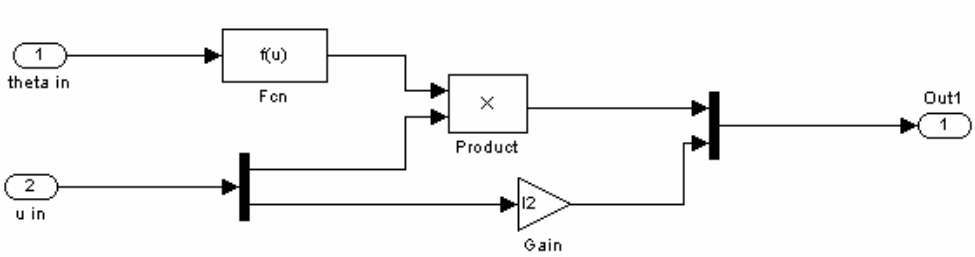

B.5 Mass matrix for CTM

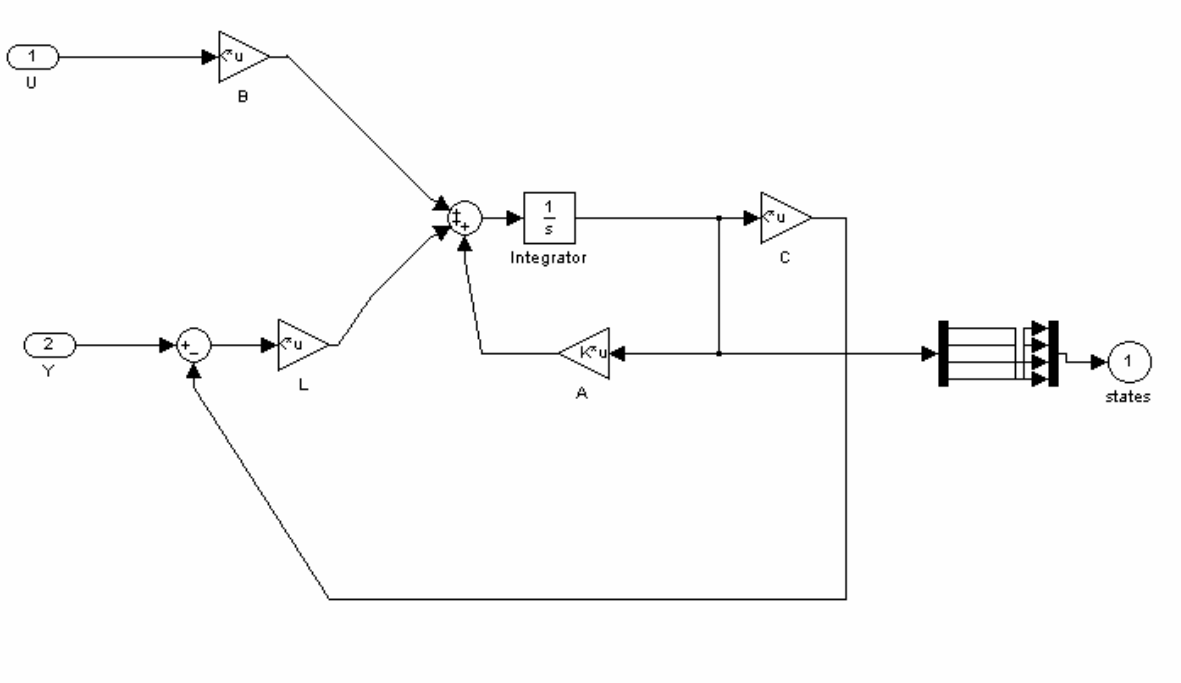

B.6 Observer subsystem

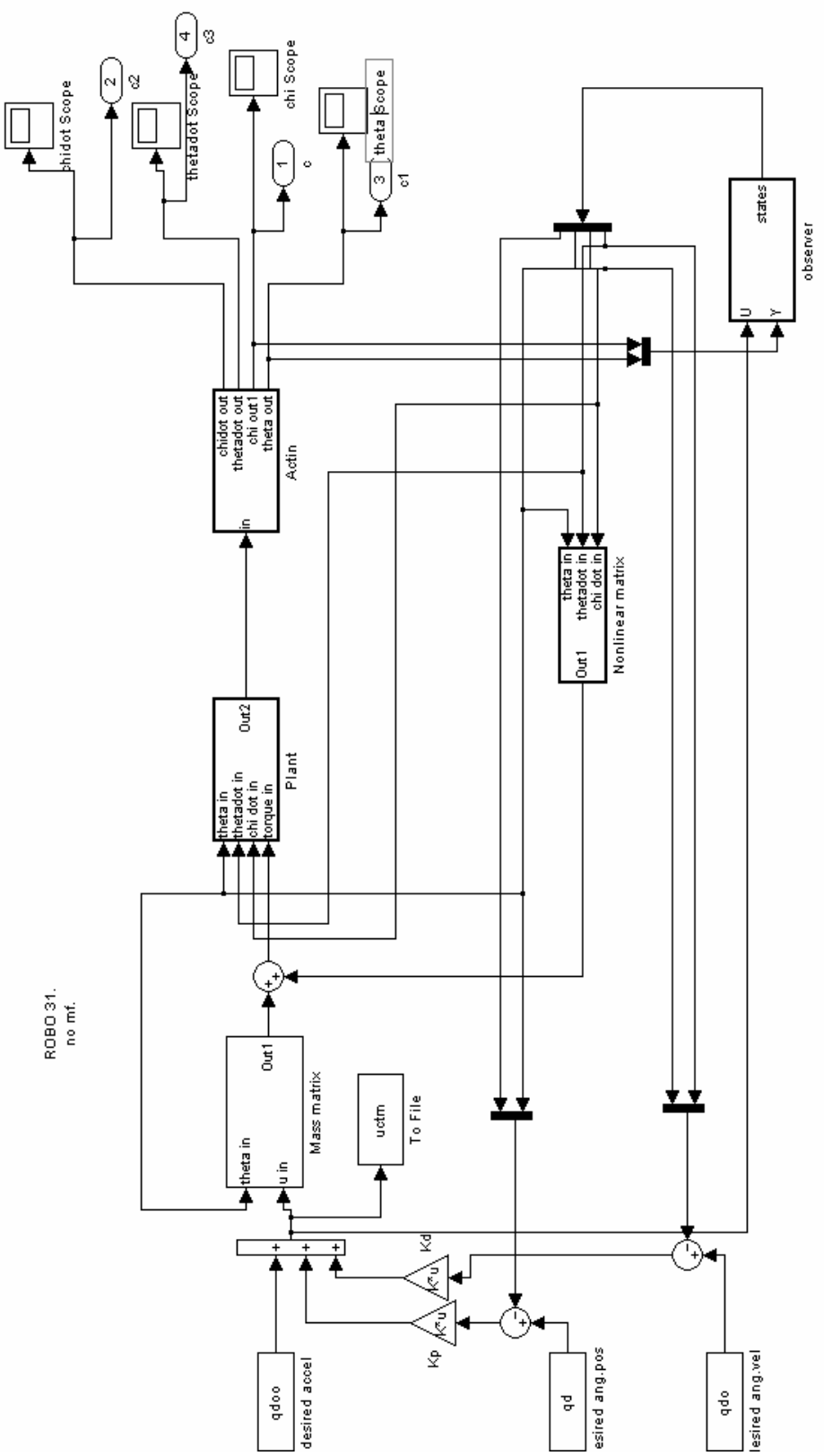

B.7 Robo31 used in section 4.7.

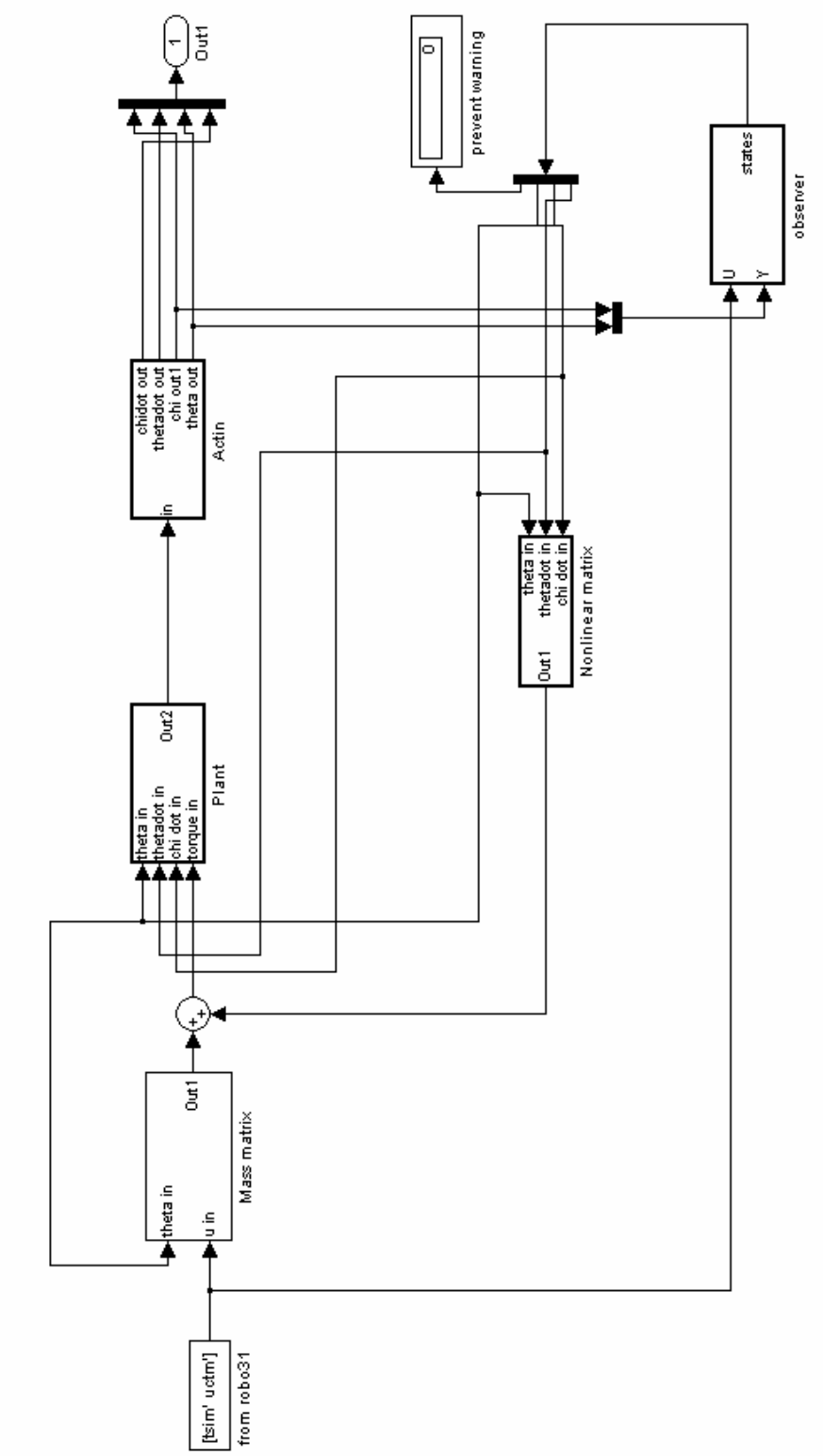

B.8 Robo33 used in section 4.8

APPENDIX C

MEMBERSHIP FUNCTIONS PROPAGATION

Propagation 1: Membership functions propagation in section 4.6.

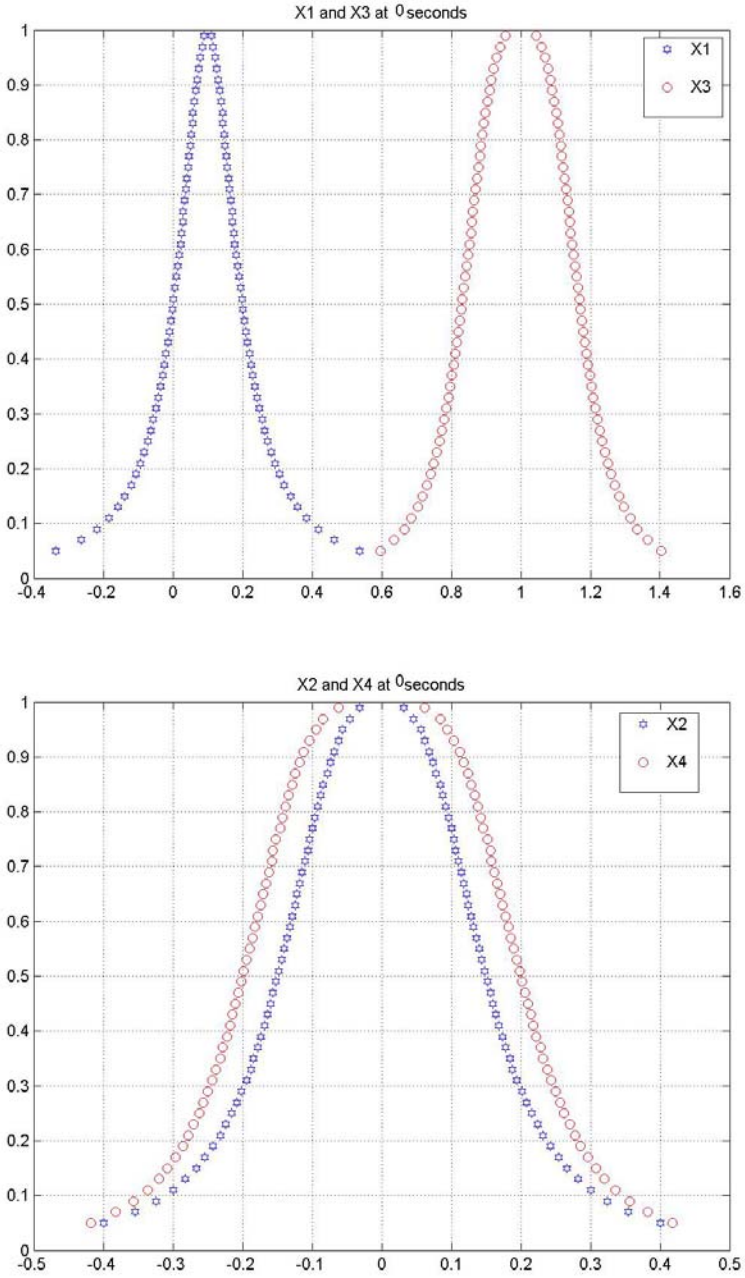

C.1.1 Membership functions propagation of a robotic grinder at 0 second

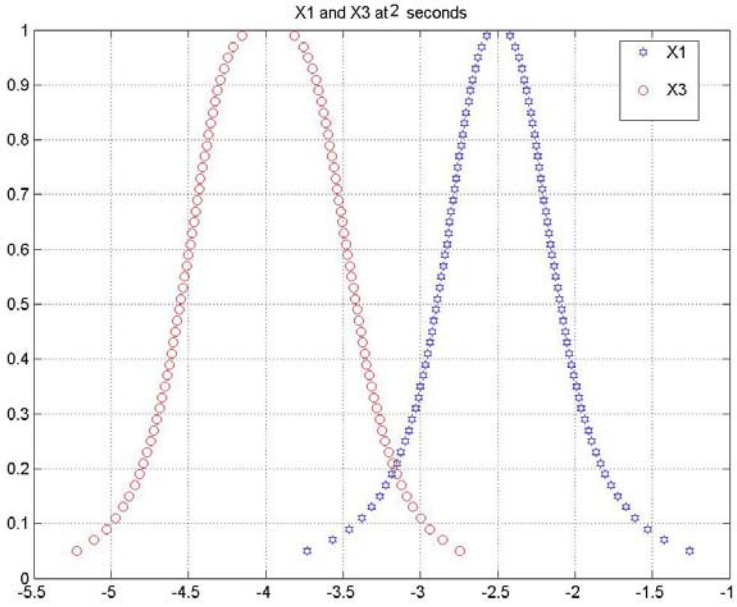

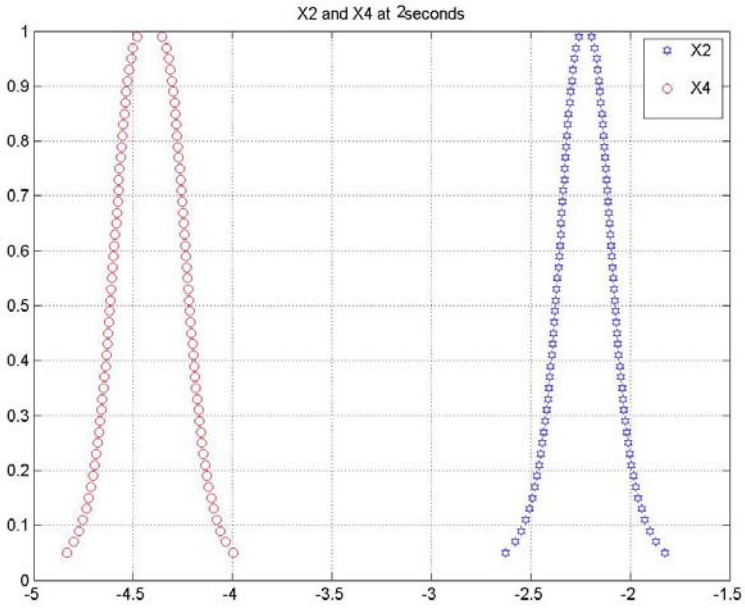

C.1.2 Membership functions propagation of a robotic grinder at 2 second

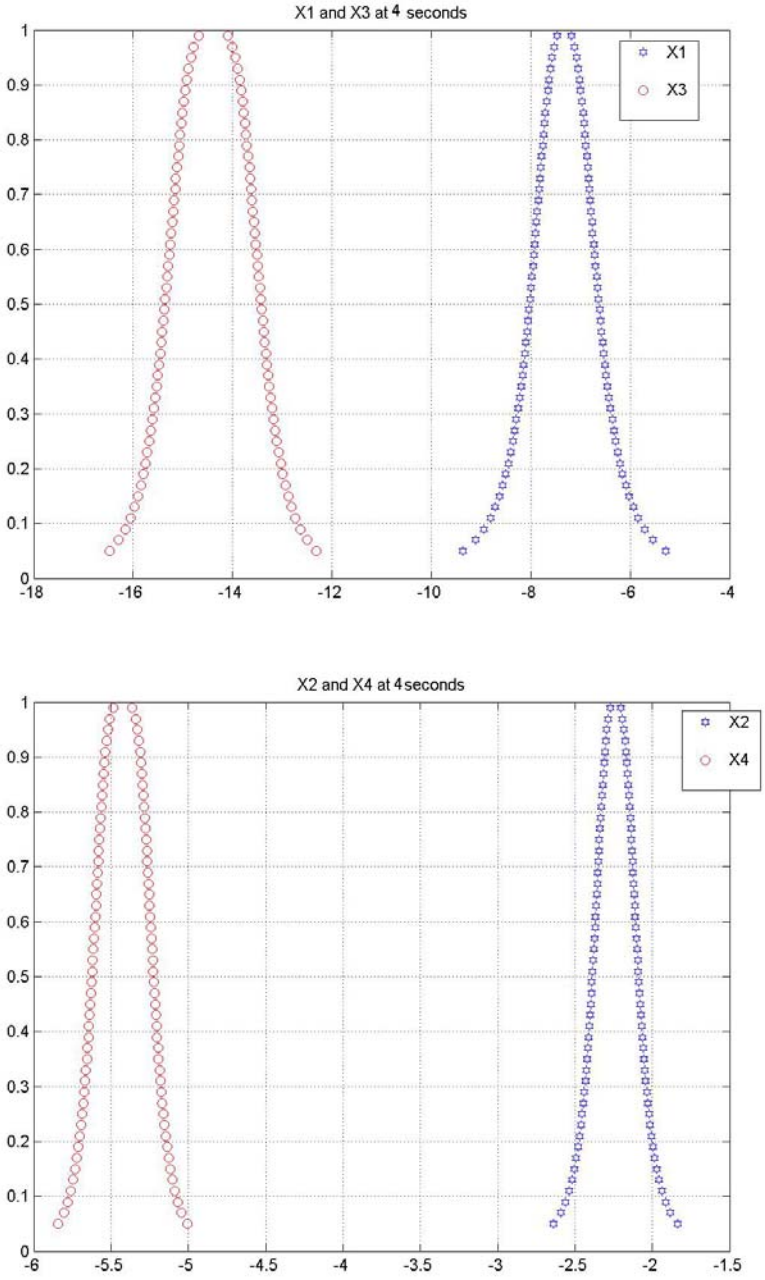

C.1.3 Membership functions propagation of a robotic grinder at 4 second

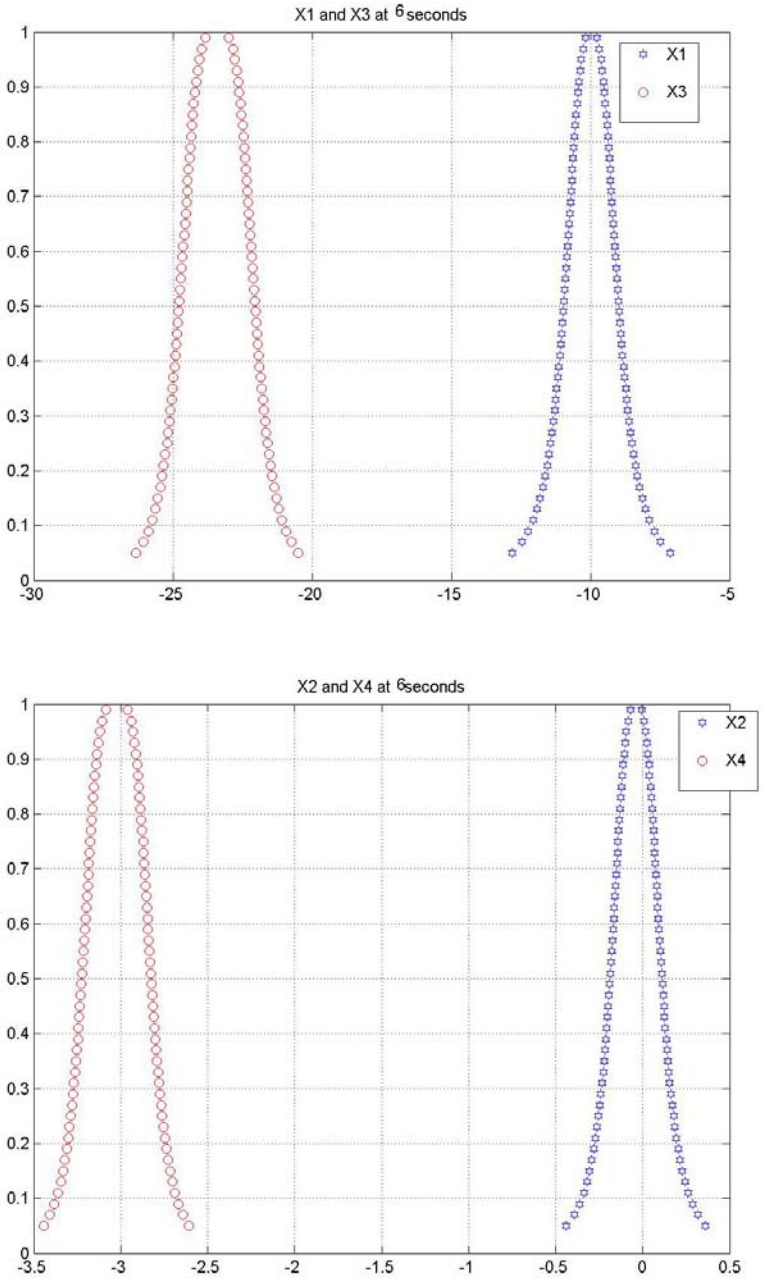

C.1.4 Membership functions propagation of a robotic grinder at 6 second

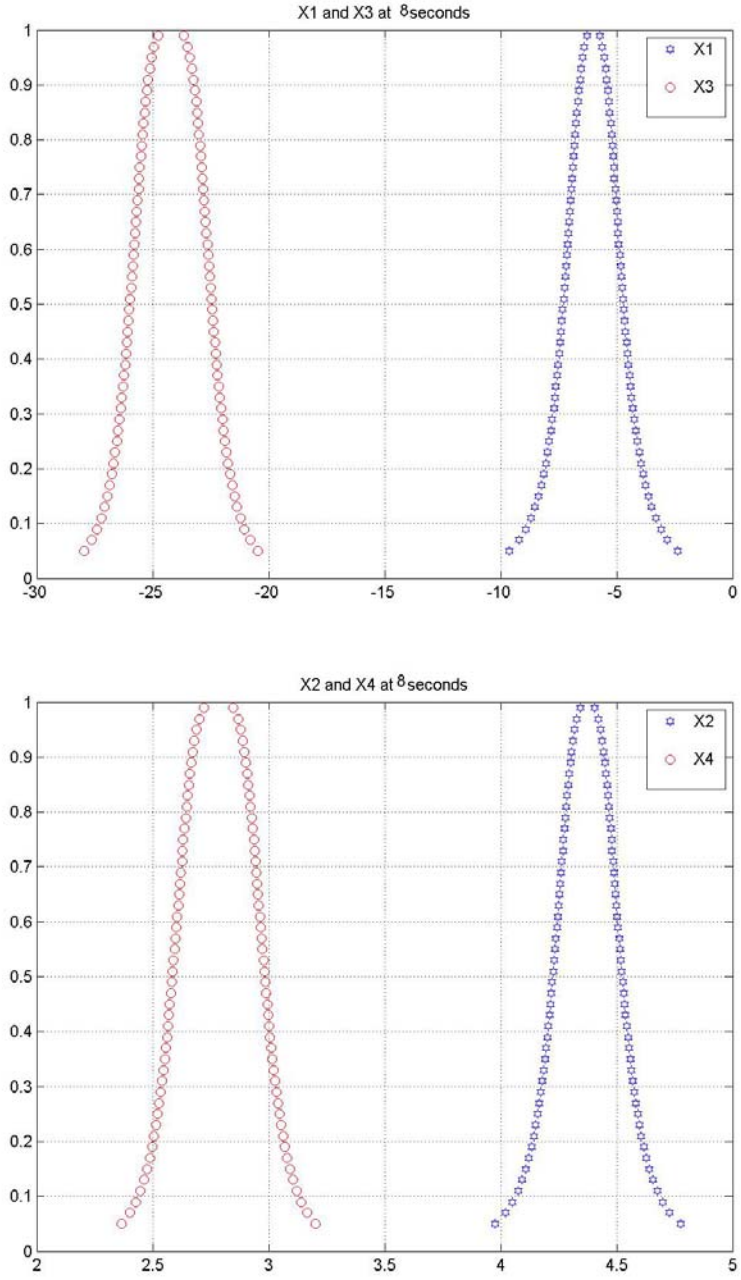

C.1.5 Membership functions propagation of a robotic grinder at 8 second

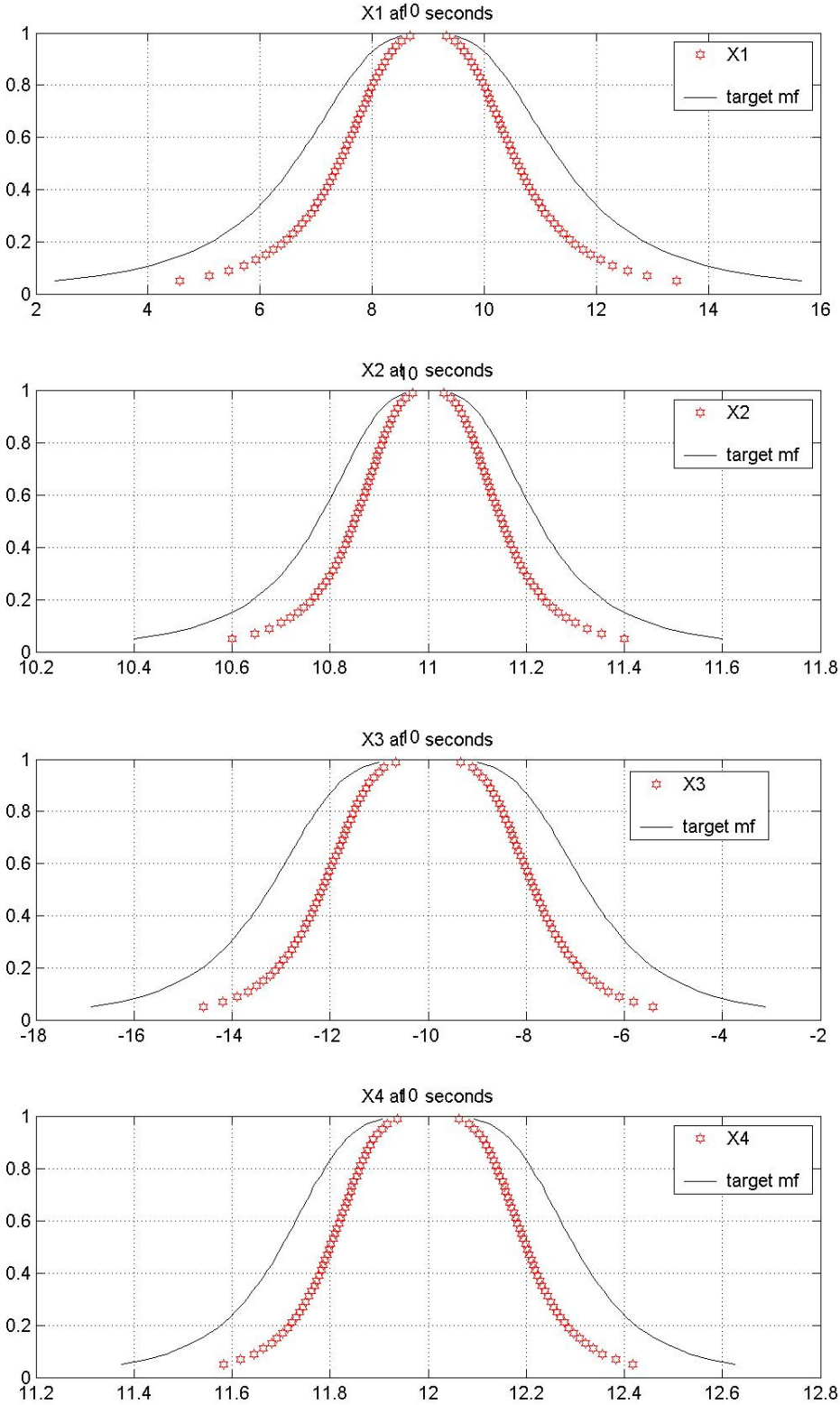

C.1.6 Membership functions propagation of a robotic grinder at 10 second with the target membership functions.

Propagation2: Membership functions propagation used in section 4.8

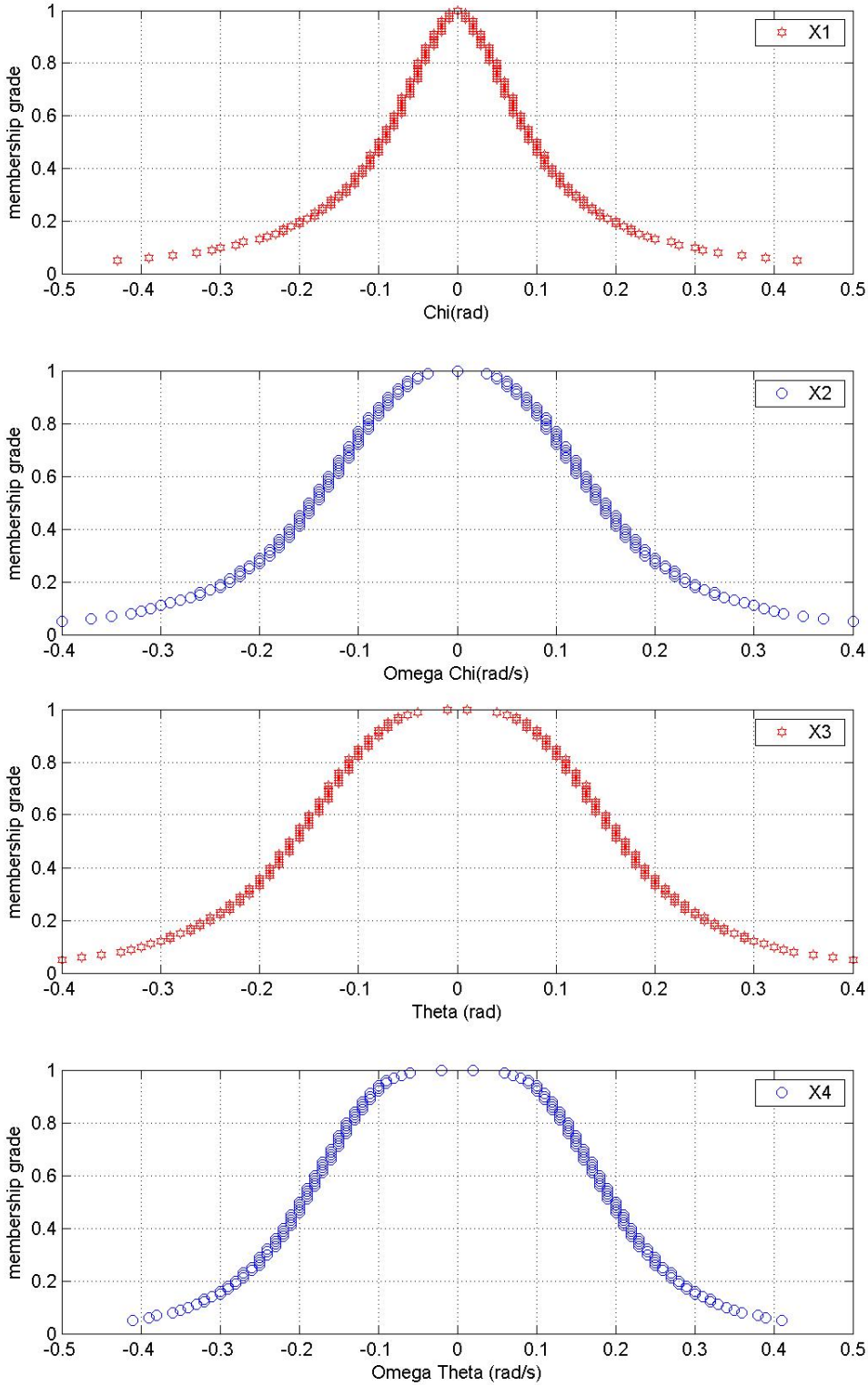

C.2.1 Membership functions propagation of a robotic grinder at 0 second

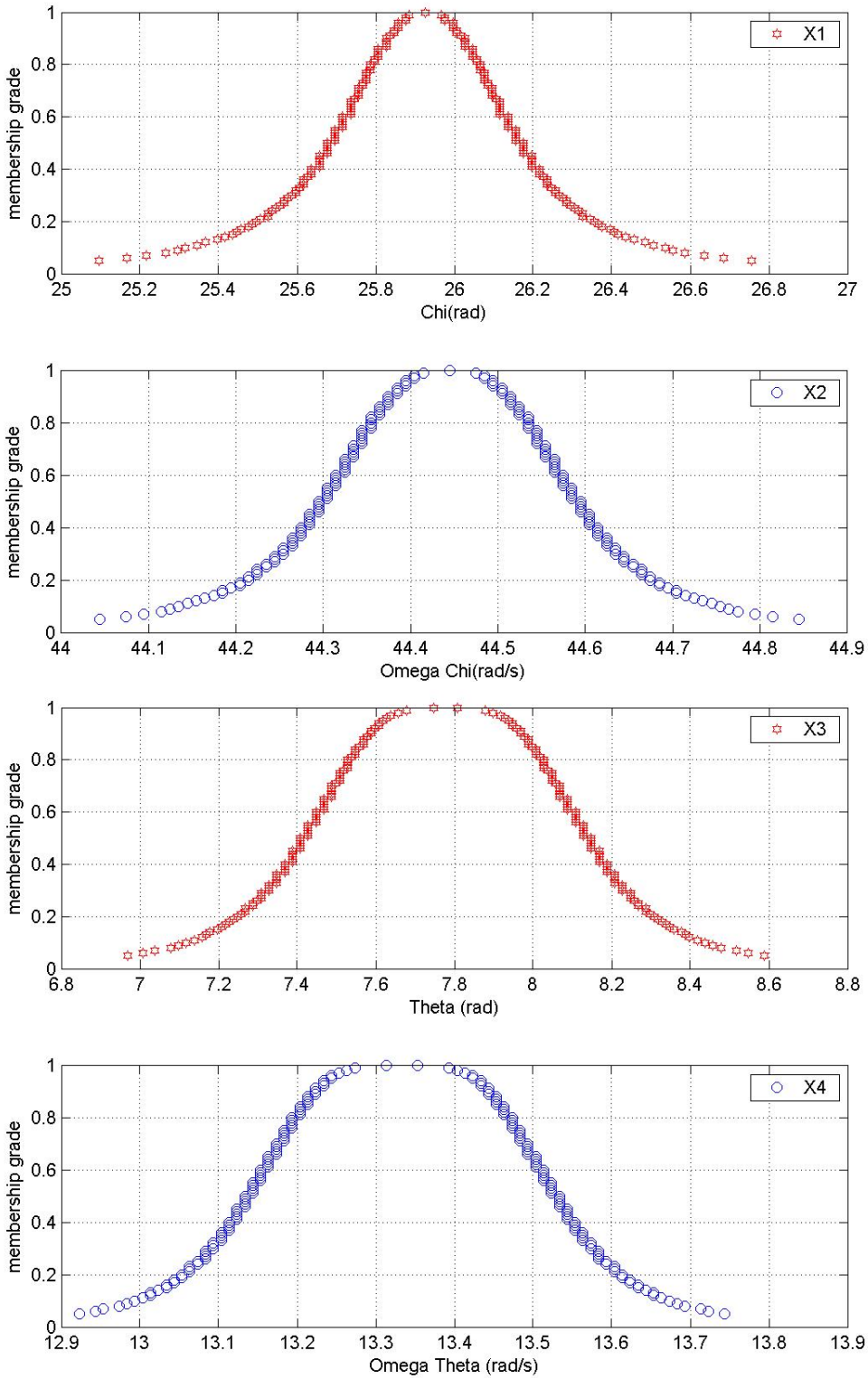

C.2.2 Membership functions propagation of a robotic grinder at 1 second

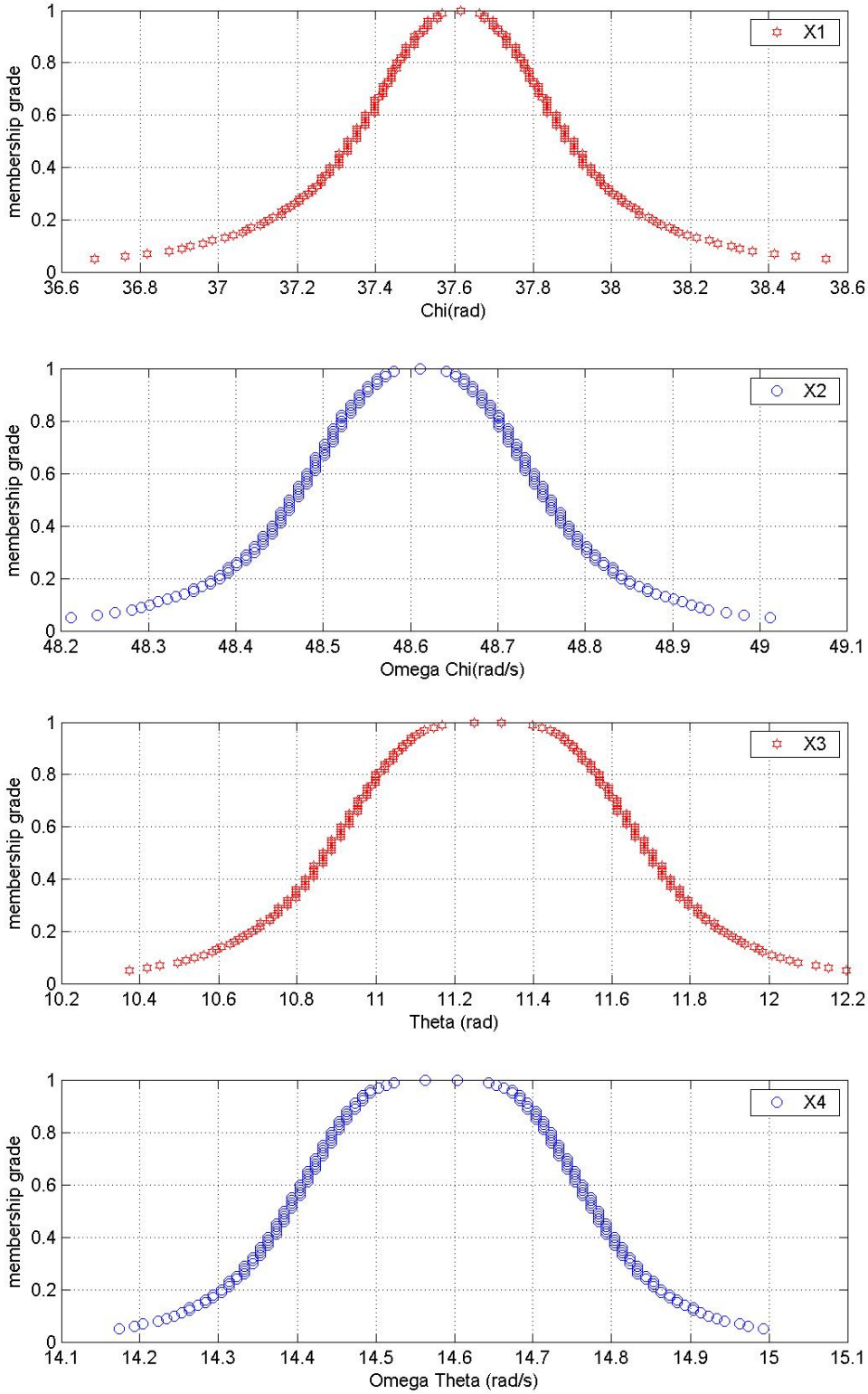

C.2.3 Membership functions propagation of a robotic grinder at 2 second

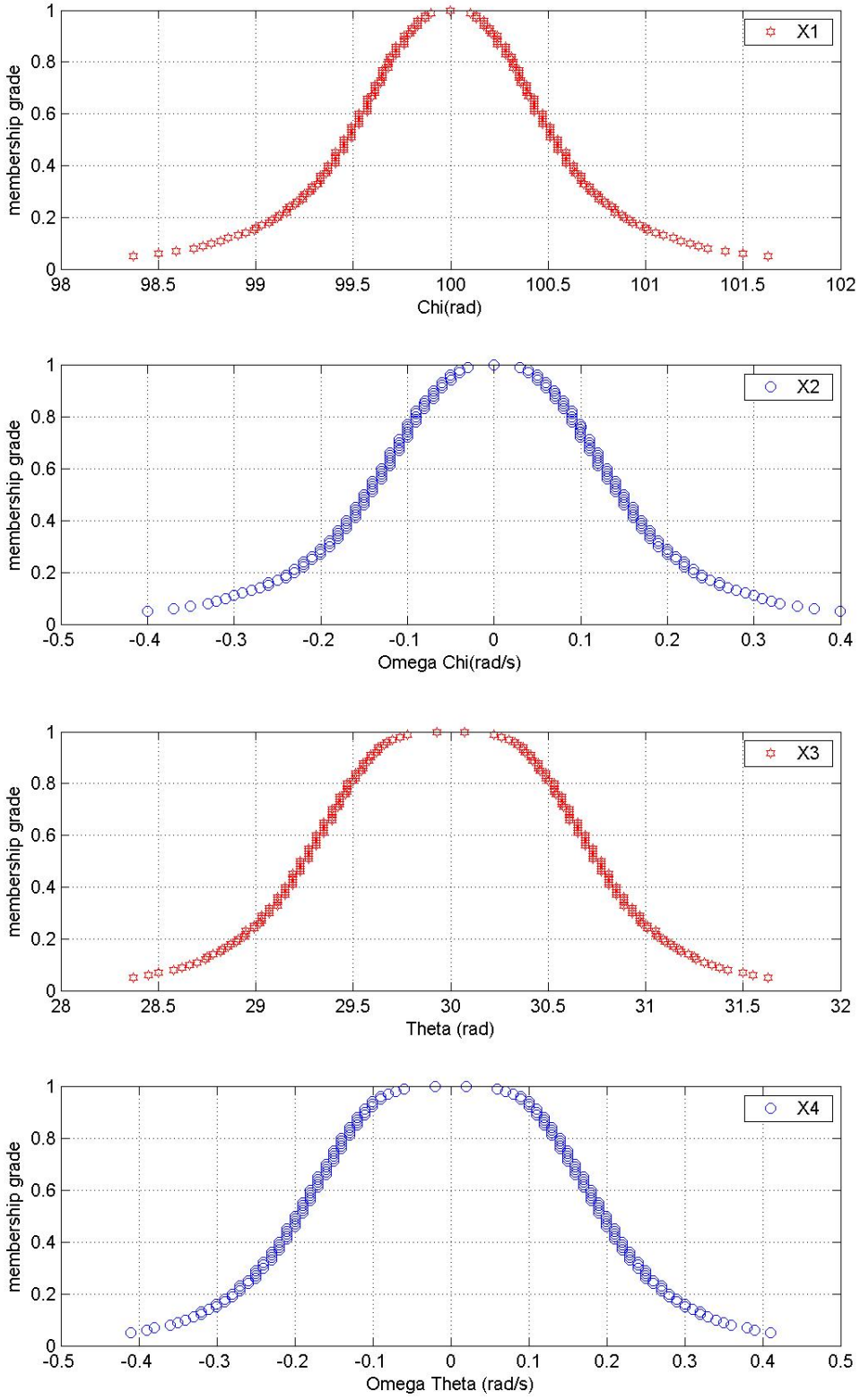

C.2.3 Membership functions propagation of a robotic grinder at 3 second

Propagation 3: Membership functions propagation used in section 4.8

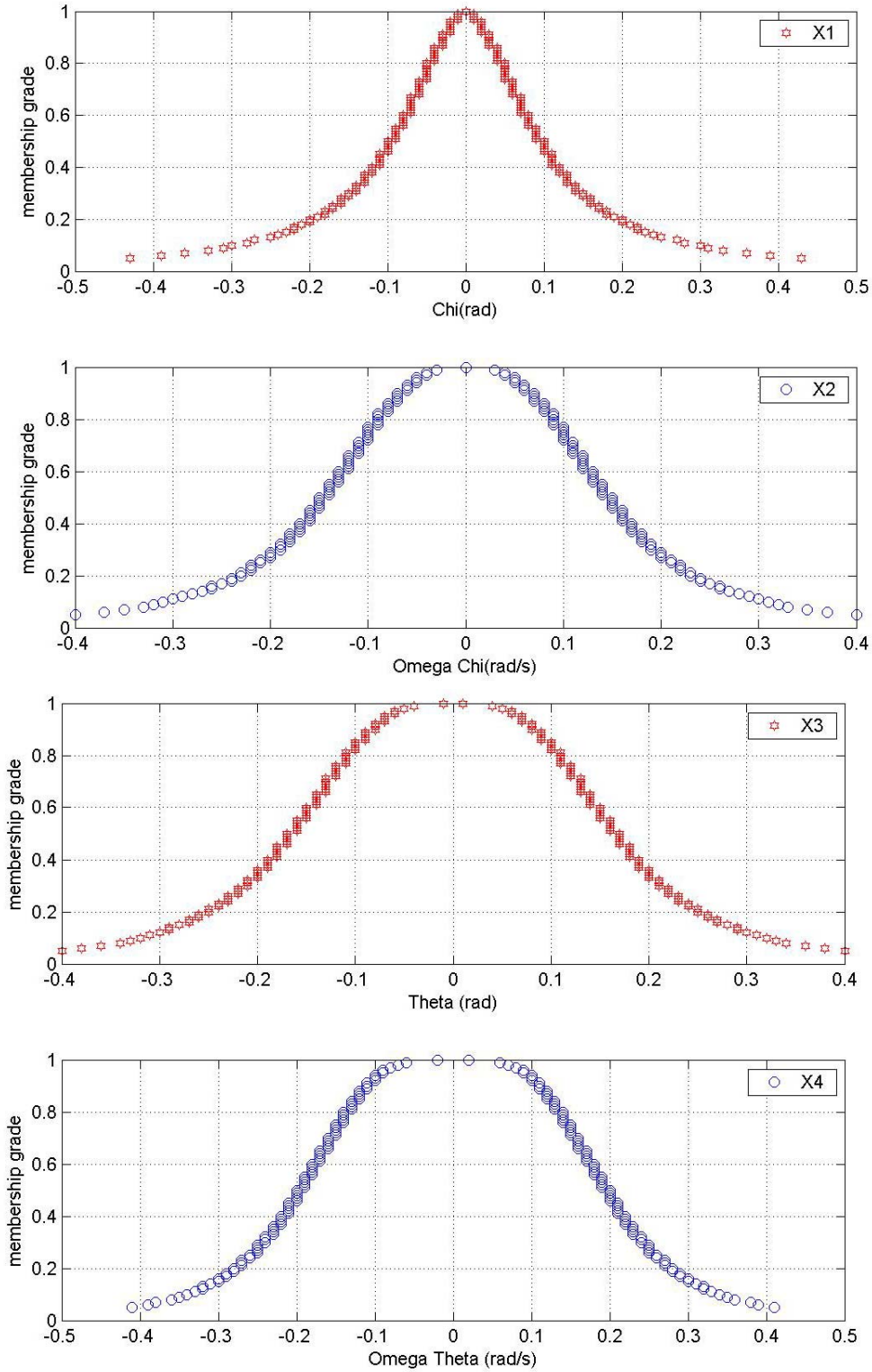

C.3.1 Membership functions propagation of a robotic grinder at 0 second

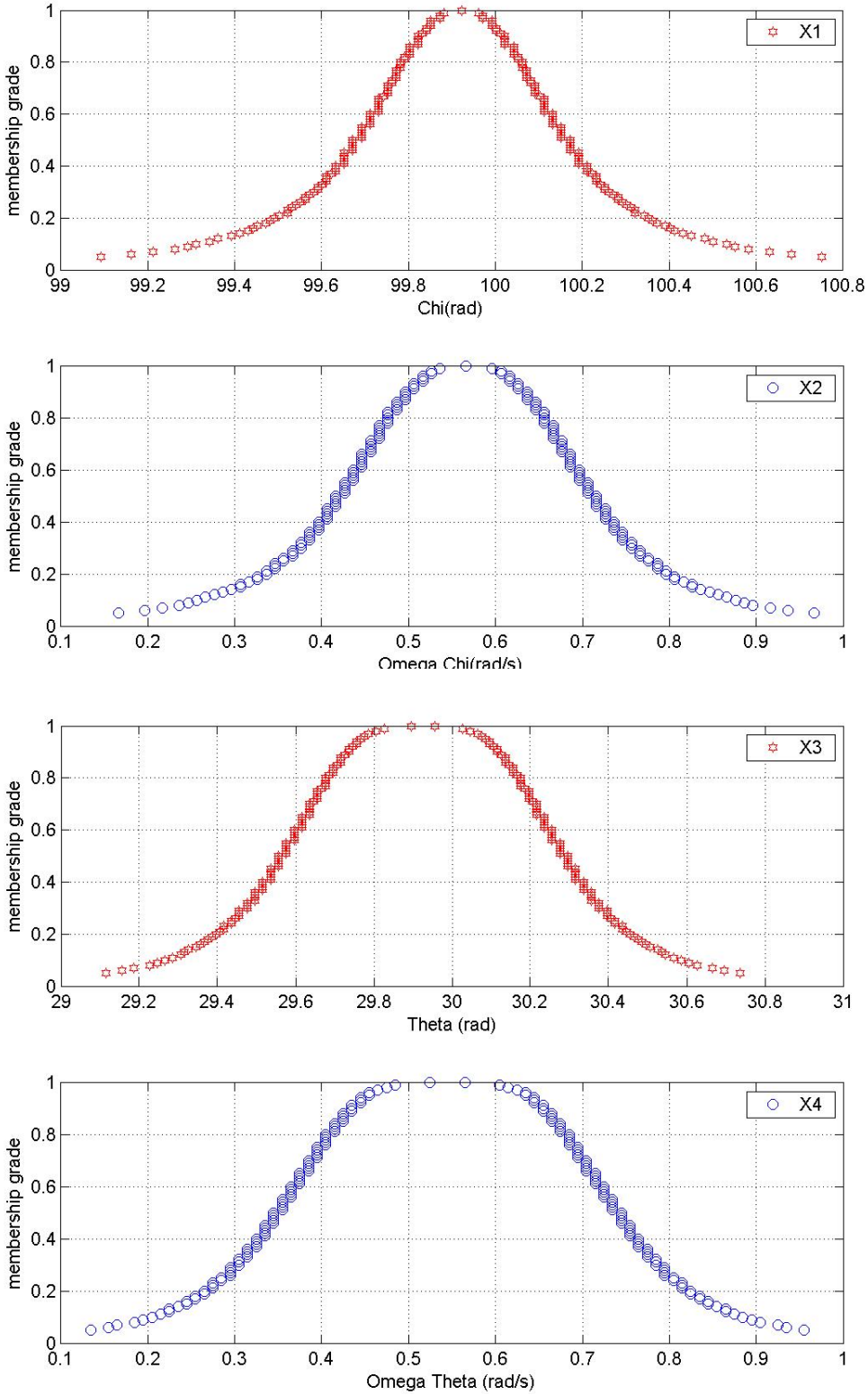

C.3.2 Membership functions propagation of a robotic grinder at 1 second

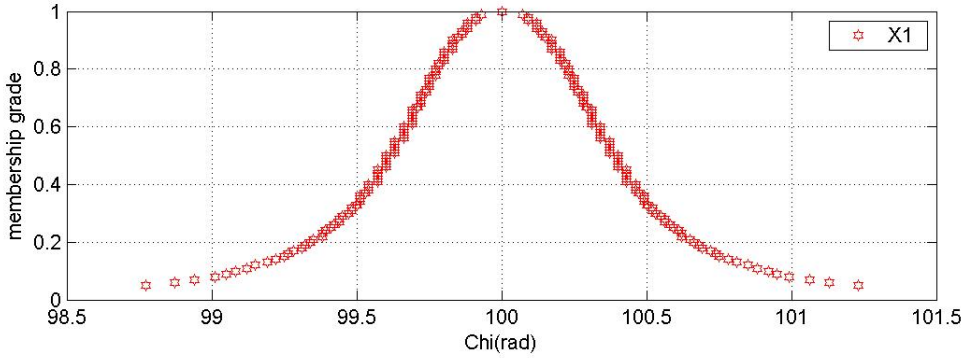

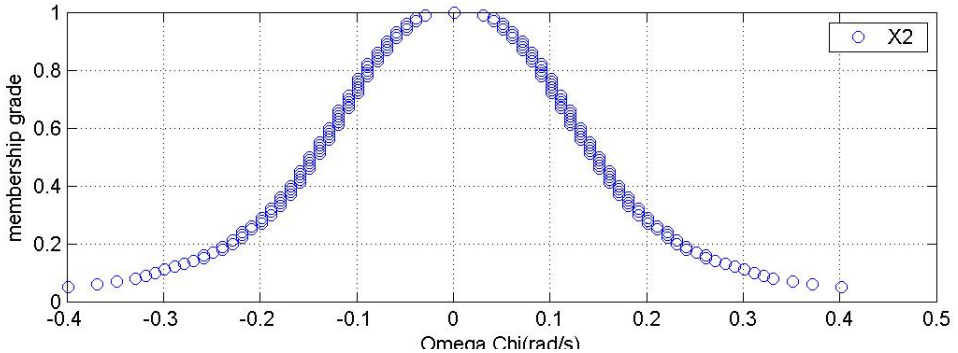

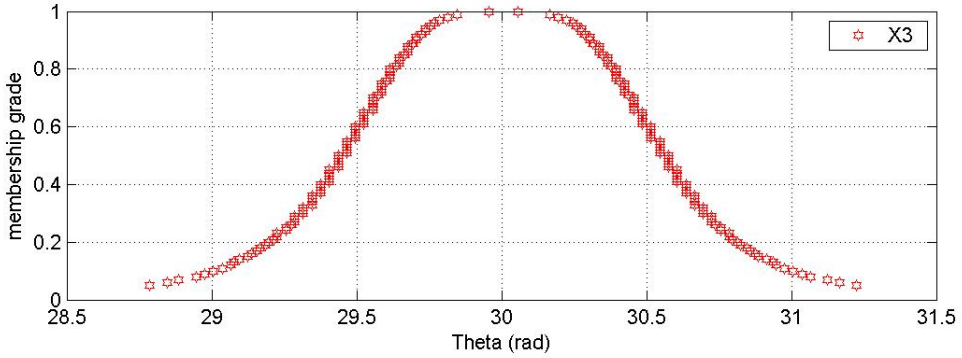

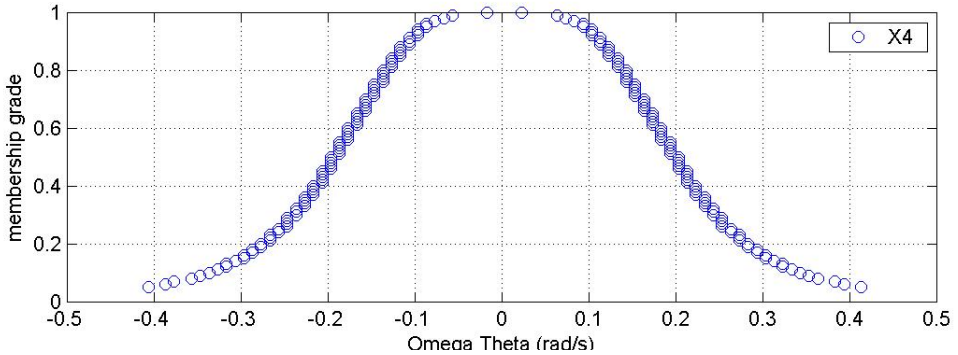

C.3.3 Membership functions propagation of a robotic grinder at 2 second

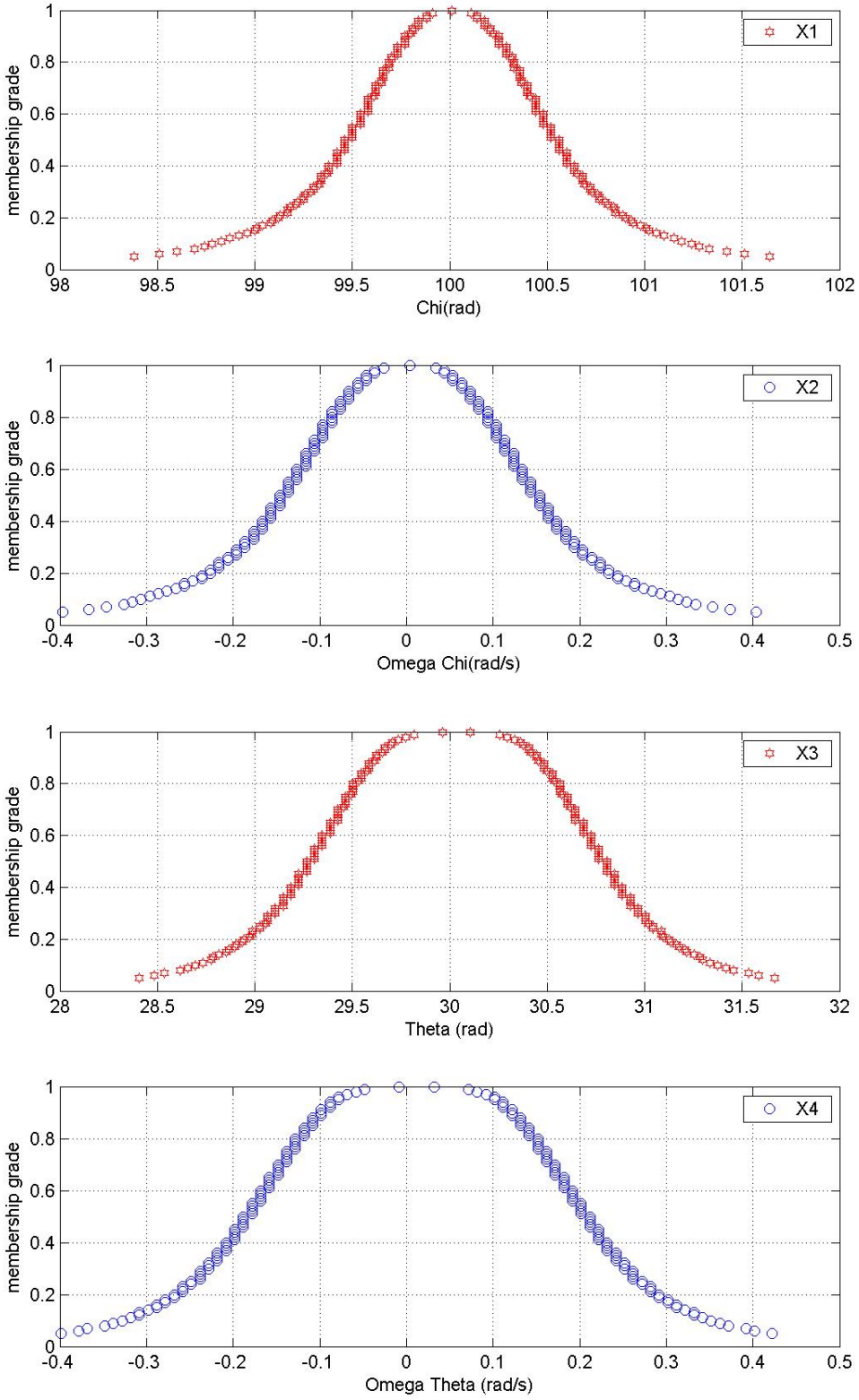

C.3.4 Membership functions propagation of a robotic grinder at 3 second

Propagation 4: Membership functions propagation used in section 4.8

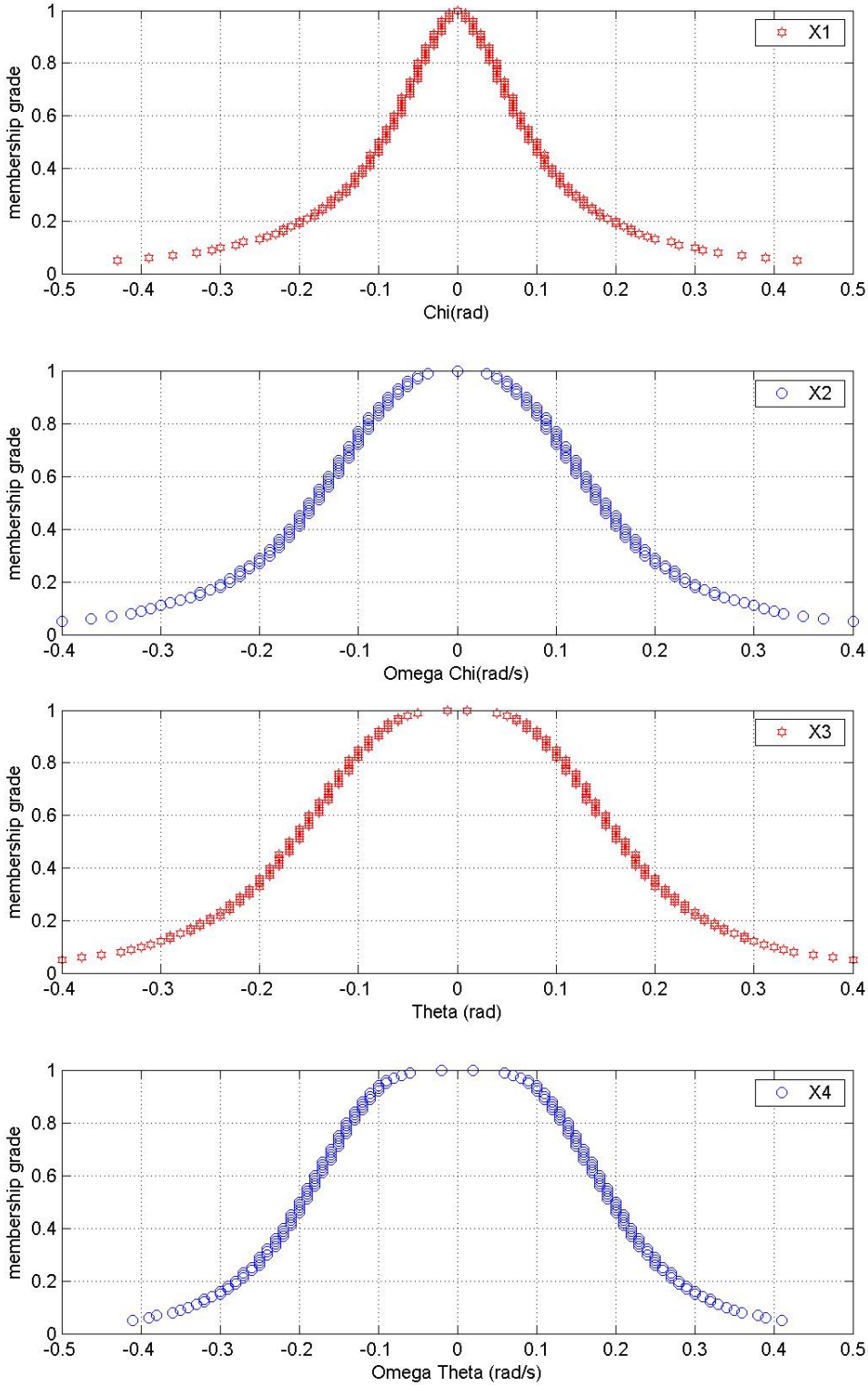

C.4.1 Membership functions propagation of a robotic grinder at 0 second

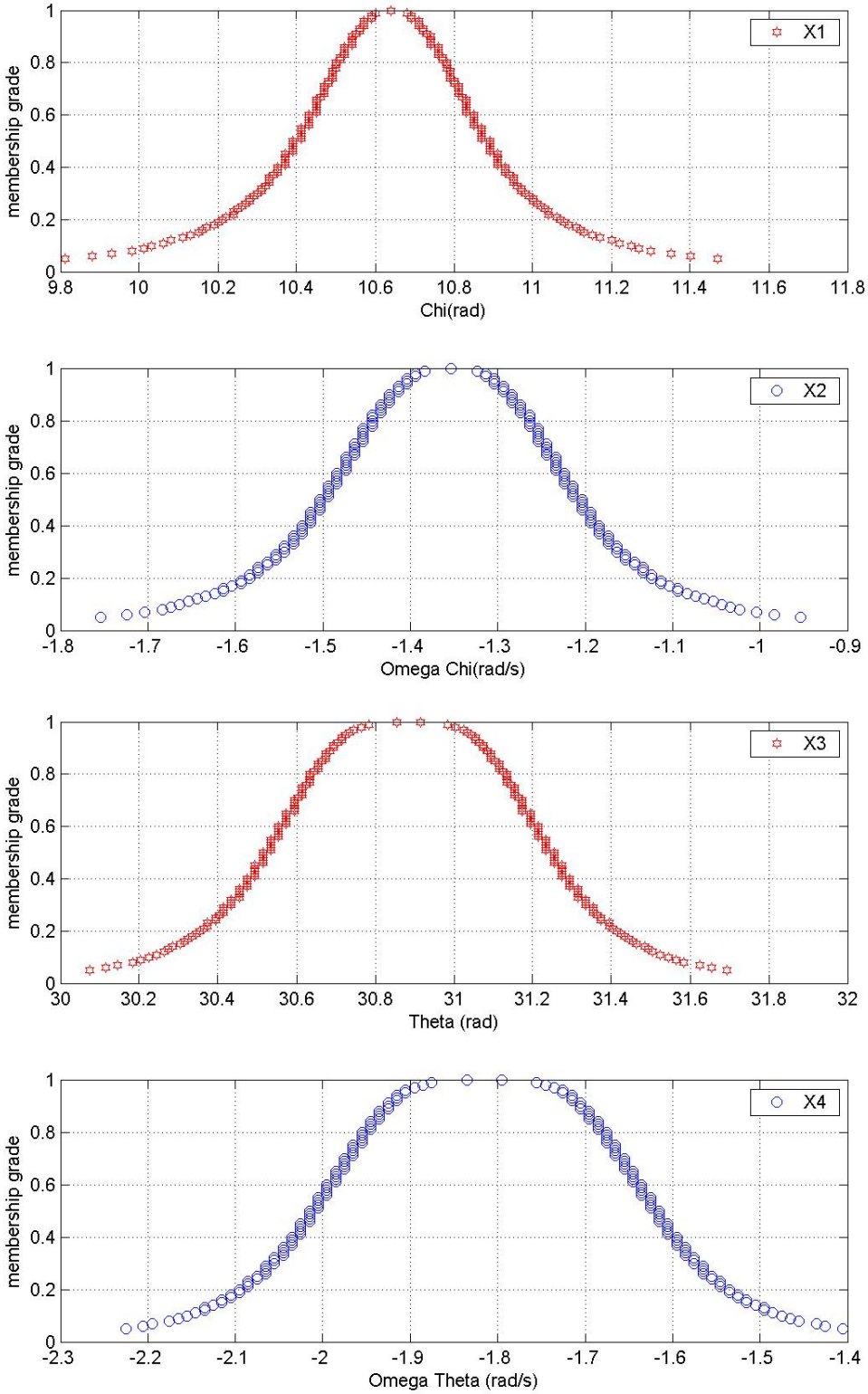

C.4.2 Membership functions propagation of a robotic grinder at 1 second

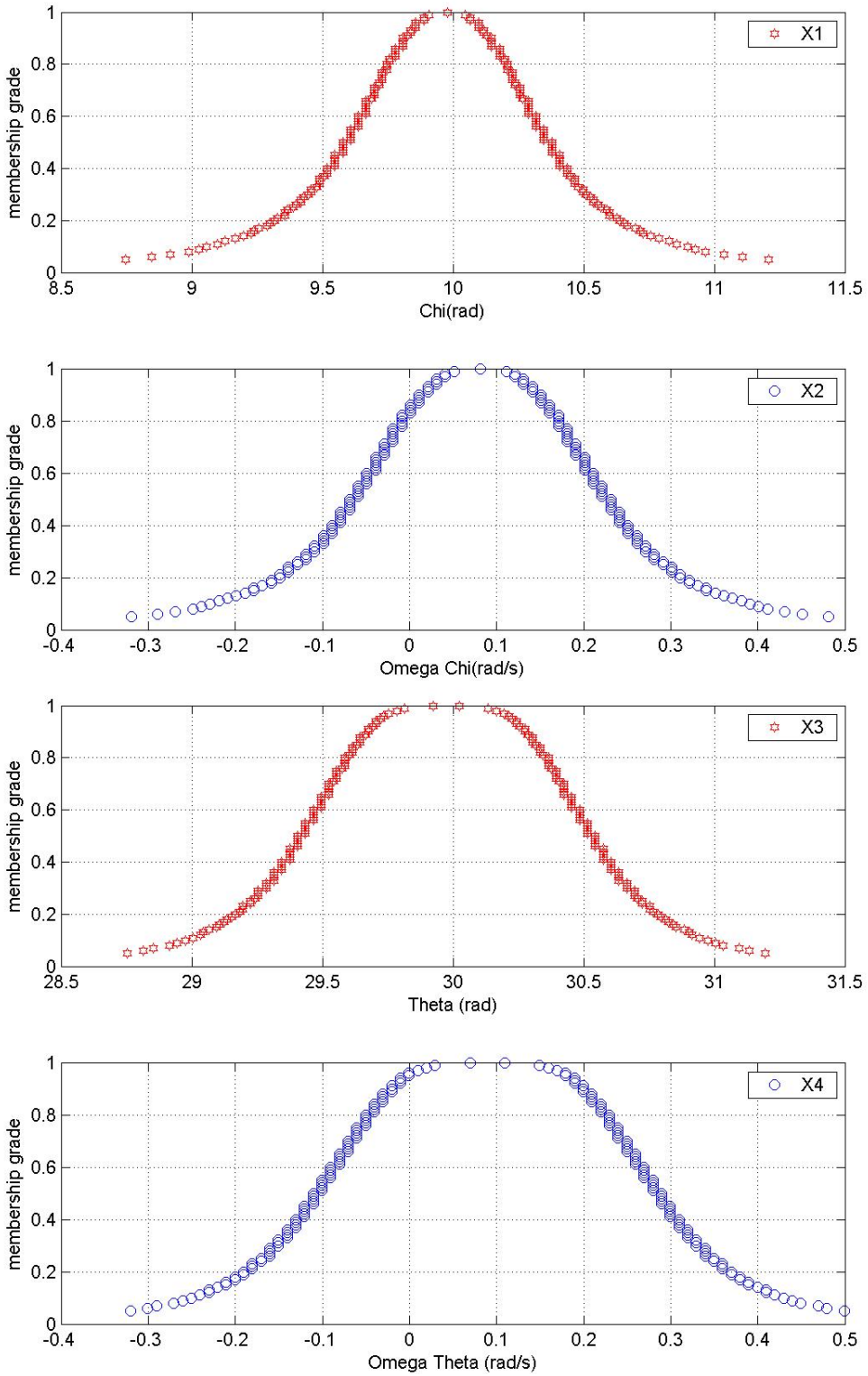

C.4.3 Membership functions propagation of a robotic grinder at 2 second

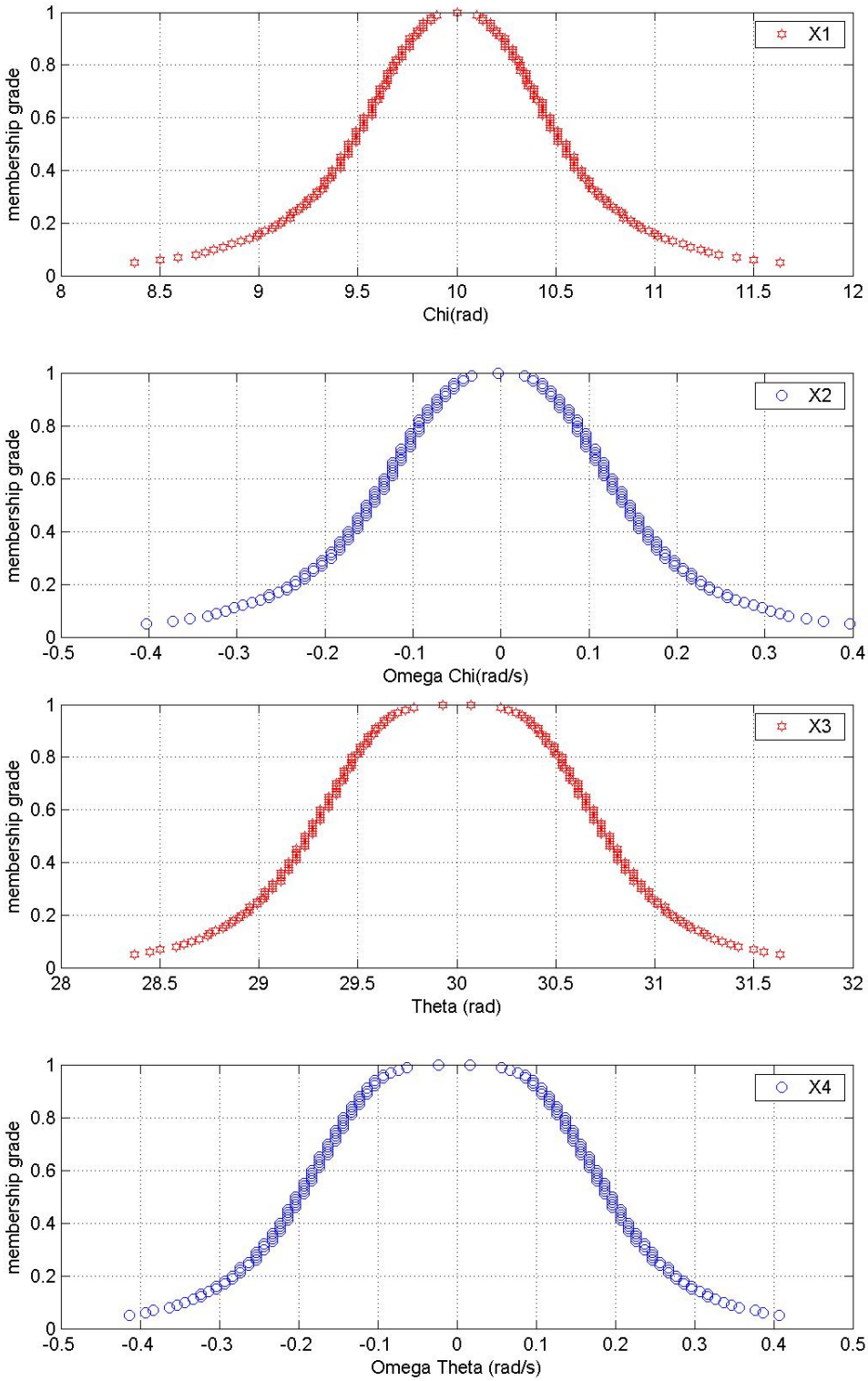

C.4.4 Membership functions propagation of a robotic grinder at 3 second

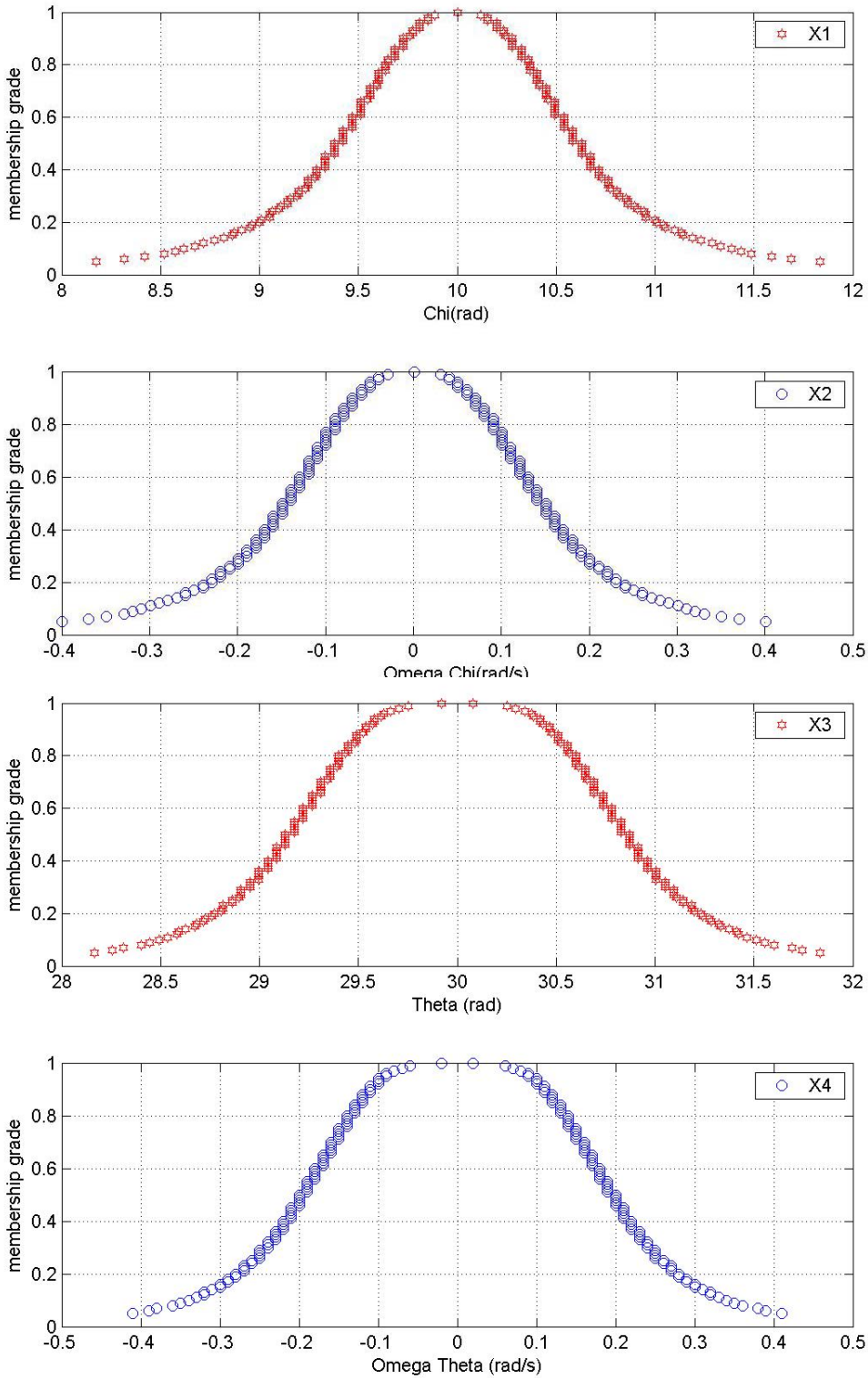

C.4.5 Membership functions propagation of a robotic grinder at 3.5 second

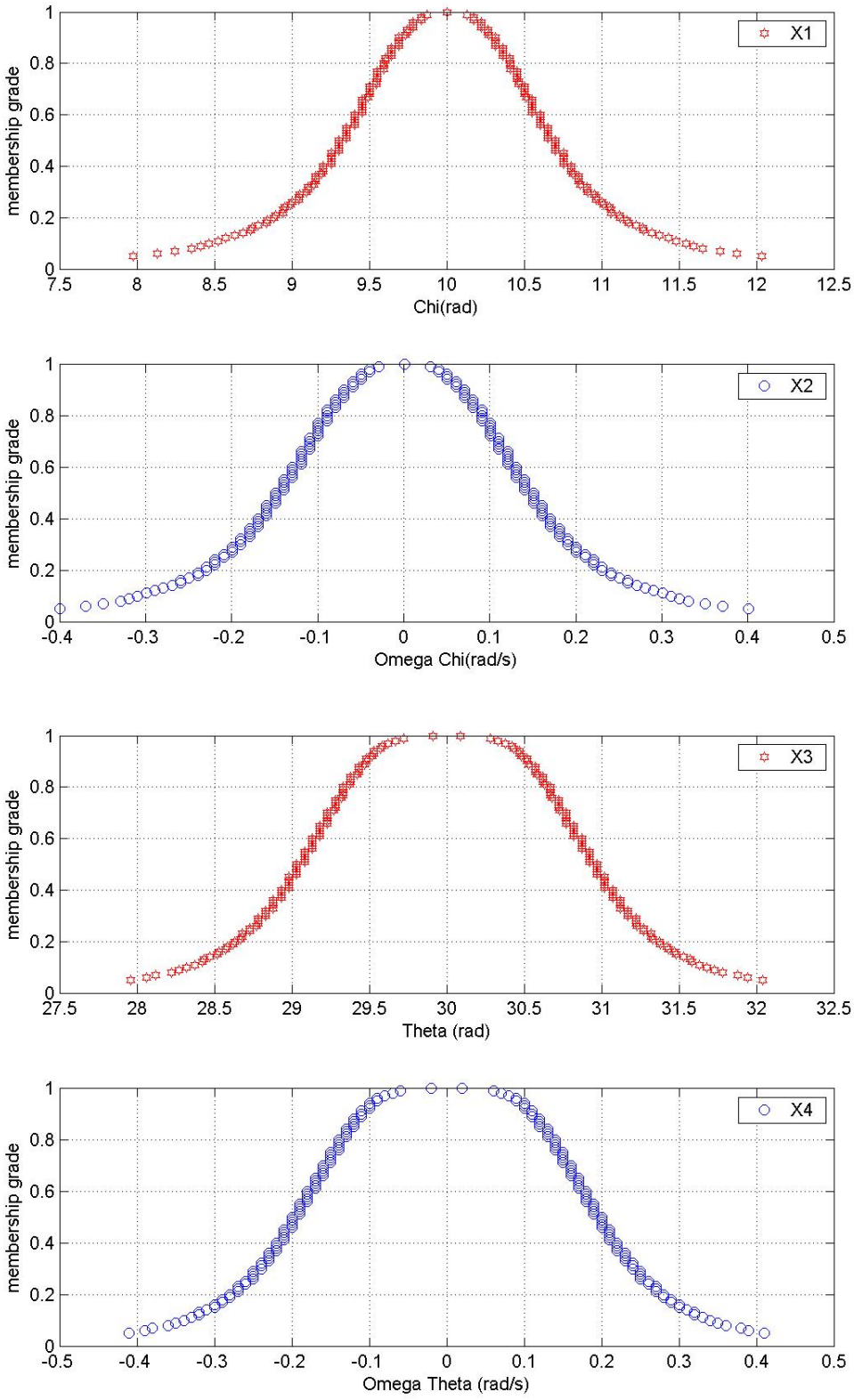

C.4.6 Membership functions propagation of a robotic grinder at 4 second

REFERENCES

[1]] J. Bay. *Fundamentals of Linear State Space Systems.*WCB/McGraw-Hill, 1999.

[2] J.F. Baldwin. *Fuzzy Logic*. John Wiley & Sons, 1996

[3] P. Bernstein, *Against the Gods*, John Wiley&Sons, 1996.

[4] J.C Bezdek. *Fuzzy Mathematics In Pattern Classification Ph.D. Thesis*. Center for Applied Mathematics, Cornell University, Ithaca, 1973

[5] J. Ginsberg. *Advanced engineering dynamics.* Cambridge University Press. 1998.

[6] M. Gopal. *Modern Control System Theory*. John Wiley & Sons, 1993.

[7] G. Graham, W. Bechtel. *A Companion to Cognitive Science*. Blackwell Publishing, 1999.

[8] G. Klir, B. Yuan. *Fuzzy Set and Fuzzy Logic:Theory and Applications* Prentice hall, 1995.

[9]G. Klir, Bo Yuan, and U. St.Clair. *Fuzzy Set Theory: Foundations and Applications.* Prentice hall, 1997.

[10] B. Kosko. *Fuzzy Thinking: The New Science of Fuzzy Logic*. Hyperion, 1993.

[11] B. Kosko, J. Bezdek, D. Dubois, and H. Prade. *Fuzziness and Probability* http://www.neuronet.pitt.edu/~bogdan/research/fuzzy/fvsp/fvsp.html

[12] E.H Mamdani. *Application of fuzzy algorithms for control of simple dynamic plant*. *IEEE* Proceedings, Vol 121, No12, 1974

[13]M. Mizumoto and K. Tanaka. *Fuzzy-Fuzzy automata*. *Kybernets* Vol5, 1976.

[14] J. Yan, M. Ryan, and J. Power, *Using Fuzzy Logic*. Prentice Hall,1994.

[15] J.Yen and R. Langari, *Fuzzy Logic: Intelligence, Control, and Information* Prentice Hall, 1st edition ,November 23, 1998.

[16] L.Zadeh, *"Fuzzy Sets"*, *Information Control 8* pp.338-353, 1965.

[17] H.J. Zimmermann. *Description and Ecopimization of Fuzzy Systems*. *Int. J. General Systm.*, Vol 2. 1975

[18]] H.J Zimmermann, A. Jones, A. Kaufmann. *Fuzzy Sets Theory and Applications* D. Reidel Publishing Company, 1986